

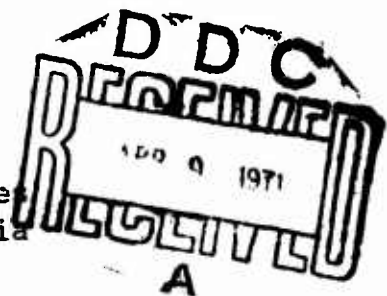
AD 721395

REPORT NUMBER USC GEOL 70-7

MINERALOGY OF HEMIPELAGIC BASIN SEDIMENTS, CALIFORNIA  
CONTINENTAL BORDERLAND: A TECHNICAL REPORT FOR CONTRACT  
N 00014-67A-0269-0009C

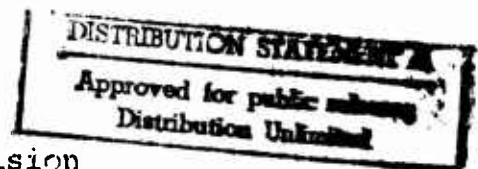
By

Peter Fleischer  
Department of Geological Sciences  
University of Southern California  
Los Angeles, California 90007



Submitted to

Ocean Science and Technology Division  
Office of Naval Research  
Washington, D.C. 20360



Reproduction in whole or in part is permitted  
for any purpose of the United States Government

November, 1970

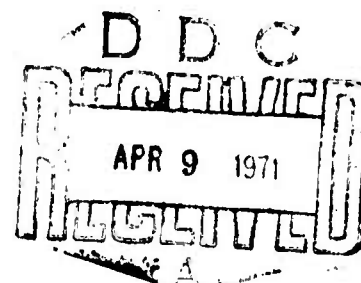
Reproduced by  
NATIONAL TECHNICAL  
INFORMATION SERVICE  
Springfield, Va. 22151

220

MINERALOGY OF HEMIPELAGIC BASIN SEDIMENTS  
CALIFORNIA CONTINENTAL BORDERLAND

by

Peter Fleischer



DEPARTMENT OF THE ARMY  
WASHINGTON, D.C. 20315  
Approved for publication  
by the Department of the Army

## CONTENTS

	Page
ILLUSTRATIONS . . . . .	vi
ABSTRACT . . . . .	x
INTRODUCTION . . . . .	1
General statement . . . . .	1
Previous work . . . . .	1
Sampling methods . . . . .	5
Core descriptions . . . . .	6
Acknowledgments . . . . .	9
ANALYTICAL METHODS . . . . .	11
Sample preparation . . . . .	11
Size analysis . . . . .	13
Purpose and methods . . . . .	13
Comparison of pipette methods . . . . .	16
Effect of sample weight . . . . .	20
Less than 2 micron centrifuge fractions	22
Carbonate analysis . . . . .	22
X-ray mineralogy . . . . .	23
Methods . . . . .	23
Pipette fractions . . . . .	23
Less than 2 micron fractions . . . . .	25

	Page
X-ray diffraction techniques . . . .	26
Non-clay minerals . . . . .	27
Identification . . . . .	27
Quantitative analysis . . . . .	29
Clay minerals . . . . .	30
Identification . . . . .	30
Quantitative aspects . . . . .	36
Long-term reproducibility . . . . .	45
BASIN AND RIVER MINERALOGY . . . . .	51
General statement . . . . .	51
Grain-size parameters . . . . .	54
Calcium carbonate . . . . .	58
Average size-mineral frequency	
distributions . . . . .	58
Less than 62 micron minerals . . . . .	69
General aspects . . . . .	69
Non-clay minerals . . . . .	74
Clay minerals . . . . .	77
Effect of particle size on mineral	
distribution . . . . .	81
Less than 2 micron minerals . . . . .	85
General aspects . . . . .	85
Clay minerals . . . . .	89



	Page
Expandable clays . . . . .	98
Mixed-layer clays . . . . .	98
Potassium-fixable and beidellitic clays . . . . .	99
Geographic distribution of minerals . . . .	103
Rivers . . . . .	103
Drainage . . . . .	103
Lithology . . . . .	107
Mineralogy of river sediments . . .	109
Basins . . . . .	115
General aspects . . . . .	115
Non-clay minerals . . . . .	118
Clay minerals . . . . .	121
CORE MINERALOGY . . . . .	125
Correlation of cores . . . . .	125
Pleistocene sea level . . . . .	129
Grain-size parameters . . . . .	130
Silt mineralogy . . . . .	135
Non-clay minerals . . . . .	135
Clay minerals . . . . .	144
Less than 2 micron clay minerals . . . . .	149
Expandable clays . . . . .	159
SANTA BARBARA BASIN MINERALOGY . . . . .	162
General aspects . . . . .	162

	Page
Comparative core mineralogy . . . . .	166
Grain size and carbonate . . . . .	166
Minerals . . . . .	172
Source of sediment . . . . .	183
Depositional process . . . . .	189
SUMMARY AND CONCLUSIONS . . . . .	194
REFERENCES . . . . .	199

## ILLUSTRATIONS

Figure	Page
1. Bathymetric map of California Continental Borderland . . . . .	2
2. Core lithology . . . . .	7
3. Precision of pipette methods . . . . .	17
4. X-ray diffraction calibration curves for quartz, feldspar, and amphibole . . . . .	31
5. Determination of 7 A kaolinite peak intensity by dissolution of chlorite with 6N HCl . . . . .	40
6. Ternary sand-silt-clay diagram . . . . .	56
7. Average mineral size-distributions of carbonate-free basin sediments . . . . .	60
8. Mineral size-distributions of river sediments . . . . .	62
9. Mineral size-histograms of river sediments . . . . .	64
10. Less than 62 micron mineral composition diagrams of average basin and river sediments . . . . .	72
11. Less than 62 micron and less than 2 micron clay mineral composition diagrams for average basin and river sediments . . . . .	78
12. Variation of minerals with particle size .	83
13. Less than 2 micron clay mineral composition diagram of Santa Barbara Basin sediments, showing chlorite enrichment . . . . .	96
14. Less than 2 micron clay mineral composition diagrams of expandable clays for average basin and river sediments . . . . .	100

Figure		Page
15.	Coastal drainage area, southern California . . . . .	105
16.	Mineral profiles of southern California river silts and clays . . . . .	111
17.	Variation of mineralogy with distance from shore . . . . .	116
18.	Carbonate content and coiling directions of <u>Globigerina pachyderma</u> . . . . .	126
19.	Pleistocene low sea level map . . . . .	131
20.	Mean diameter, standard deviation, and sorting index of cores . . . . .	133
21.	Quartz and amphibole size-fraction weight percents of cores . . . . .	136
22.	Plagioclase and potassium feldspar size-fraction weight-percents of cores . . . . .	138
23.	Quartz-feldspar, plagioclase-K-feldspar, montmorillonite-illite, and kaolinite-montmorillonite ratios of cores . . . . .	141
24.	Montmorillonite and illite size-fraction weight-percents of cores . . . . .	145
25.	Chlorite, kaolinite, and vermiculite size fraction weight-percents of cores . . . . .	147
26.	Less than 2 micron montmorillonite and illite ratio percents of cores . . . . .	151
27.	Less than 2 micron kaolinite and chlorite ratio percents of cores . . . . .	153
28.	Less than 2 micron vermiculite ratio percents and mixed-layer clay of cores . . . . .	155
29.	Potassium-fixable clay and beidellitic clay in the less than 2 micron expandable clay fraction of cores . . . . .	160

Figure	Page
30. Grain-size parameters and carbonate content, Santa Barbara Basin core 11270 .	168
31. Average mineral size-distributions for Santa Barbara Basin green mud and gray layers . . . . .	170
32. Bulk mineral and quartz-feldspar composition diagrams of less than 62 micron Santa Barbara Basin and river sediments .	173
33. Less than 2 micron clay mineral composition diagrams, Santa Barbara Basin and rivers . . . . .	176
34. Less than 62 micron size-fraction mineralogy, Santa Barbara Basin . . . . .	179
35. Less than 2 micron clay mineral ratio percents, Santa Barbara Basin . . . . .	181
36. Fit of less than 62 micron river mineral-suites to gray layers and green mud of Santa Barbara Basin by ranking . . . . .	186

Table	Page
1. Precision of standard measures for pipette methods . . . . .	19
2. Effect of sample size on precision of pipette analysis . . . . .	21
3. Long-term reproducibility . . . . .	46
4. Average grain size and carbonate . . . . .	55
5. Average less than 62 micron mineral ratio percents . . . . .	70
6. Average shale compositions compared to basin and river sediments . . . . .	76
7. Less than 2 micron clay mineral ratio percents . . . . .	87
8. Drainage areas and discharges . . . . .	94
9. Comparison of green mud and gray layers, Santa Barbara Basin . . . . .	167

## ABSTRACT

Minerals in Holocene and late Pleistocene basin sediments of the northern California Continental Borderland are derived from local sources, and in minor amounts from wind- and current-borne sediment. Source, sea level fluctuations, differential settling, and sedimentation by floods control the distribution of the mineralogy.

The sediments are clayey silts composed of illite, montmorillonite, and quartz, with subordinate kaolinite, chlorite, vermiculite, feldspar, and amphibole. Montmorillonite consists partly of mixed layers with illite, and of trioctahedral, iron-rich varieties. Quartz and feldspar are abundant only in the silt-sizes, and their proportions are strongly affected by sediment size.

River-sediment mineralogy can be divided into northern sedimentary, central igneous-metamorphic, and southern batholithic suites. Basin sediments, however, are relatively homogenous owing to mixing by currents. Basin sediments are higher in montmorillonite and chlorite, and lower in illite than the river sediments. Chlorite enrichment is caused by deposition of chlorite-rich sediment transported by the California Current from the North Pacific coast. This process is recognizable in Santa Barbara Basin, where chlorite in hemipelagic sediment is twice that in rapidly deposited local flood-layers. Montmorillonite enrichment may also be caused by the same process, but could be due to the dominance of several rivers. An offshore increase of montmorillonite and a corresponding decrease of illite appears to be the result of segregation by differential settling. Fine-grained quartz increases offshore and reflects the increase in importance of the eolian component.

Analysis of cores reveal mineralogic variations that are largely controlled by sea-level fluctuations. High quartz-feldspar ratios in Pleistocene sections of cores from the outer borderland are similar to those on Santa Rosa-Cortes Ridge, which was subject to wave erosion during low sea level 18,000 years B.P. In Catalina Basin, a distinct metamorphic plagioclase-chlorite-amphibole suite from Catalina Island was diluted by a volcanic suite

from Santa Barbara Bank during low sea level. An increase in montmorillonite-illite ratios coincident with rising sea level is attributable to a differential settling effect, and to the removal of offshore banks as sources as they were flooded and submerged by the rising sea. Decrease of kaolinite since the Pleistocene is related to climatic change.

Numerous well-sorted gray silt layers in Santa Barbara Basin appear to be flood-deposits that formed after unusually heavy storms, such as occurred in 1969. Comparison of mineralogy and sedimentologic parameters shows that the Santa Clara River is the dominant source of these deposits.



## INTRODUCTION

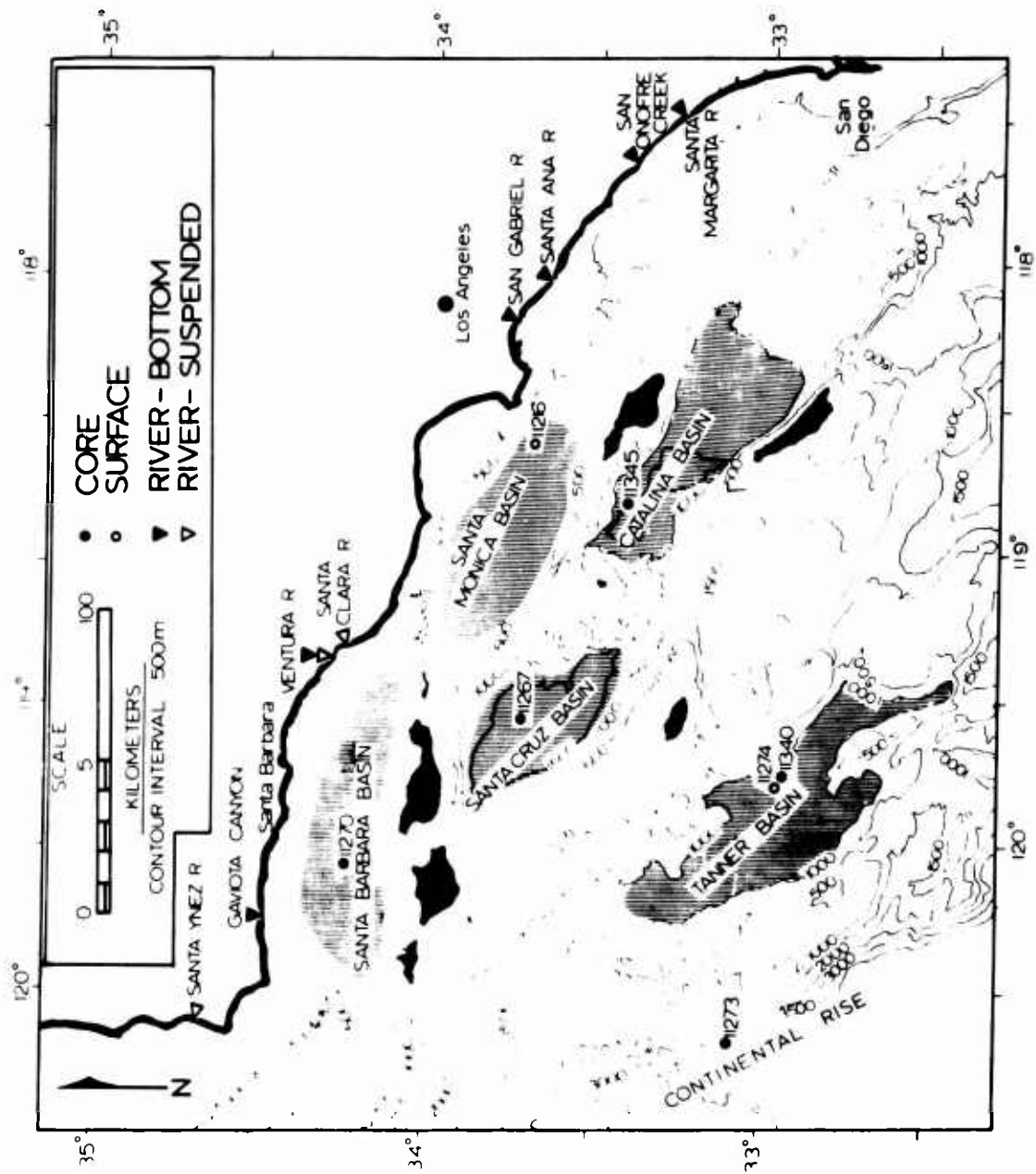
### General Statement

The purpose of this study is to determine the silicate-mineral composition of fine-grained basin sediments in the California Continental Borderland. Two portions comprise the study: the relation of basin sediment mineralogy to sources and sedimentation processes, and the effect of late Pleistocene-Holocene climatic and sea-level fluctuations on the basin mineralogy. The location of the area studied is the northern California Continental Borderland from Lat.  $32^{\circ} 45' N$  to Lat.  $35^{\circ} 00' N$ , and from Long.  $117^{\circ} 15' W$  to Long.  $121^{\circ} 00' W$  (fig. 1). Basins that were studied are Santa Monica Basin, Santa Barbara Basin, Santa Cruz Basin, Catalina Basin, Tanner Basin, and the continental rise. In addition, major and representative rivers along the southern California coast were sampled to determine the source-area mineralogy.

### Previous Work

Emery (1960) adequately summarized the geology and oceanography of the California Continental Borderland. This work also serves as a reference for most studies

Figure 1. Bathymetric map of California Continental Borderland and sample locations with RV Velero IV station numbers.



made in this area up to 1960.

There has been a general absence of mineralogic studies on borderland sediments as compared to other parts of the continental margins of the United States. The earliest and only major work is a clay-mineral study by Dietz (1941), also presented in part by Grim, Dietz, and Bradley (1949). This work demonstrated the predominance of montmorillonite and illite in the basin sediments. It was also concluded that kaolinite is gradually being lost from the sediments, and that degraded illite is being reconstituted by potassium uptake. This work was undertaken at a time when x-ray diffraction technology and especially its application to clay mineralogy was in an early stage of development. In addition, the number of samples analyzed was relatively small, and only core tops and bottoms were used. These considerations show that the basis of the conclusions drawn from this work may be questionable and should be reexamined.

Subsequent mineralogic work has been of minor extent. Clay minerals in cores from Santa Barbara Basin, Santa Monica Basin, and Santa Catalina Basin were studied by H. M. Thorne in 1955 (Emery, 1960); he found that illite was dominant and concluded that there were no variations in the cores. Orr and Emery (1956) reported montmorillonite and illite to be dominant in several analyses from Santa Barbara Basin.

Quartz and feldspar determinations have been made on a few samples by E. D. Goldberg and D. S. Gorsline (Emery, 1960). They noted quartz-feldspar ratios of 2.2 and plagioclase-orthoclase ratios of 4.5 for borderland sediments.

A number of studies of clay minerals from submarine canyons in the borderland have been undertaken by students at the University of Southern California. These, like the above work, are plagued by lack of uniformity of methods and interpretation, and are therefore of limited value. Of interest is a study by H. B. Zimmerman (unpublished report, 1965) of clay minerals from Catalina Submarine Canyon, in which he used electron microscope and x-ray diffraction methods. He reported the presence of frequent tubular objects that he identified as halloysite. Although this interpretation is probably correct, the objects may also be sepiolite or attapulgite.

Work on the mineralogy of fine-grained river sediments is virtually nonexistent. A few diffraction analyses by Rodolfo (1964) show the presence of quartz, feldspar, illite, montmorillonite, and chlorite.

#### Sampling Methods

The intent of the sampling approach was to obtain maximum geographic coverage of the late Pleistocene to Holocene stratigraphic interval with a minimum number of

samples. This objective was partially attained with a set of cores from nearshore, intermediate, and offshore basins. In this manner, a profile from nearshore to offshore environments was obtained.

Cores were collected in the centers of the above-mentioned basins (fig. 1) with a modified Kullenberg piston corer aboard R.V. Velero IV. A Reineck box core taken on Redondo Submarine Fan was used as a surface sample from that basin, and also as a standard to develop analytical methods and to measure reproducibility.

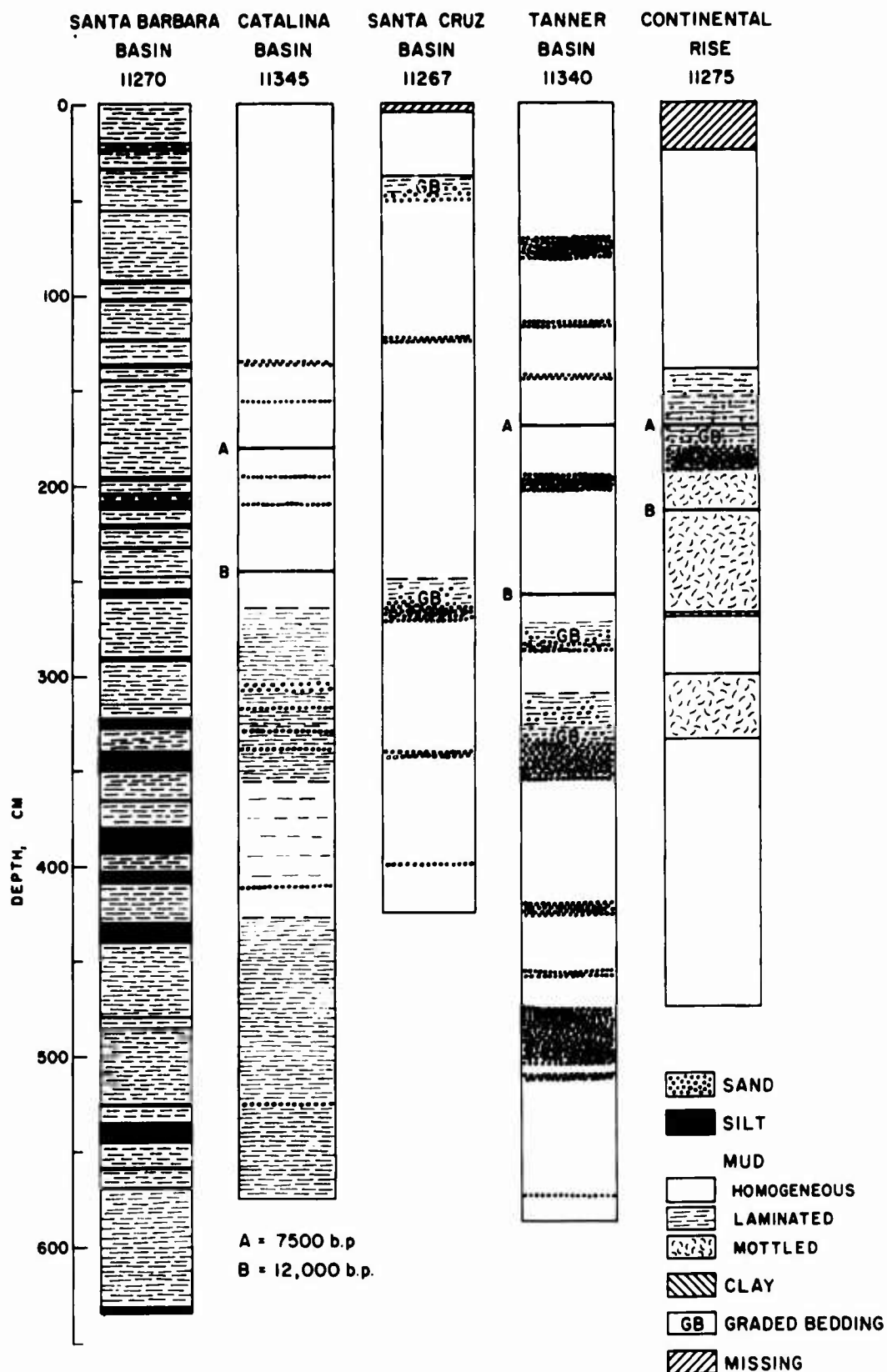
Bed-load sediment was collected from Gaviota Creek, Ventura River, San Gabriel River, Santa Ana River, San Onofre Creek, and Santa Margarita River. Suspended-load sediment was sampled from Santa Ynez, Ventura, and Santa Clara Rivers during the February-March flood of 1969 (fig. 1).

#### Core Descriptions

Cores range in length from 435 to 665 cm (fig. 2). Most of the sediment consists of uniform-appearing olive gray mud of varying shades. Small sand layers are common in most of the cores, and several thicker, graded sand layers are present in the Santa Cruz, Tanner Basin, and continental rise cores. A thick graded bed and some mottling in the core from the continental rise indicates possible slumping, reworking, and unconformities. The

Figure 2. Core lithology and station numbers.  
Approximate locations of time  
horizons A and B based on carbonate  
and coiling ratio markers.

# CORE LITHOLOGY





location of this core (fig. 1) makes it subject to these processes.

Laminations were observed in the Santa Barbara Basin core and in lower portion of the Santa Catalina Basin core. In addition, numerous, distinctly gray silt layers mark the Santa Barbara Basin core.

#### Acknowledgments

This work was made possible through the support, assistance, and helpful criticism of many people. I sincerely thank Profs. Donn S. Gorsline, Richard O. Stone, and Anton B. Burg of the University of Southern California for their assistance, for the many discussions, and for reading the manuscript.

Thanks also go to Dr. Ronald L. Kolpack, Mr. David E. Drake, Mr. Robert L. Fleisher, Sister Damien Marie, Prof. James L. Bishoff, and Mrs. Barbara E. Haner of the University of Southern California; Dr. Norman J. Hyne, University of Tulsa; and Dr. Robert W. Rex, University of California, Riverside, for providing suggestions and help in carrying out this study.

Special thanks are extended to Dr. Peter W. Barnes, U. S. Geological Survey, Menlo Park, for performing the carbonate analyses.

Appreciation is expressed to Captain Fred C. Ziesenhenné and the crew of the R.V. Velero IV for their

assistance in the coring operations; Miss Julie Gunther, University of California, Los Angeles, for a portion of the drafting; and to Mrs. June E. Brown for typing the manuscript.

This work was supported by the Department of Geological Sciences, University of Southern California, and by funds from Office of Naval Research Contracts NR 083-144 and N00014-67A-0269-009C. Ship time was provided under National Science Foundation Grant GB8206.

## ANALYTICAL METHODS

### Sample Preparation

The cores were extruded and split lengthwise into two sections while still moist. After the cores were described, 5 cm increments were sampled at 50 cm intervals from one split for size and mineralogical analysis. These increments correspond to about 20 to 50 gm of sample on a dry-weight basis. Only fine-grained "pelagic" sediment was sampled, and sand layers were avoided. The 5 cm samples were preserved in a moist condition until used.

In order to provide adequate dispersion for size analysis, and to obtain good x-ray diffraction patterns, both core and river sediments were cleaned by removal of carbonates, organic matter, and iron oxides. The methods for the removal of these components were adapted from procedures outlined by Jackson (1956).

Carbonates were removed by digestion of the sample in 100 ml of 1N, pH 5 sodium acetate buffer solution at about 85°C. The solution was removed from the sample by centrifugation, and the procedure repeated until digestion was complete, usually two to four times.

The carbonate-free samples were then transferred to 1 L beakers for removal of organic matter with hydrogen peroxide. All samples were heated to 85°C, and 30 percent

hydrogen peroxide was added in 5 to 10 ml increments until the reaction was completed. This required 50 to 100 ml hydrogen peroxide.

During this treatment, the characteristic olive-green color of the basin sediments, which was already partly lost during the acid digestion, changed to a grayish tan. The color change seems in part to be caused by removal of organic pigments, but also probably by oxidation of colloidal iron oxides adsorbed on mineral grains.

After the organic matter was removed, the samples were washed by centrifugation with 100 ml of pH 5 sodium acetate, with 100 ml of 95 percent ethanol, and twice with 100 ml of 1N, pH 7 sodium acetate in preparation for removal of iron oxides.

Free iron oxides were removed by the sodium dithionite-citrate-bicarbonate method developed by Jackson (1956). Because of the size of the samples, the quantities used by Jackson were quadrupled. The samples were placed in 1 L beakers, 160 ml of 0.3M sodium citrate and 20 ml of 1M sodium bicarbonate were added, and the suspension heated to 75° to 85°C. Four grams of sodium dithionite was added and the suspension agitated for 5 minutes; this step was repeated twice. The sample was then cooled, 40 ml of acetone and 50 ml of saturated sodium chloride solution were added to promote flocculation, and the liquid removed by centrifugation. After the

iron oxides were removed, the color of the sediments was a faint greenish gray. The green color appears to be associated with clay minerals, such as chlorite, and with montmorillonite, because the greenish color is enhanced in the finest size fractions.

To achieve uniform and adequate dispersion during size analysis of the samples, the exchangeable cations were replaced with sodium. Sodium saturation was carried out by centrifuge-washing the samples five times in 100 ml of 1N sodium chloride solution. Acetone was added when it was necessary to increase flocculation. The samples were then washed with 150 ml of 95 percent ethanol and cold-stored until used.

## Size Analysis

### Purpose and Methods

The purpose of the size analyses was twofold; to determine the size-frequency distribution of the detrital portion of the sediments, and to determine individual size frequency distributions for each mineral. Mineralogical analysis of individual size fractions usually requires laborious decantation procedures, and weight determinations of the fractionated sample are difficult to combine with x-ray clay-mineral determinations. The method developed here combines the fractionation and size analysis.

This method is a modification of the standard pipette analysis (Krumbein and Pettijohn, 1938), in which two pipette aliquots are taken simultaneously at each interval. One aliquot is placed in a tared beaker, dried, and weighed in the usual manner, and the other is processed for mineralogical analysis. By multiplying the mineral percents of each fraction by the pipette-weight fraction percent, cumulative distributions for each mineral are obtained. Mineral size-frequency distributions can then be derived by incremental or graphic differentiation of the cumulative mineral distributions in a way analogous to the method used for total size distributions (Krumbein, 1934).

A one-half split of the cleaned samples was used for size analysis; this was equivalent to 10 to 20 gm in most instances. The half-split was wet-sieved through a  $62\mu$  mesh, and the coarse fraction dried and weighed. The less than  $62\mu$  fraction was placed in a 1 L cylinder, and the volume of the suspension adjusted to 1000 ml. A dispersing agent was not needed. Aliquots were taken at 1-Phi unit intervals with a double 25 ml pipette. One 25 ml aliquot was used for weight determination, and the other saved for x-ray analysis. After the less than  $1\mu$  pipette was taken, another double aliquot was removed; these aliquots were centrifuged to obtain the less than  $0.25\mu$  fraction. The centrifugation was repeated five times,

until no less than  $0.25\ \mu$  sediment remained in the decantate. The less than  $0.25\ \mu$  fractions were then treated like the pipette fractions.

A computer program was used to calculate size fraction weight percents, mean diameter, standard deviation, skewness, kurtosis, and a nonparametric sorting index. Calculation of these measures requires the use of equal increments. Since the pipette analysis was based on 1-Phi intervals, the finer fractions were also treated in these intervals. The  $0.25$  to  $1.0\ \mu$  fraction was included as two intervals with equal weight fractions,  $0.5$  to  $1.0\ \mu$  and  $0.25$  to  $0.5\ \mu$ . The less than  $0.25\ \mu$  fraction was divided into three equally weighted 1-Phi intervals to spread out the tail of the distribution, extending it to  $0.031\ \mu$ . This figure is close to the minimum size of clay minerals; only a small portion of the clay minerals appear to be smaller than  $0.02\ \mu$  (Jackson, 1956).

The sorting index used in this work was derived by Sharp and Fan (1963) to provide a better measure of dispersion for multimodal or non-normally distributed sediments. It is based on a 25-interval 1-Phi scale from +15 to -10 Phi units. The sorting index, S, in percent sorting, is given by

$$S = 100 + 71.5338 \left( \sum_{i=1}^n f_i (\log_{10} f_i) \right)$$

where  $f_i$  is the fraction observed in the  $i$ th class.

#### Comparison of Pipette Methods

A study of four pipette techniques was undertaken to examine the precision and accuracy of the double pipette method. The methods investigated were (1) one standard 50 ml pipette, (2) one manual 25 ml pipette, (3) a double 25 ml (50 ml total) pipette, and (4) a combination of a 50 ml semiautomatic and a 25 ml manual pipette.

A cleaned, well-homogenized sediment from Santa Monica Basin was used as a standard. Approximately equal quantities of this sediment were put into 1000 ml suspensions after removal of the greater than  $62\mu$  fractions. A total of four analyses was made with each technique.

Average frequency distributions, standard deviations, and coefficients of variation for these analyses are shown in Figure 3. The average frequency distributions from the four methods are similar, and there are no systematic differences detectable among these methods. Average coefficients of variation are lowest, at 4.6 and 4.7 percent, for the 25 ml and 25-25 ml methods. For the 25-50 ml and 50 ml methods, average coefficients of variation are 5.8 and 8.5 percent, respectively.

Reproducibility of standard measures is high for all methods (Table 1). Only the 50 ml method has significantly higher variation than the other methods.



Figure 3. Precision of pipette methods. Weight fractions, standard deviations, and coefficients of variations for four types of pipettes and for sieve analysis.

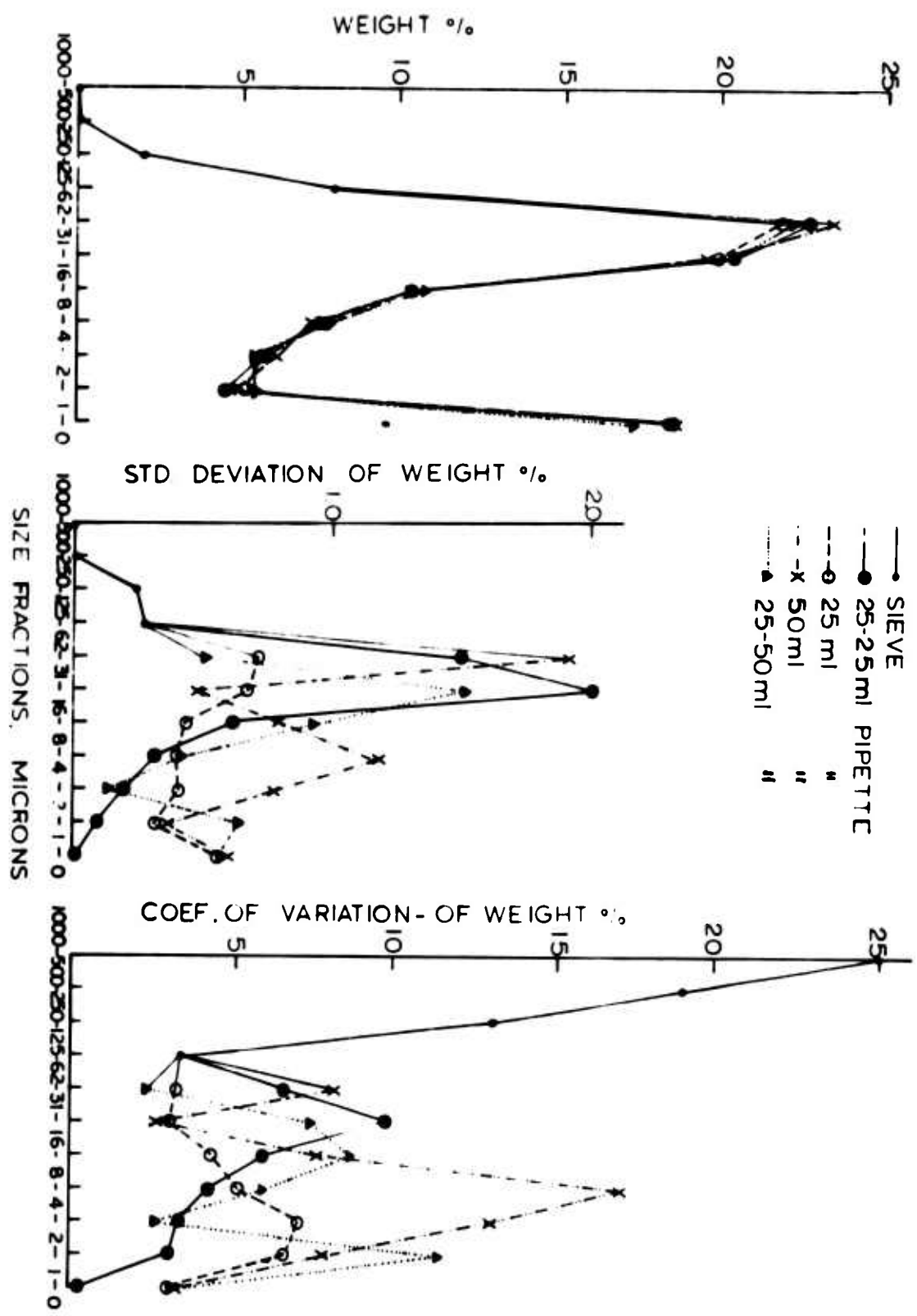


Table 1. Precision of standard measures for pipette methods; coefficients of variation, C (mean/standard deviation) for 4 replicate analyses

Pipette Method	C, %, standard measures				
	Mean Phi	Mean Diam. mm	Std. Dev.	Skew- ness	Kurtosis
25 ml	0.2	0.0*	0.1	4.8	1.6
25-25 ml	0.2	0.0*	0.5	2.2	1.6
50 ml	1.2	0.0*	0.2	10.9	2.8
25-50 ml	0.2	0.0*	0.1	1.7	0.9

\* Variation is less than 0.01 mm.

The double 25 ml pipette method is therefore at least as accurate as the normal 50 ml method, and probably more so. The reason for this may be that the suspension is withdrawn at two points rather than one, which gives a closer approximation of the theoretical cylindrical sampling increment.

#### Effect of Sample Weight

The effect of variation in sample weight for size analysis was studied in order to detect any systematic errors and to find the optimum sample size. Four sample weights, approximately 8, 12, 15, and 19 gm, were used; and four pipette analyses were made for each sample weight, one by each of the four methods described above. The variation in sample weights was about 2 to 6 percent.

Coefficients of variation for pipette size fractions are shown in Table 2. There is no systematic error in the frequency distributions with sample size. Average coefficients of variation are between 5 and 6 percent for all except the 8 gm samples, for which they are 10 percent.

Coefficients of variation for standard measures are again very low (Table 2), but there seems to be no relation between sample size and precision of the measure.

From these data it may be concluded that sample weights of 10 to 20 gm are adequate. The error in individual size fractions increases with samples under 10

Table 2. Effect of sample-size on precision of pipette analysis; coefficients of variation, C (mean/standard deviation) for 4 replicate analyses

Sample Weight, gm	C, % Sample Weight	C, %, Size Fractions, Microns					Ave.
		32-62	16-32	8-16	4-8	2-4	
7.6	5.7	9	9	10	14	15	7
11.6	2.1	3	5	8	4	6	4
15.1	2.0	5	5	5	5	4	5
18.9	2.6	6	5	5	6	9	5
						10	6

Sample Weight, gm	C, %, Standard Measures			
	Mean Phi	Mean Diam. mm	Std. Dev.	Kurtosis
7.6	0.4	0.C*	0.8	1.4
11.6	0.5	0.0*	0.8	2.1
15.1	0.9	0.0*	0.8	3.2
18.9	0.1	0.0*	0.6	1.0

\* Error is less than 0.01 mm.

gm, but the standard measures are not affected by samples as small as 8 gm.

#### Less Than 2 Micron Centrifuge Fractions

A comparison was made between less than  $2\mu$  fraction weights as determined by centrifugation and by pipette methods, because less than  $2\mu$  centrifuge fractions were used to make a detailed determination of clay mineralogy in addition to the pipette fraction analysis. Fifty-ml aliquots for centrifugation were removed from eight suspensions on which pipette analyses had been performed. A total of six centrifugations was made on each aliquot, and the less than  $2\mu$  decantate dried and weighed. The centrifuge fraction weight was compared to the less than  $2\mu$  pipette fraction weight after the former had been corrected for the removal of a less than  $1\mu$  aliquot from the suspension as part of the pipette analysis. For six of the analyses, the variation between the two methods is about 5 percent at the 95 percent confidence limit. For the remaining two analyses, clay cake contamination raised the centrifuge fraction weights about 20 percent.

#### Carbonate Analysis

Samples for calcium carbonate determination were obtained from the remaining one-half split of the cores at intervals corresponding to those at which the samples for

size and mineral analysis were taken. The samples for carbonate analysis were then dried and finely ground. Calcium carbonate was determined gasometrically by hydroxide absorption on a LECO machine by a technique described by Kolpack and Bell (1968).

### X-Ray Mineralogy

#### Methods

##### Pipette Fractions

Five size fractions in 2-Phi unit intervals, the less than 62, 16, 4, 1, and 0.25  $\mu$  fractions, were used for x-ray diffraction analysis. These fractions were saturated with  $Mg^{++}$  in order to reduce variations caused by exchangeable cations, and to allow determination of vermiculite. The aliquots were centrifuge-washed twice with 10 ml of 1N magnesium chloride, then with 1N, pH 7 magnesium acetate to remove exchangeable  $H^+$ , and once with 1N magnesium chloride. Excess salts were removed by three to four centrifuge washes with 50 ml water-ethanol mixtures. For the final wash, 95 percent ethanol was used to keep the sediment flocculated during centrifugation.

An internal standard, reagent-grade calcium carbonate powder was added to the magnesium-saturated sediment in amounts 30 percent of the dry weight of the aliquots. The standard was used to make quantitative

x-ray determinations of the non-clay minerals.

Sufficient water was then added to the sediment and standard to make a thick suspension. After thorough agitation, 1 to 2 ml of the suspension was transferred to a porous porcelain plate and onto a glass slide. The porcelain mount was used for clay mineral analysis, and the slide for the non-clay minerals. One ml of 10 percent glycerol solution was added to the tiles while the sediment was still moist. Glass slides had to be used for the non-clay minerals because the diffraction pattern of the tiles interferes in the angular range where the non-clay minerals were determined. The slide mount was scanned three times, for higher precision, over the major peaks of the non-clays and the standard.

The problem of clay mineral segregation on glass slides has been noted by Gibbs (1965), and porous porcelain plates were used for all clay mineral analyses to avoid this error. The porosity of the porcelain plates is enough to remove about 3 ml of water in a few minutes by capillary suction, thus preventing most settling effects. In addition, the high density of the suspension also inhibits segregation.

To find the degree of segregation actually taking place when mounting sediments studied in this work on glass slides, five replicate analyses of less than 2  $\mu$  clays were made by tiles and by slides. Segregation was



significant formontmorillonite, which was 24 percent higher on the slide, and for kaolinite, which was 25 percent lower on the slide. Other clay minerals varied 5 percent or less.

#### Less Than 2 Micron Fractions

In addition to the pipette fractions, clay mineral analyses were performed on less than  $2\mu$  centrifuge fractions of the cleaned samples. This was done because it was desirable to have a clay mineral analysis of higher precision and greater scope than is possible with the pipette fractions, where small sample size and dilution by addition of the standard reduce diffraction intensity.

The less than  $2\mu$  fractions were recovered by centrifugation from a quarter-split of the cleaned samples. Three aliquots were taken from the centrifuged suspension and saturated with  $Mg^{++}$ ,  $K^+$ , and  $Li^+$ . The magnesium-saturated aliquots were used for the basic clay mineral analysis, the potassium-saturated aliquots for a determination of potassium fixing, and the lithium-saturated aliquots for a determination of beidellitic montmorillonite by a method developed by Greene-Kelly (1953). Potassium and lithium saturation procedures were similar to the procedure for magnesium described above. The washes were with 99 percent methanol followed by 100 percent acetone to keep the clay flocculated; also,

saturated lithium chloride was substituted for the 1N solution in the first step of the lithium-saturation procedure.

One mount on a porous porcelain was made for each of the magnesium, potassium, and lithium-saturated aliquots. The magnesium clay was additionally treated with glycerol, and the potassium saturated mount vapor-saturated with ethylene glycol. The magnesium-saturated mounts, including those from the pipette fractions, were scanned after glycerol treatment, and again after they had been heated 12 hours at 400°C and at 600°C. Potassium-saturated mounts were scanned after the glycol treatment, and again after a 12 hour heating at 400°C. The lithium-saturated mounts were scanned, heated at 200°C for 12 hours, treated with glycerol, and scanned again.

#### X-Ray Diffraction Techniques

X-ray diffraction analyses were made with Norelco wide-angle goniometers and instrumentation. Copper K-alpha radiation; 1° divergence and antiscatter slits, and a receiving 0.006" slit; a scanning rate of 1° 2-theta/min; and a recorder chart speed of 0.5 in/min, with a 2 sec time constant, was used for all scans.

Non-clay mineral determinations were made with a proportional counter and graphite-crystal monochromator system using 50 kv and 30 ma full-wave power. For the clay

analyses, a scintillation counter and nickel-filter system at 40 kv and 30 ma continuous power was employed because this system allowed scanning as low as  $2^{\circ}$  2-theta, as compared to  $3^{\circ}$  2-theta for the monochromator.

During the clay-mineral scans, the x-ray intensity was monitored every hour with a silicon powder standard. Two 100 sec scans were made over the silicon (111) peak, and the count number used to calibrate the clay mineral peak intensities. This procedure was required because multiple scans were needed for the clay mineral determinations.

Integrated peak intensities of the clay mineral basal reflections were determined planimetrically after the low-angle background had been faired with a French curve. Peak areas were then adjusted for variations in x-ray intensity with the silicon calibration-standard intensity.

### Non-Clay Minerals

#### Identification

Non-clay minerals detected in the silt and clay fractions were quartz, plagioclase, potassium feldspar, and amphibole.

Quartz is an abundant constituent in the silt fractions and was identified on the basis of its 4.26 Å

(100) and 3.34 Å (101) peaks. For quantitative determination, both peaks were measured, but only the weaker (100) peak was used because the 3.33 Å (003) illite peak was found to interfere significantly with the (101) quartz peak.

Feldspars were identified by their 6.4 Å (020) and 3.17 Å to 3.25 Å (040) peaks. In the coarse silt fractions, a number of intermediate peaks were also observed. The distinction between plagioclase and K-feldspar is made difficult by overlapping peaks, and by peak shifts in both minerals caused by compositional variation and temperature of crystallization. Since the feldspars were usually present in quantities under 10 percent of the total sediment, only the (040) peak complex could be used as a quantitative estimate. For plagioclase, this peak is at 3.19 Å, and for K-feldspar it is at 3.24 Å. However, there is some ambiguity in these peaks which cannot be resolved because both feldspars may in some instances have peaks at 3.19 Å and 3.24 Å.

Amphibole was identified in many samples on the basis of its 8.4 Å (110) peak. This spacing is normal to the 110 cleavage of amphibole. The prominent cleavage causes preferred orientation of amphibole, with the result that the (110) peak is enhanced. This allows detection of minute quantities of amphibole.

### Quantitative Analysis

Quartz, plagioclase, K-feldspar, and amphibole were determined quantitatively by x-ray diffraction with an internal standard technique (Klug and Alexander, 1954). The method can be expressed by the relations

$$X_1 = \frac{K'}{1-X_s} \cdot \frac{I_1}{I_s} = K \cdot \frac{I_1}{I_s}$$

where  $X_1$  and  $X_s$  are the weight fractions of the 1th component and the internal standard,  $s$ ;  $I_1$  and  $I_s$  are the integrated peak intensities of the 1th component and the internal standard, and  $k'$  and  $K$  are constants. The advantage of this method is that when the standard is added in a constant proportion, the concentration of the unknown component is a linear relation of  $I_1/I_s$ .

Calibration curves were made by preparing a number of mixtures in varying proportions of finely ground quartz, low andesine, orthoclase, and hornblende with aliquots of less than 2  $\mu$  suspensions of known sediment concentration from Santa Monica Basin sediment. Reagent-grade calcite powder was used as the internal standard and added in amounts equal to 30 percent of the dry weight of the aliquot plus the standard mineral. After thorough mixing, two glass-slide mounts were made for each concentration of each mineral. Five scans over different portions of each slide were recorded, average  $I_1/I_s$  ratios deter-

mined for each concentration, and calibration curves drawn from these. The curves were corrected for the small amounts of minerals to be determined that were present in the less than 2/ $\mu$  fraction of the sediment, and the final curves (fig. 4) used to determine mineral concentration in unknown mixtures. Because of the ambiguities encountered in the feldspar determinations, particularly K-feldspar, the andesine calibration curve was used for both plagioclase and K-feldspar.

Because of the large number of determinations made, peak heights, rather than integrated peak areas, were employed in these analyses, and this accounts for the deviation from linearity in the calibration curves at very low concentrations.

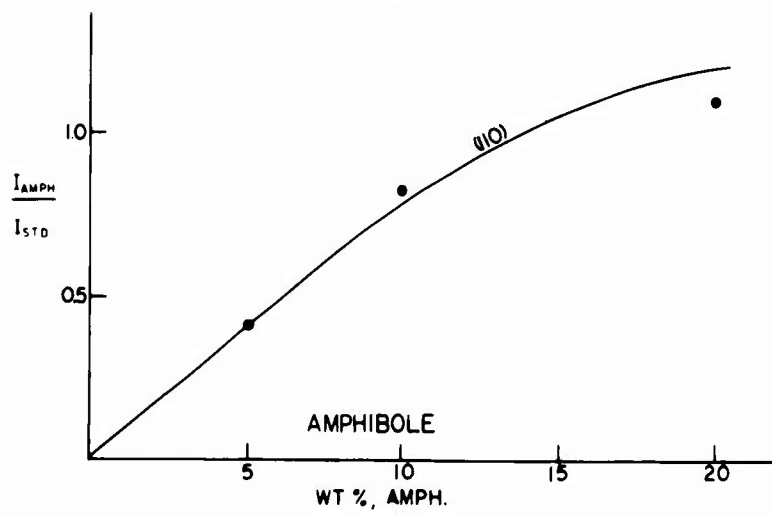
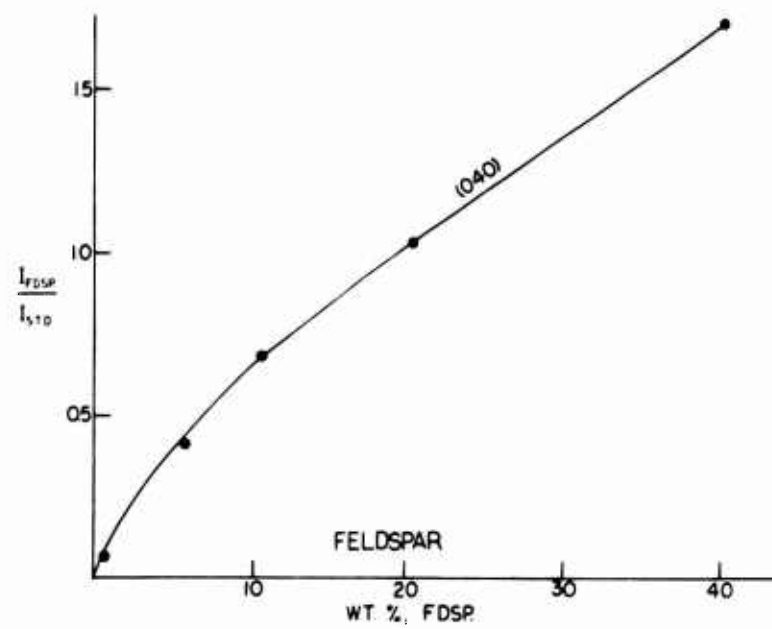
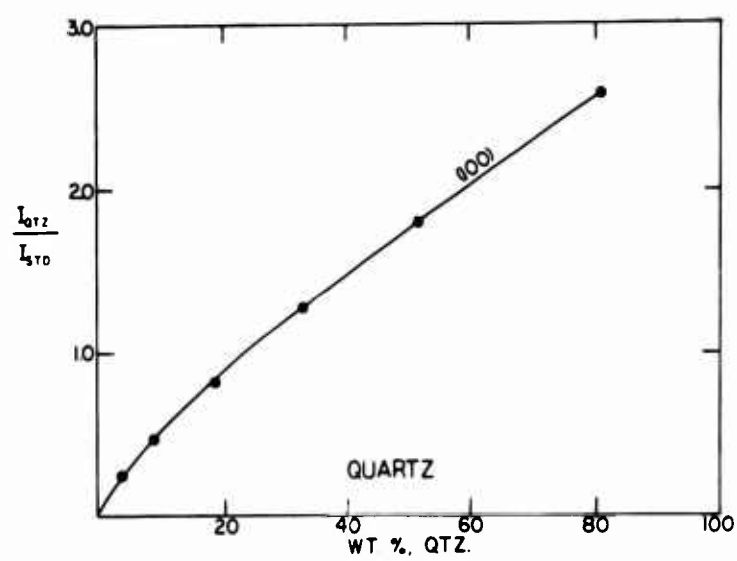
### Clay Minerals

#### Identification

The clay mineral groups identified in the basin sediments include kaolinite, chlorite, vermiculite, illite, montmorillonite, and talc/pyrophyllite. In addition, expandable mixed layer clays, beidellitic montmorillonite, and potassium-fixable clays are present to some degree.

Kaolinite was identified by basal spacings of 7.1 Å and 3.5 Å. These spacings remain unaffected by all treat-

Figure 4. X-ray diffraction calibration curves for quartz, feldspar, and amphibole using 30 percent calcite ((104) peak) as internal standard.





ments except heating at  $600^{\circ}\text{C}$ , which eliminates them. The kaolinite peaks are moderately sharp, indicating fairly good crystallization. Upon glycerol saturation, the 7 Å peak often developed a low shoulder that extended to about 8 Å. This reflection appears to be caused by partly expanded halloysite (Brindley, 1961). Tubular structures believed to be halloysite have been observed in electron micrographs of clays from submarine canyons in the borderland (H. B. Zimmerman, unpublished report).

Chlorite is characterized by a basal spacing of about 14 Å, and a sequence of higher order peaks at 7 Å, 4.8 Å, and 3.5 Å. Upon heating at  $600^{\circ}\text{C}$ , a sharp peak develops at 13.8 Å, and the higher order peaks disappear.

Vermiculite could not be identified directly since its basal spacings are similar to those of chlorite. Its presence, however, could be inferred by comparison of the 14 Å, magnesium-glycerol peak with the 13.8 Å chlorite peak after  $600^{\circ}\text{C}$  heat treatment. Magnesium-glycerol treatment is the only sure method of distinguishing vermiculite from montmorillonite. With this treatment, vermiculite will not expand as it may under other conditions (Walker, 1961). This means of vermiculite identification does not give unequivocal results in the presence of chlorite, and may result in erroneous identification if poorly crystallized chlorites that do not develop a good 13.8 Å peak are present in the mixture.

Illite was identified as being those minerals which give a series of basal reflections at 10 Å, 5 Å, and 3.3 Å that is unaffected by cation exchange, glycerol saturation, and heat treatments. The borderland illites have fairly sharp peaks, indicating reasonably good crystallinity. Although (060) reflections were not measurable owing to the number of minerals in the mixture, most of the illite may be assumed to be dioctahedral. Minor amounts of biotite, glauconite, and mixed-layer clays may also be included in this classification.

Montmorillonite was identified by a 14.5 Å basal reflection that expanded to 17.8 Å with glycerol treatment after magnesium saturation. In the potassium-saturated state, it contracts to 12.3 Å. Upon heating to 400°C or more, all these spacings collapse to 10 Å. Normal magnesium montmorillonite has a basal spacing of 15.5 Å, which corresponds to the presence of two molecular water layers; and potassium montmorillonite has a spacing of 12.4 Å spacing, which corresponds to one molecular water layer (MacEwan, 1961). The observed lack of complete expansion in the magnesium-saturated state may indicate some random mixed-layering with illite (Weaver, 1956). The (060) spacing of montmorillonite could not be determined. However, its greenish color, which becomes a rusty buff upon heat treatment, suggests that a considerable amount of iron may be present in the montmorillonite; and there-

fore trioctahedral montmorillonite may occur in significant amounts.

Expandable mixed-layer clay appears to be fairly abundant in the basin sediments. Mixed layering was estimated by a method developed by Schultz (1964), in which an excess intensity of the 10 Å peak after heating to 400°C, when the intensities of illite and montmorillonite have been accounted for, is attributed to mixed layers. The mixed-layer clay appears to be mainly montmorillonite with minor amounts of illite because expansion to 17 Å or more was always observed with glycerol treatment, and also because no other spacings attributable to mixed layering were present after the 400°C heating. A "crystallinity index" as used by Biscaye (1965), which is a ratio of the 17 Å montmorillonite peak heights to the depth of the "valley" at about  $4^{\circ}$  2-theta, was determined in a few basin sediments in a preliminary study. Because of the large errors encountered in measurement at very low angles, and because a number of factors can affect this index, it was not further used. There was no correlation between the mixed layer clay as determined by Schultz's method and Biscaye's crystallinity index.

Beidellite, as determined with a test developed by Greene-Kelly (1953), was present in all samples. With this test, an expanded spacing of 17.7 Å for lithium-saturated montmorillonite, after heating at 200°C to

300°C and subsequent treatment with glycerol, indicates the presence of beidellite or a trioctahedral montmorillonite. The presence of beidellitic montmorillonite by this test supports the observation that trioctahedral montmorillonite is present on the basis of the green color.

Expandable minerals which are irreversibly contracted to 10 Å, or "fixed" by interlayer potassium ions, were found in minor quantities in the basin sediments. These minerals do not re-expand with ethylene glycol treatment after the exchangeable cations are replaced with potassium. In addition, the expansion that did occur in the montmorillonite was always incomplete, which again confirms the illitic character of some of the montmorillonite as was seen in the mixed-layer clay.

Talc and/or pyrophyllite was identified in Santa Catalina Basin sediments by a 9.1 Å to 9.3 Å shoulder on the 10 Å illite peak. Because of the lack of resolution, the mineral is probably talc, which has a basal spacing of 9.3 Å.

#### Quantitative Aspects

Proportions of clay minerals were determined semi-quantitatively by multiple ratio methods (Copeland, 1963), similar in principle to that first used on clays by Johns, Grim, and Bradley (1954); and in part by a technique developed by Schultz (1964).

To make the multiple ratio method truly quantitative, intensity factors must be determined experimentally for each phase, and all phases must be included in the calculation. These requirements were approximated by using estimated peak-intensity factors, and by assuming that the clay minerals comprise 100 percent of the fraction analyzed. The latter requirement is closely approached in the less than 2  $\mu$  fractions, and partly corrected for in the coarser fractions by quantitative analysis of the non-clay minerals. X-ray-amorphous matter and minor quantities of other minerals are not included in the calculation.

The estimation of intensity factors is a more difficult problem. These could be determined experimentally only in one instance; and intensity factors similar to those used by other workers (Johns, Grim, and Bradley, 1954; Schultz, 1964; Gibbs, 1967a) were taken for the remainder.

The intensity factors used were: (a) unity for all 10 A peak areas and peak heights, including illite on the glycerol-saturated mount, and illite, montmorillonite, and mixed-layer clays after 400°C heat treatment; (b) 4 for the 18 A montmorillonite peak area; (c) 3 for the 18 A montmorillonite peak height; (d) 2 for the 7 A kaolinite peak area; (e) 3 for the 13.8 A chlorite peak area after heating to 600°C; and (f) 3 for the 14 A vermiculite peak area on the glycerol saturated mount. A chlorite peak

height ratio of 2 was assumed for the 600°C-peak at 14 Å to the untreated 14 Å peak; and a 14 Å-600°C chlorite to 7 Å untreated chlorite peak area ratio of 1.5 was experimentally determined.

The quantitative distinction of chlorite and kaolinite is one of the more difficult and critical problems in clay mineralogy. One solution is to use a 3.5 Å (002) kaolinite to (004) chlorite peak ratio (Grim, Bradley, and White, 1957); another is to use the 4.8 Å (003) chlorite peak (Griffin and Goldberg, 1963); and a third is utilizing the 14 Å (001) peak after 600°C heat treatment (Schultz, 1964). The third method was applied in this study. Resolution of the 3.5 Å peaks was poor, and the diffraction patterns of the tiles resulted in interference. It was also difficult to accurately measure these superimposed peak heights. The (003) chlorite peak was weak, and suffered from interference by the (002) illite peak. The 14 Å-600°C peak, on the other hand, is free from interferences, but careful temperature control during heating and close monitoring of the x-ray intensity are essential.

Kaolinite was measured on the basis of its 7 Å peak area on the glycerol-saturated mount. In order to determine the true intensity of this peak, the interfering chlorite was removed from a sample of Santa Monica Basin clay by acid dissolution. The intensity of the 7 Å

chlorite peak as compared to the 14 A-600°C chlorite peak can then be expressed by:

$$\frac{I_{14A-600^\circ \text{ chlorite}}}{I_{7A-\text{untreated chlorite}}} = \frac{I_{14A-600^\circ \text{ chlorite}}}{I_{7A \text{ kaol+chlor}} - I_{7A-\text{kaol, acid-leached}}}$$

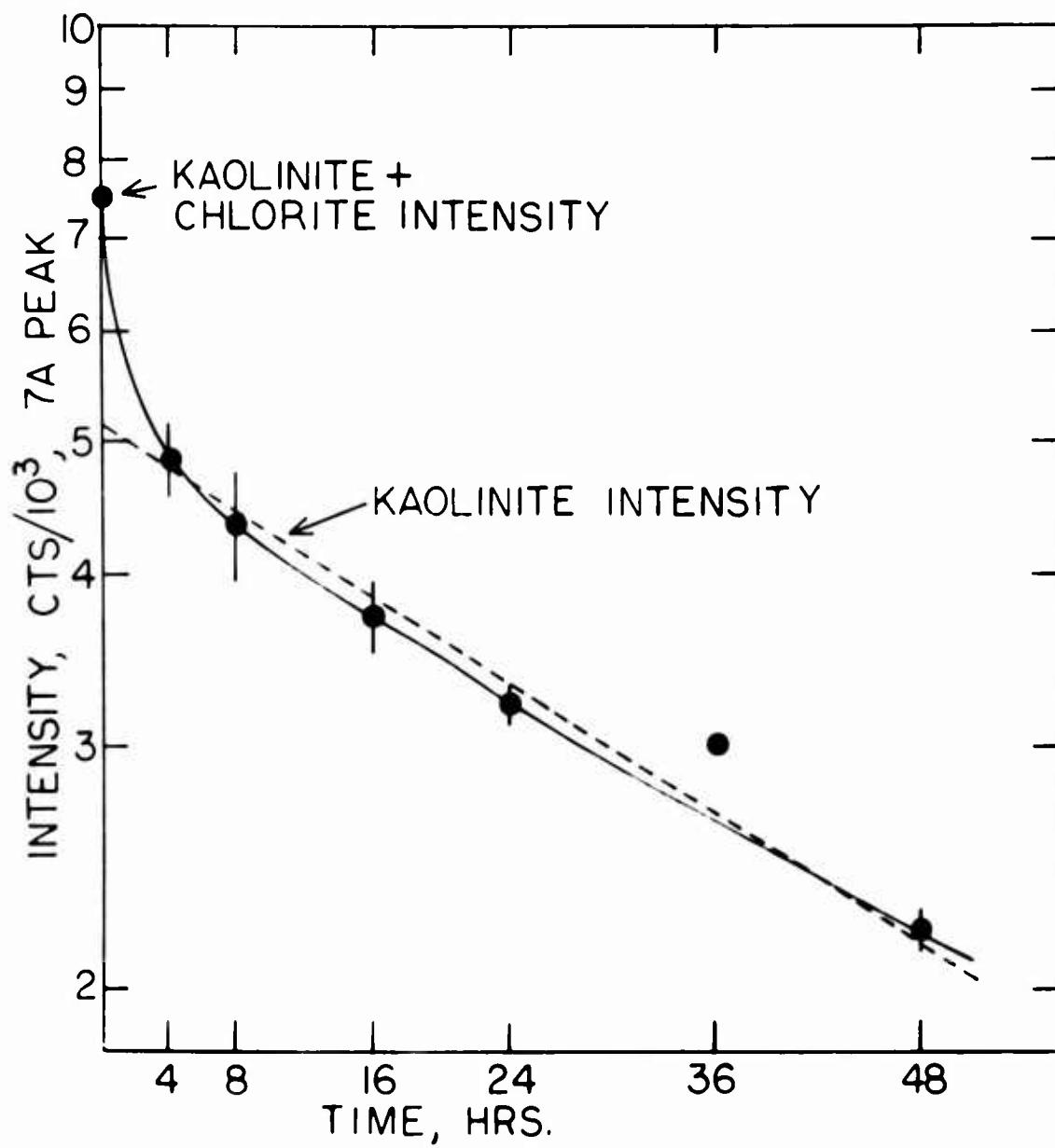
where I is the integrated peak area.

Chlorite was removed by leaching the less than 2 $\mu$  fraction in 6N HCl at 60°C for varying lengths of time. Absolute intensities of the 7 A peaks were measured on the leached aliquots and also on the unleached sample, and a time-intensity curve plotted. This was necessary because the chlorite was removed faster than expected, and some kaolinite was also lost (fig. 5). Since kaolinite solution seemed to follow a slow, linear rate, a straight-line extrapolation was made, and the extrapolated intensity of the 7 A kaolinite peak was used in the computation of the chlorite ratio. By this method, a value of 1.5 was obtained for the 14 A-600°C-7 A chlorite ratio; and with this factor, the kaolinite peak area can be derived by subtracting 1/1.5 of the 14 A-600°C chlorite peak area.

Quantitative estimation of vermiculite in the presence of chlorite and montmorillonite apparently has not been reported before. The method employed here utilizes the difference in peak heights between the 14 A-glycerol and 14 A-600°C chlorite peaks as an estimate of vermiculite. Peak heights were used because the uncertain-

Figure 5. Determination of 7 A kaolinite peak intensity by dissolution of chlorite with 6N HCl. Dashed line is kaolinite solution curve.





ties of the method do not make it advantageous to use peak areas. Conversion to peak area, in order to include vermiculite in the multiple-ratio calculation, is made by obtaining a vermiculite-chlorite peak height ratio and multiplying by the 14 A-600°C chlorite peak area.

The ratio percent, X, of any particular included clay phase can be calculated from the equation

$$X, \% = 100. \frac{kP}{3C + 2K + I + 4M + 3V}$$

where C, K, I, M, and V are the intensities of chlorite, kaolinite, illite, montmorillonite, and vermiculite; P is any of the phases in the denominator; and k is its corresponding intensity factor. Peak intensities of the phases are given by the equations

$$C = (14A-600^\circ \text{ peak area})$$

$$K = (7A\text{-glycerol peak area}) - (1.5 (14A-600^\circ \text{ peak area}))$$

$$I = (10A\text{-glycerol peak area})$$

$$M = (18A\text{-glycerol peak area})$$

and

$$V = (14A-600^\circ \text{ peak area}).$$

$$= \frac{(14A\text{-glycerol peak height}) - (0.5(14A-600^\circ \text{ peak height}))}{(14A-600^\circ \text{ peak height})}$$

The percent of expandable mixed-layer clay was estimated by the method of Schultz (1964). With this calculation, the proportions of illite, montmorillonite, and mixed-layer clay are based on their common 10 A peak after

heating to 400°C. In calculating this parameter, it is necessary to determine the ratio percents of the other clay minerals because

$$\text{mixed-layer clay, \%} = 100 - (\text{kaolinite, \%} + \text{chlorite, \%} + \text{illite \%} + \text{vermiculite, \%})$$

The equations to determine kaolinite, chlorite, illite, and montmorillonite are the same as those presented by Schultz (1964), and the intensity factors listed above were used. Vermiculite was calculated by the equation

$$\text{vermiculite, \%} = (100 - \text{kaolinite, \%} - \text{chlorite, \%}) \cdot \frac{(\text{14A-glycerol peak height}) - (0.5(\text{14A-600}^\circ \text{ peak height}))}{3 (\text{10A-400}^\circ \text{ peak height})}$$

These calculations were originally used for all minerals. However, errors resulting from the 10 A-400°C peak were larger than expected because temperature control was not satisfactory. Therefore, this method was discarded save for the mixed-layer clay calculations.

The percent beidellitic montmorillonite was calculated from ratios of the 10 A-glycerol peaks to the 10 A-200-400°C peaks of the lithium and magnesium-saturated fractions by the equation

beidellitic montmorillonite of total montmorillonite and mixed-layer clays, % =

$$\left[ \frac{1 - \frac{(10A-Li-200^\circ \text{ glycerol peak area})}{(10A-Li-200^\circ \text{ peak area})}}{1 - \frac{(10A-Mg \text{ glycerol peak area})}{(10A-Mg \text{ peak area})}} \right] \cdot 100$$

The percent of potassium-fixable expandable clay was similarly calculated; here 10 A peaks of potassium and magnesium-saturated clays were compared after glycerol and glycol treatment, and after heating to 400°C, by the equation

Potassium-fixable expandable clay in the total expandable fraction, % =

$$\left[ 1 - \frac{1 - \frac{(10A-K \text{ glycol peak area})}{(10A-K-400^\circ \text{ peak area})}}{1 - \frac{(10A-Mg \text{ glycerol peak area})}{(10A-Mg-400^\circ \text{ peak area})}} \right] \cdot 100$$

Computation of the clay mineral ratio percents was performed with a computer because of the large number of calculations which had to be made on each sample. In the case of the pipette size-fraction calculations, weight fractions, non-clay mineral weight-percents, and clay mineral peak intensities were combined in one program which calculated the total mineralogy on a weight-percent basis of all size fractions.

### Long-term Reproducibility

Long-term reproducibility was determined for all parameters in order to estimate cumulative errors in all analyses. For this purpose, eight splits of the standard sample were processed at intervals with all analyses as they were performed on the sediments. Mean values, standard deviations, and coefficients of variation (standard deviation/mean) were calculated for all parameters (Table 3).

Standard deviations are generally low for carbonate and size parameters. An exception is kurtosis; the large variation of this parameter appears to be due to the low values encountered. Individual size fractions are less reproducible, and have coefficients of variation of 10 to 20 percent, and 10 to 15 percent for all but the very small fractions and the sieve fractions.

Less than 2% clay mineral ratio percents have good reproducibility for the amounts present. Mixed-layer clay, potassium-fixable clay, and beidellite ratio percents, however, have large standard deviations. These are attributable mostly to the 10 Å peak after heat treatment at 400°C. The reproducibility of this peak proved to be low because temperature control during heat treatment was inadequate. Disorientation of the clay mount upon glycerol saturation, and possibly incomplete cation exchange in the lithium-saturated clays, contribute to the

Table 3. Long-term reproducibility of sediment and mineral parameters of 8 replicate analyses of a basin sediment

$\bar{X}$ = mean, s = standard deviation, C, % = 100 ( $\bar{X}/s$ )			
	$\bar{X}$	s	C, %
Mean Phi	6.90	0.094	1.4
Mean diam., $\mu$	8.4	0.58	7
Standard deviation	2.97	0.037	3
Skewness	0.91	0.051	6
Kurtosis	-0.06	0.11	195
Sorting index	29	1.18	4
CaCO <sub>3</sub> , %	5.19	0.19	4
<u>Size Fraction Weight Percents, Microns</u>			
500-1000 (sieve)	0.03	0.019	62
250- 500 (sieve)	0.12	0.038	31
125- 250 (sieve)	2.40	0.41	17
62- 125 (sieve)	6.90	0.62	9
31- 62 (pipette)	23.68	3.31	14
16- 31 (pipette)	17.12	2.66	16
8- 16 (pipette)	13.23	1.52	12
4- 8 (pipette)	7.27	0.79	11
2- 4 (pipette)	6.20	0.74	12
1- 2 (pipette)	4.77	0.72	15
1-0.25 (pipette)	9.94	1.63	16
Less than 0.25 (centrifuge)	8.13	1.55	19

Table 3. Long-term reproducibility of sediment and mineral parameters of 8 replicate analyses of a basin sediment (continued)

	$\bar{X}$	S	C, %
<u>Less Than 2 Micron Clay Mineral Ratio Percents</u>			
Illite	37.4	1.4	4
Montmorillonite	47.1	2.2	5
Vermiculite	3.3	0.6	20
Chlorite	4.2	0.5	13
Kaolinite	8.0	1.7	21
Mixed-layer clay	29.5	8.1	27
K-fixable clay	6.2	6.1	99*
Beidellitic clay	51.7	18.1	35*
* Of expandable clay fraction.			
<u>Pipette Fraction Mineral Percents, Fractions in Microns</u>			
<u>Quartz</u>			
16-62	14.0	3.4	24
4-16	5.0	1.2	23
1- 4	0.94	0.19	21
0.25-1	0.40	0.061	15
< 0.25	0.0	0.0	0.0
<u>Plagioclase</u>			
16-62	4.2	1.5	36
4-16	0.94	0.21	22
1- 4	0.13	0.046	35
0.25-1	0.05	0.014	28
< 0.25	0.0	0.0	0.0
<u>K-feldspar</u>			
16-62	1.5	0.60	41
4-16	0.24	0.077	32
1- 4	0.047	0.023	50
0.25-1	0.026	0.006	21
< 0.25	0.0	0.0	0.0

Table 3. Long-term reproducibility of sediment and mineral parameters of 8 replicate analyses of a basin sediment (continued)

	$\bar{X}$	S	C, %
<u>Pipette Fraction Mineral Percents, Fractions in Microns</u> (continued)			
<u>Amphibole</u>			
16-62	0.25	0.076	31
4-16	0.091	0.035	38
1- 4	0.047	0.008	18
0.25-1	0.0	0.0	0.0
< 0.25	0.0	0.0	0.0
<u>Illite</u>			
16-62	16.5	5.8	35
4-16	7.8	2.3	29
1- 4	5.4	1.7	31
0.25-1	4.4	1.3	29
< 0.25	1.5	0.42	28
<u>Montmorillonite</u>			
16-62	0.93	5.0	540
4-16	3.9	1.9	48
1- 4	1.4	1.2	83
0.25-1	2.8	1.0	36
< 0.25	6.0	1.0	17
<u>Vermiculite</u>			
16-62	2.3	0.87	38
4-16	0.42	0.41	97
1- 4	0.29	0.23	81
0.25-1	0.42	0.21	49
< 0.25	0.038	0.027	70
<u>Chlorite</u>			
16-62	2.5	1.5	59
4-16	1.1	0.70	63
1- 4	0.61	0.13	21
0.25-1	0.44	0.097	22
< 0.25	0.049	0.053	109



Table 3. Long-term reproducibility of sediment and mineral parameters of 8 replicate analyses of a basin sediment (continued)

	$\bar{X}$	s	C. %
<u>Pipette Fraction Mineral Percents, Fractions in Microns</u> (continued)			
<u>Kaolinite</u>			
16-62	1.1	1.9	166
4-16	0.97	1.1	110
1- 4	2.1	0.85	41
0.25-1	1.4	1.0	73
< 0.25	0.60	0.40	67
<u>Less Than 62 Micron Fractions</u>			
Quartz	22.5	3.7	16
Plagioclase	5.9	1.7	28
K-feldspar	2.0	0.64	32
Amphibole	0.42	0.095	22
Illite	38.9	7.7	20
Montmorillonite	14.5	4.8	33
Vermiculite	3.8	1.1	28
Chlorite	5.2	1.3	26
Kaolinite	7.0	2.1	30

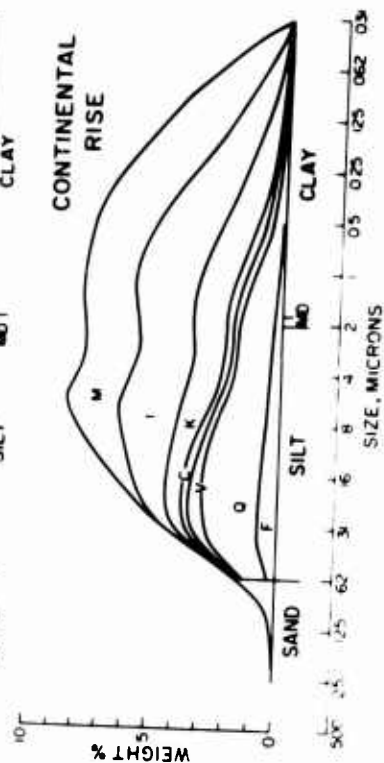
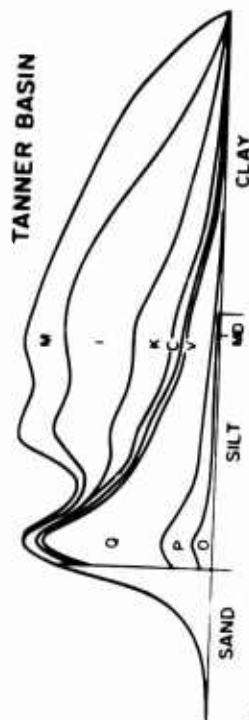
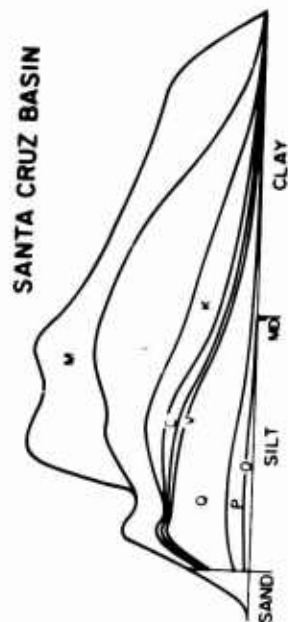
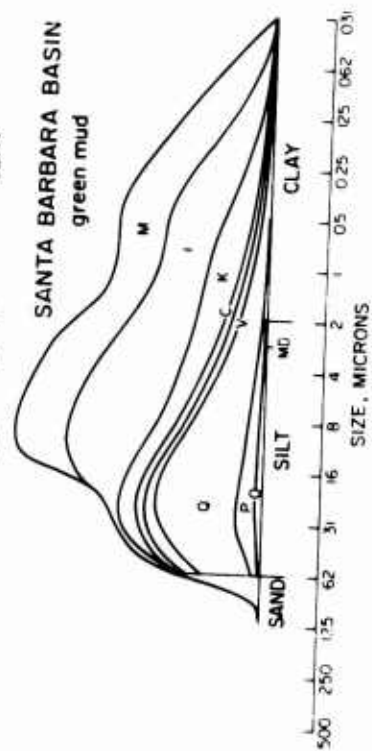
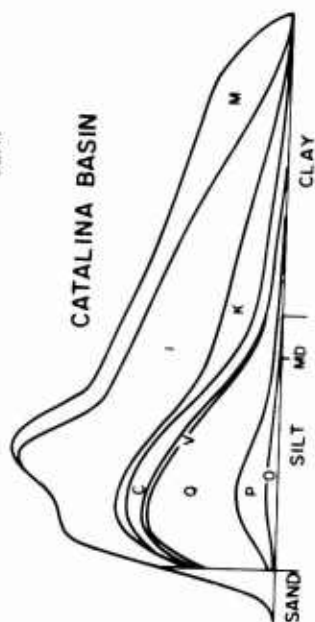
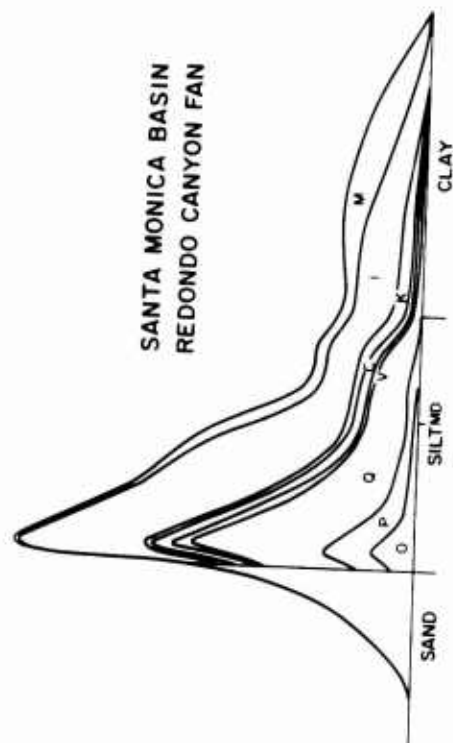


Figure 8. Mineral size-distributions of river sediments. M, montmorillonite; I, illite; K, kaolinite; C, chlorite; V, vermiculite; Q, quartz; P, plagioclase; O, K-feldspar; MD, mean diameter.

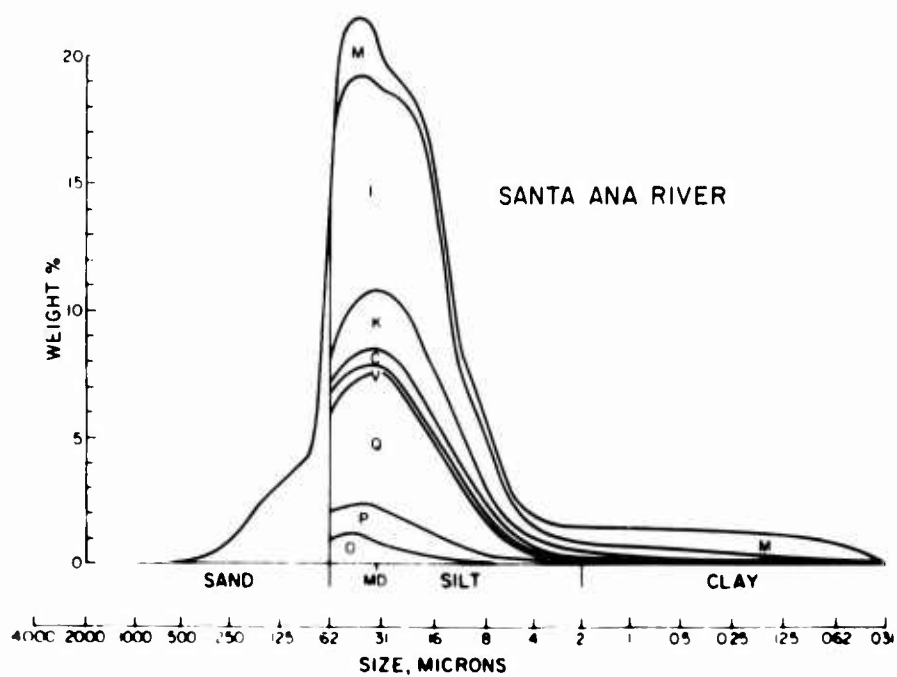
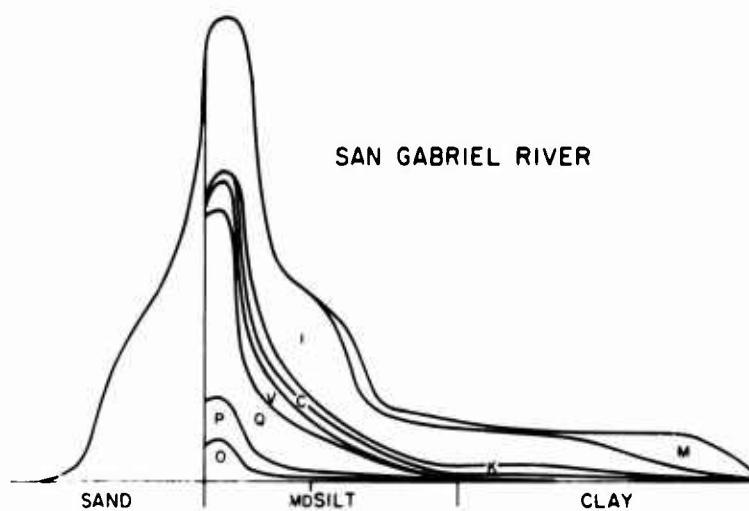
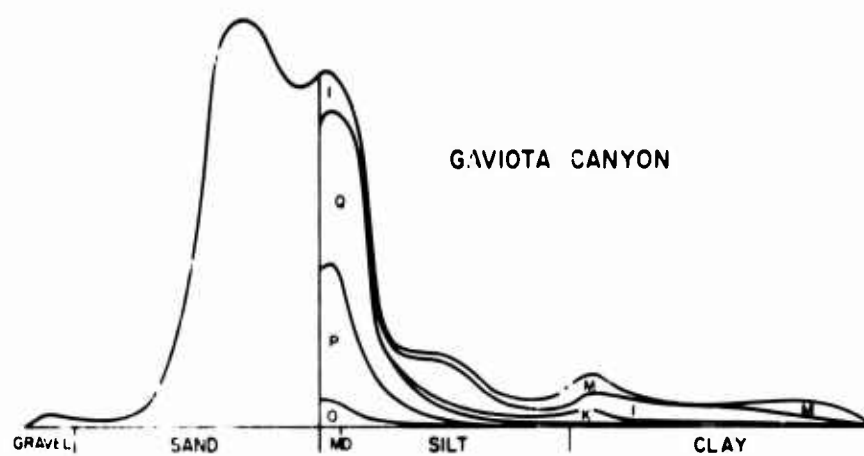
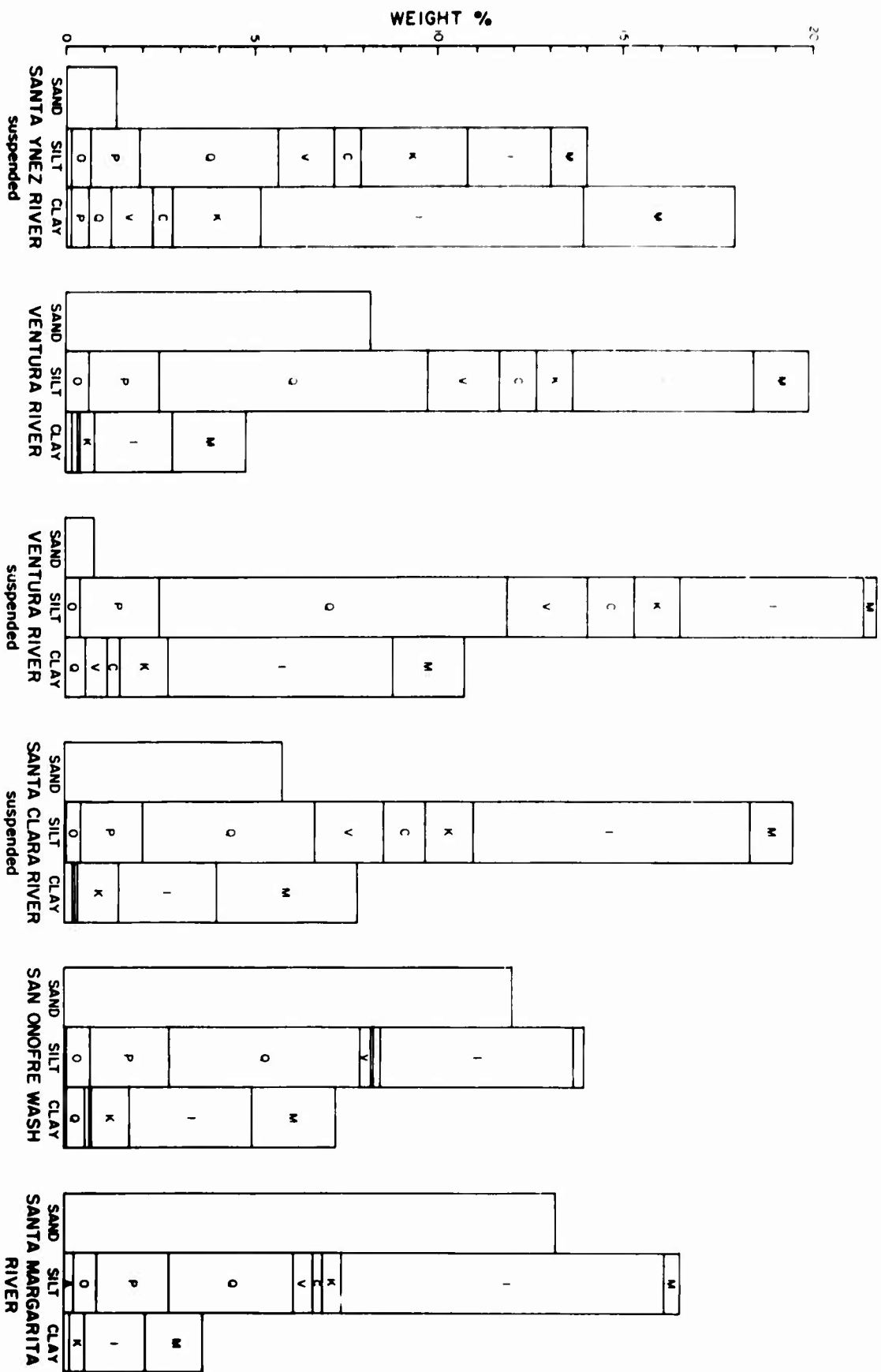


Figure 9. Mineral-size histograms of river sediments. M, montmorillonite; I, illite; K, kaolinite; C, chlorite; V, vermiculite; Q, quartz; P, plagioclase; O, K-feldspar; A, amphibole. Minerals are arranged in order listed. Sand, 62-2000  $\mu$ ; silt, 2-62  $\mu$ ; clay, less than 2  $\mu$ .



is supplied directly from the mainland shelf, and Tanner Basin receives turbidite sands from Santa Rosa-Cortes Ridge. The coarse mode seems to be the result of winnowing of sediments by local short-term bottom currents. Measurements of such currents on the La Jolla Submarine Fan near San Diego (Shepard, Dill, and von Rad, 1969) has shown that velocities of 5 to 30 cm/sec are frequent and almost continuous in the lower range. For particle sizes between 31 and 62  $\mu$ , current velocity-particle size relations (Hjulström, 1939) are such that erosion will occur at velocities over about 30 cm/sec, and deposition takes place at velocities under about 0.3 cm/sec. The measured current velocities thus fall well within the upper velocity range required for transportation of this mode. They are high enough to keep the coarse silt suspended much of the time, but only occasionally great enough to erode it. This size range is also close to the erosional velocity minimum (Hjulström, 1939). Together with the current velocities, this fact explains the presence of a distinct mode. Smaller particles require increasingly higher erosional velocities and these occur only infrequently. Hence coarse silt has greatest mobility under these conditions.

The dominant mode in the basin sediments is in the fine- to medium-silt range. Here the importance of mineralogic control on the size distribution must be con-

sidered. As expected, quartz and feldspar dominate in the coarse silt range, and montmorillonite and illite in the clay sizes. The dominant fine-silt mode, however, owes its presence to a rapid increase over the coarse mode in illite and expandable montmorillonite-mixed layer (?) minerals. Quartz, feldspar, and other clay minerals do not increase correspondingly in this range, which would be expected if the dominant mode were entirely controlled by sedimentologic processes. Thus, although a portion of the fine-silt mode is undoubtedly deposited as discrete particles, and therefore by current-dominated processes, its dominance in the basin sediments is controlled by mineral composition. The medium- to fine-silt mode is also present in the river sediments (Fig. 8); here it is again caused mainly by an increase in illite.

Presentation of the size distributions on Figures 7 and 8 has been terminated at  $0.032\mu$  because only a relatively small part of the clay fraction occurs below  $0.02\mu$  (Jackson, 1956). A  $0.032\mu$  cutoff then should produce relatively little distortion in the size distribution, and most of the basin sediments indeed show a smooth decrease to  $0.032\mu$ . When attempting to interpret the less than  $0.25\mu$  portion of these size distributions, the cleaning procedures, particularly the acid leaching, must be recalled. Solution of very fine particles may quantitatively decrease the fine-clay fraction, but breakdown of



large particles may increase it. It is difficult to test for these effects. Comparison with unleached basin sediments (Emery, 1960) shows no significant differences between leached and unleached sediments, but this comparison is made almost meaningless by abundant calcium carbonate in the unleached sediments.

The clay and fine silt portions of the size distributions are probably not indicative of sedimentation processes, but represent the size distribution of minerals in this range. Sedimentation of clay-size particles is slow enough that bottom currents keep them in suspension indefinitely; therefore, some process like flocculation or coagulation by organic agencies must be called upon to promote deposition. In this regard, it is interesting to note that the importance of organisms in marine sedimentation processes has been generally ignored (R. H. Meade, oral communication). Considering the high content of organic matter and the frequency with which fecal pellets are observed in these sediments, it is likely that the fine fraction becomes coagulated with organic matter by processes such as passing through the gut of organisms. Organic coagulation would seem to be a particularly attractive process whereby suspended sediment could be transferred from the turbid bottom layer and "fixed" to the bottom.

## Less Than 62 Micron Minerals

### General Aspects

Inasmuch as carbonate-free basin sediments contain only 1 or 2 percent material coarser than  $62\mu$ , the bulk mineralogy of the less than  $62\mu$  fraction represents essentially the total mineral fraction of these sediments. The river sediments analysed contain an appreciable fraction greater than  $62\mu$ ; here the less than  $62\mu$  mineralogy is fractional and influenced by the sand modes.

Average percents of less than  $62\mu$  minerals for basins and rivers are listed on Table 5. Illite, montmorillonite, and quartz are most abundant and make up 70 percent of the sediments; kaolinite, plagioclase, and chlorite make up another 20 percent; and vermiculite, K-feldspar, and amphibole are in the remaining 10 percent.

A glance at Table 5 reveals an important aspect of basin sediments in the California Continental Borderland, namely a striking mineralogic similarity. Coefficients of variation (Table 4) for the basin sediments support this observation; the average coefficient of variation is only 22 percent. The river sediments are considerably more varied, and have a coefficient of variation of 50 percent. A tight clustering of basin sediments also can be seen on a total mineralogy ternary diagram (fig. 10). Here it is evident that the river sediments are considerably more

Table 5. Average less than 62 micron mineral percents and ratios

Santa Monica Basin	22	6	2.0	0.42	39	15	3.8	5.2	7	2.75	3.0
Santa Barbara Basin	21	4	1.4	0.08	27	26	4.2	3.5	13	3.89	2.9
Santa Cruz Basin	18	4	1.4	0.28	30	30	2.7	3.9	10	3.33	2.9
Catalina Basin	20	5	1.2	0.50	35	19	2.0	6.8	10	3.22	4.2
Tanner Basin	21	5	1.7	0.25	29	25	2.4	3.3	12	3.13	2.9
Continental Rise	20	4	1.2	0.20	28	24	3.0	4.2	14	3.85	3.3
Santa Ynez River*	15	4	1.7	0.66	35	16	8.3	3.9	16	2.63	2.4
Gaviota Canyon	29	15	2.2	0.10	26	16	0.4	0.0	11	1.69	6.8
Ventura River	30	7	2.5	0.0	28	14	8.1	4.4	6	3.16	2.8
Ventura River*	30	6	1.3	0.0	34	7	8.5	4.8	8	4.11	4.6
Santa Clara River*	18	6	1.6	0.16	38	19	7.2	0.5	9	2.37	3.8
San Gabriel River	14	4	1.7	0.32	45	12	7.1	4.7	11	2.45	2.4
Santa Ana River	23	6	2.5	0.26	37	13	2.0	3.8	13	2.70	2.4
San Onofre Creek	27	10	3.1	0.41	39	12	2.0	0.8	6	2.06	3.2
Santa Margarita River	18	10	3.1	1.39	51	9	2.7	1.2	5	1.37	3.2
Ave., basins	20	5	1.5	0.29	31	23	3.0	4.5	11	3.08	3.3
Ave., rivers	23	8	2.2	0.37	37	13	5.1	2.7	9	2.25	3.6

Table 5: Average less than 62 micron mineral percents and ratios (continued)

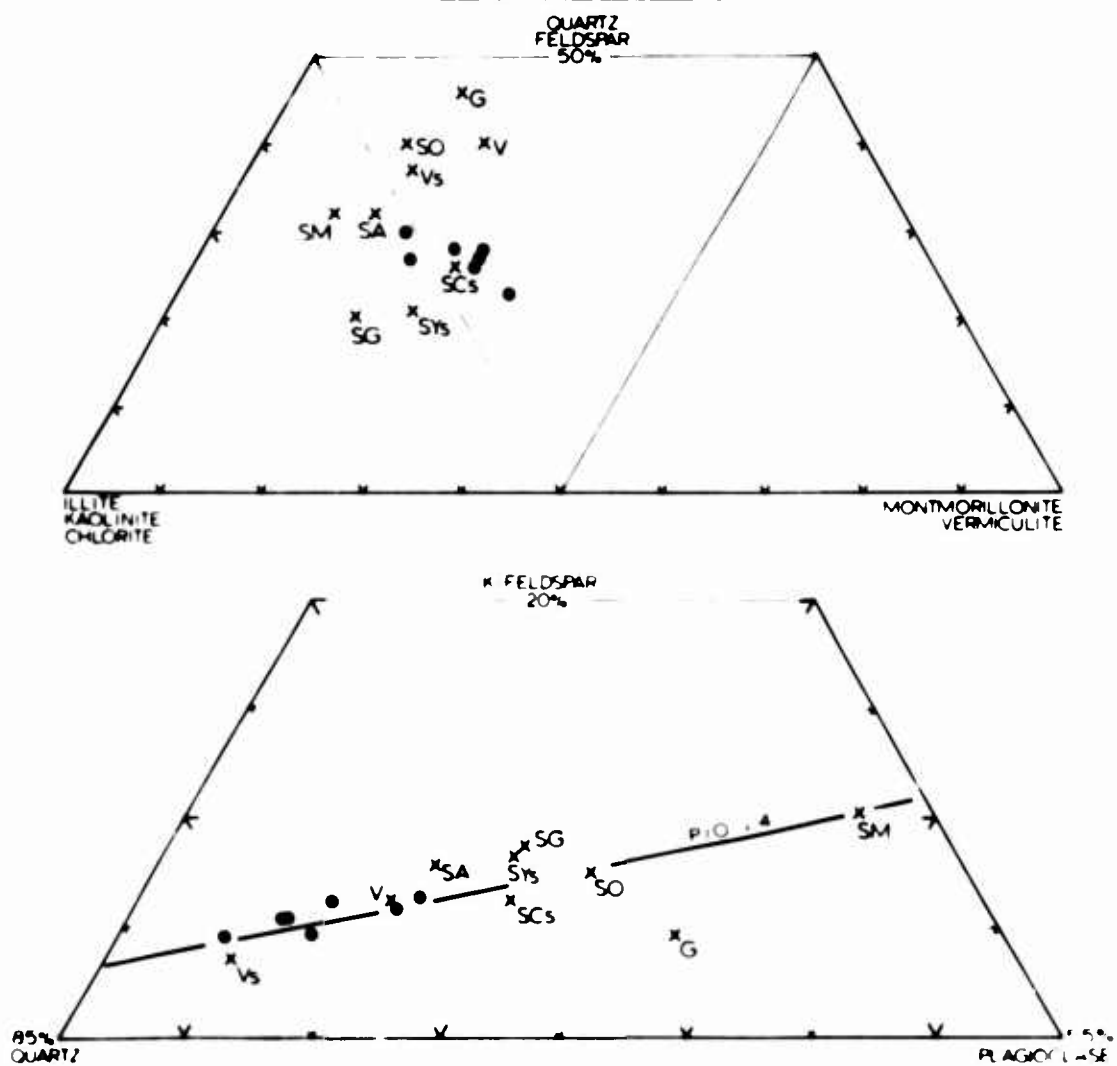
	Quartz	Plagioclase	K-feldspar	Amphibole	Illite	Montmor- illonite	Vermiculite	Chlorite	Kaolinite
Coefficients of Variation, %	7	17	8	53	15	23	23	29	23
Basins		47	30	119	21	28	64	75	38
Rivers	30								

\* Suspended load, 1969 storm.

Figure 10. Less than 62  $\mu$  mineral composition diagrams of average basin and river sediments. SYs, Santa Ynez River, suspended load; G, Gaviota Canyon; V, Ventura River; Vs, Ventura River, suspended load; SCs, Santa Clara River, suspended load; SG, San Gabriel River; SA, Santa Ana River; SO, San Onofre Creek; SM, Santa Margarita River.

<62  $\mu$  MINERALS

● BASINS x RIVERS



scattered and also that they are richer in illite than basin sediments. The similarity among basin sediments suggests that considerable mixing of source material occurs during transport over the borderland.

#### Non-Clay Minerals

Quartz and feldspar comprise the bulk of the non-clay silicates in the less than 62 $\mu$  fraction. Amphibole is present only in very small quantities or absent (Table 5); it is highly variable and serves well as a source indicator.

Quartz-feldspar ratios for basin sediments range from 2.8 to 3.9 with an average of 3.0, and river sediments range from 1.4 to 4.1 with an average of 2.2. These figures correspond to 25 and 31 percent feldspar in the non-clay fractions for basins and rivers, respectively. The greater spread and higher feldspar content in the river sediments is displayed on a quartz-plagioclase-orthoclase ternary diagram (fig. 10).

A ready petrologic interpretation of the ratios is not possible because these sediments are clayey silts and would be classified petrologically as argillaceous siltstone, mudstone, or shale. Because little work has been performed and no compositional classification is in use for fine-grained rocks (with the possible exception of clay mineralogy), it becomes necessary to interpret the quartz-

feldspar ratios in terms of sandstone classifications. By Gilbert's classification (Williams, Turner, and Gilbert, 1954) the sediments border between an arkosic and a feldspathic wacke; according to Pettijohn's classification (1954) they would be on the border of feldspathic gray-wackes (less than 25 percent quartz). Because of the predominant silt size of the sediments, however, arkosic or feldspathic mudstone is a more appropriate name.

The apparently high feldspar content of basin and river sediments is not surprising; it has been long known (Reed, 1928) that feldspar in Mesozoic and Tertiary California sandstones averages 50 percent. Even beach sands on the southern California coast average 40 percent feldspar (Gorsline, 1968). The question then is not why the high proportion of feldspar, but rather why it is not higher. Although the significance of feldspar in arenaceous rocks has been extensively investigated, its importance in argillaceous sediments is not as well known. Early estimates of mineral composition of average shales, calculated from chemical analyses (Leith and Mead, 1915; Clarke, 1924), give high values of feldspar and low values of clay minerals (Table 6). These often-quoted estimates have been shown to be somewhat erroneous by Shaw and Weaver (1965), who calculated the mineral composition for average shales directly from quantitative x-ray diffraction analyses. Basin and river sediments examined in this study have



Table 6. Average shale compositions compared to California Continental Borderland basin sediments and southern California river sediments

	Leith & Mead, 1915	Clarke, 1924	Shaw Weaver 1965	Basins	Rivers
Quartz	32	22.3	30.8	16.6	22.1
Feldspar	18	30	4.5	5.4	9.8
Clay minerals	34	25	60.9	60.2	64.3
Iron oxides	5	5.6	0.5	-	-
Carbonates	8	5.7	3.6	12	1.8
Other minerals	1	11.4	< 2	< 1	< 1
Organic matter	1	-	1	5 (est)	1(est)

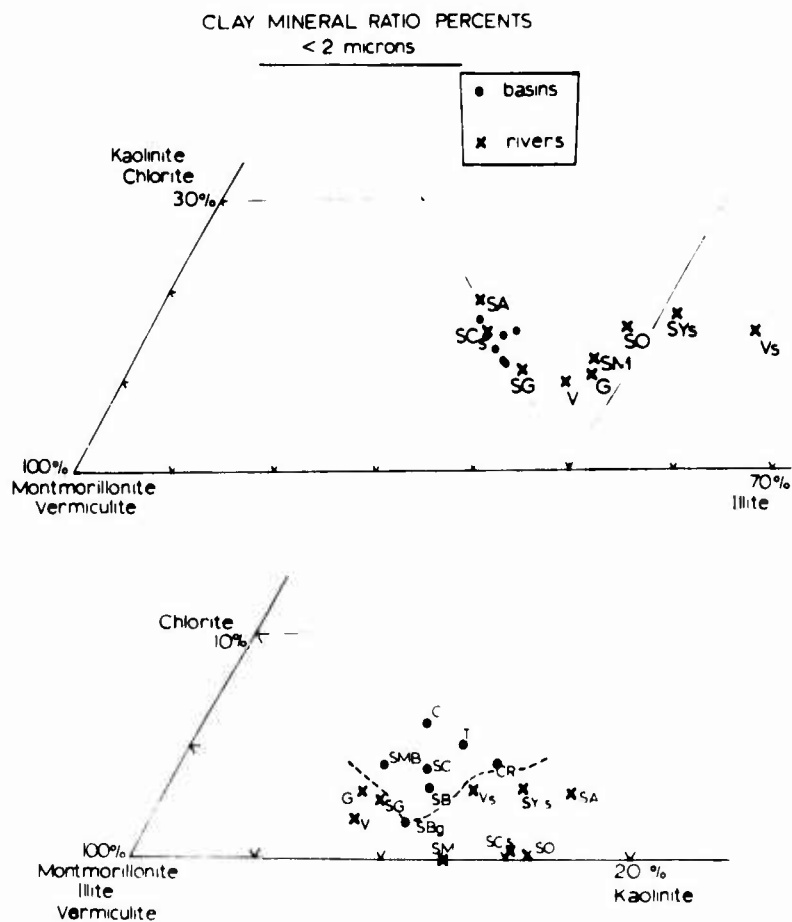
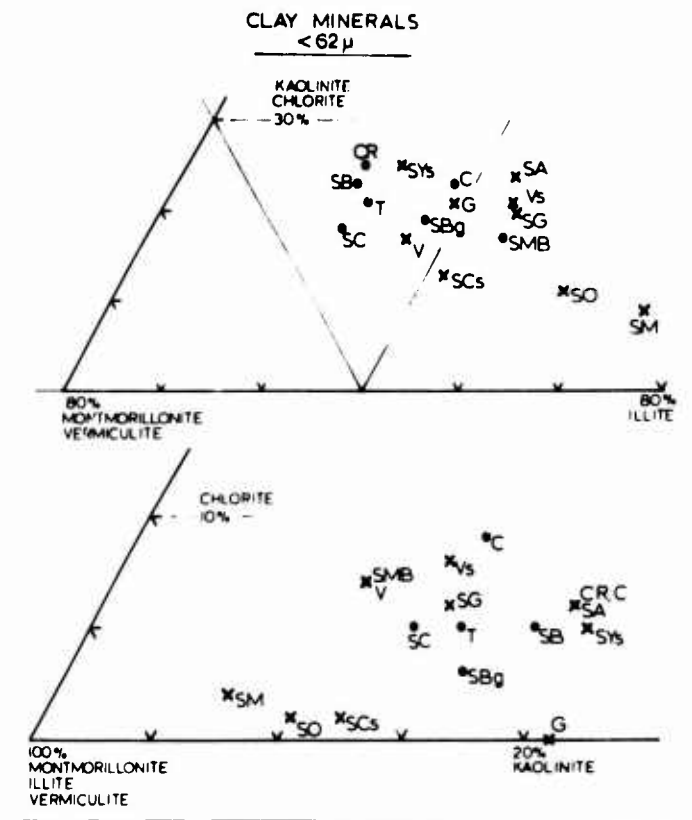
feldspar and clay mineral percents similar to Shaw and Weaver's average shale (Table 6). Somewhat higher feldspar and lower quartz percents are doubtless a reflection of the feldspathic nature of California sediments.

Plagioclase-K-feldspar ratios are more uniform than quartz-feldspar ratios; they are about 3.5, and show relatively little variation (fig. 10). Figure 10 also reveals that the plagioclase-K-feldspar ratio is independent of quartz; therefore, plagioclase and K-feldspar appear to behave similarly in the less than  $2\mu$  fractions of these sediments. Studies on river sands by Gorsline (1968) have shown that the southern California sands are distinctly bimodal in their plagioclase-K-feldspar ratios, with a large mode at 1.0 and a smaller mode at 16. This division is not evident in the less than  $62\mu$  fraction of river sediments in this study. One explanation is that plagioclase-K-feldspar ratios converge in the smaller size fractions; another is that the x-ray technique employed in this study has a determinate error which significantly raises the value determined for very small amounts of K-feldspar.

#### Clay Minerals

The less than  $62\mu$  clay mineral fraction, or essentially the total-sediment clay mineralogy, is predominantly illite-montmorillonite (Table 5, fig. 11), with

Figure 11. Less than 62  $\mu$  and less than 2  $\mu$  clay mineral composition diagrams for average basin and river sediments. SMB, Santa Monica Basin; SB, Santa Barbara Basin, green mud; SBg, Santa Barbara Basin, gray layers; SC, Santa Cruz Basin; C, Santa Catalina Basin; T, Tanner Basin; CR, continental rise. SYS, Santa Ynez River, suspended load; G, Gaviota Canyon; V, Ventura River; Vs, Ventura River, suspended load; SCs, Santa Clara River, suspended load; SG, San Gabriel River; SA, Santa Ana River; SO, San Onofre Creek; SM, Santa Margarita River.



minor amounts of kaolinite, chlorite, and vermiculite. This assemblage is typical of those developed in arid and semiarid regions. The predominance of montmorillonite and illite in soils developed in these climatic regions has been shown by Knox (Grim, 1968, p. 515) and Winters and Simonsen (1951).

Two anomalies are apparent in Figure 11. First, although river sediments do show more scatter, they are on the whole more illitic than the basin sediments. Second, chlorite is very low in a number of river sediments, and lower on the average than in the basin sediments. The same pattern is displayed even better in the less than  $2\mu$  fraction, and its implications will be discussed. The less-than  $62\mu$  clay mineral fraction is not a particularly useful interval because it includes both silt and clay modes which were affected by somewhat different transportation and depositional processes. This problem does not occur in non-clay minerals because the quantity of these in the less than  $2\mu$  fraction is negligible. The average size-fraction mineralogy of basins and rivers is discussed in the section on geographic variations.

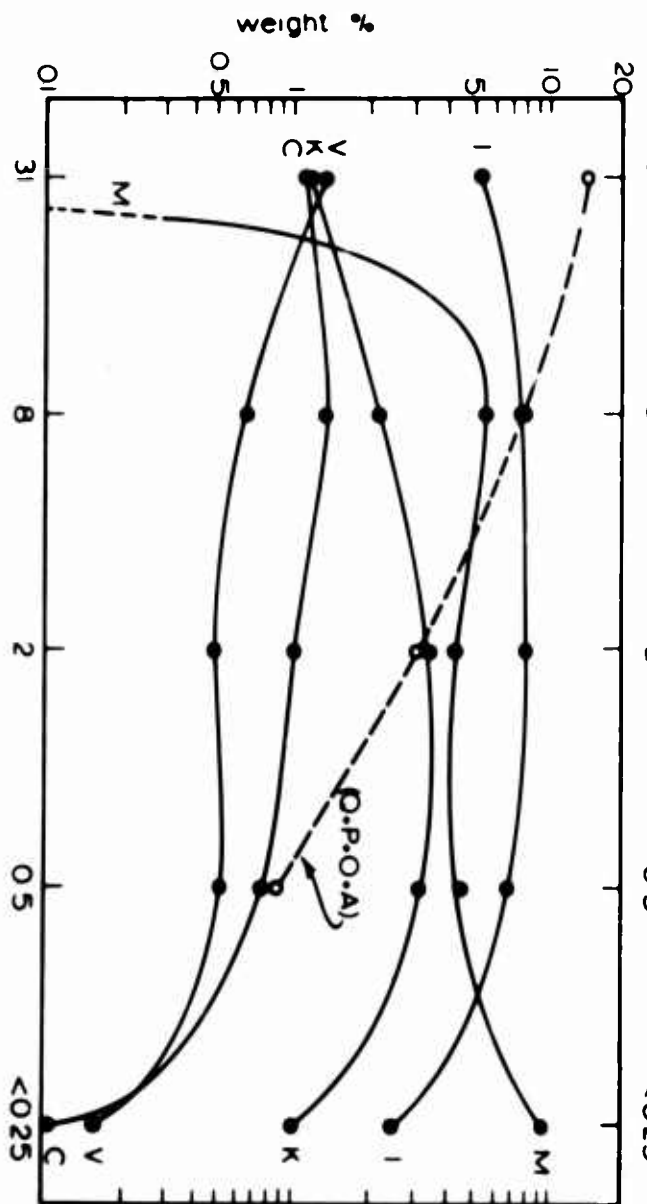
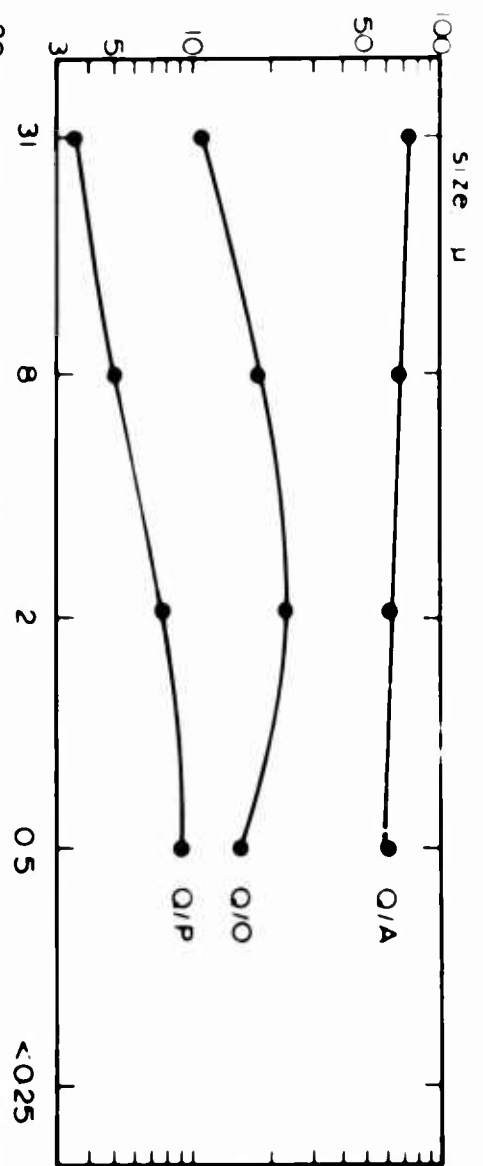
#### Effect of Particle Size on Mineral Distribution

A question which arises from the discussion of the mineralogic trends above is: To what degree does a shift in size distribution affect the mineral composition in a

given fraction? Or, put more generally, how does mineral composition vary with grain size? It is obvious from the work on this subject, including this study, that the non-clay minerals are more abundant in the silt sizes, whereas the clay minerals predominate in the clay sizes. Size ranges of clay particles are well-known, and can be rather extensive (Grim, 1968). Among studies in which minerals were quantitatively determined in size fractions (Mielenz and King, 1955; Gibbs, 1967b; Windom, 1969) including the present one, there is considerable variety in size distributions of individual minerals, both clay and non-clay. Source, weathering, and depositional process all influence these distributions, and for this reason no general relations for individual mineral distributions can be devised. However, even if mineral size-distributions are consistent for a given group of sediments, as they appear to be in this case (fig. 7), variations in the grain size distribution will affect the mineral composition of any given fraction because analysis requires a finite and often large size fraction. This size effect is generally ignored or only indirectly considered in many studies in which one or two size fractions of a sediment are analysed.

To investigate the grain-size effect in the basin sediments, average ratios and ratio percents of all basin samples were plotted for each mineral in the five fractions analysed (fig. 12). All minerals have essentially the same

Figure 12. Variation of minerals with particle size, basin sediments, California Continental Borderland. Q, quartz; P, plagioclase; O, K-feldspar; A, amphibole; I, illite; M, montmorillonite; K, kaolinite; C, chlorite; V, vermiculite.





mineral size-distributions; therefore, an average of all samples was used.

The proportions of clay minerals (fig. 12) are relatively constant between 0.5 and  $8\mu$ ; below  $0.5\mu$ , all decrease rapidly except montmorillonite, which increases. Above  $8\mu$ , only vermiculite increases; possibly this coarse vermiculite is altered biotite. The persistence of montmorillonite into the medium silts, and its absence in the coarse silt fraction, could be related either to a limit on montmorillonite aggregates or to a size limit on expandable illitic-montmorillonitic clays. The behavior of the clay ratios in sizes over  $2\mu$  is more erratic than below  $2\mu$ . For this reason, clay minerals of the coarse to medium silt fractions, and of the less than  $62\mu$  fraction, may be difficult to interpret and may obscure characteristics in the more distinctive less than  $2\mu$  fraction.

The non-clay minerals decrease steadily with grain size and are difficult to detect in sizes under  $0.5\mu$  (fig. 7). Quartz-plagioclase and quartz-K-feldspar ratios increase considerably with smaller particle sizes, indicating that the feldspars are less persistent into these sizes. This relationship explains the quartz-feldspar problem discussed above, and indicates that finer sediments will have higher quartz-feldspar ratios. Thus the basin sediments have higher quartz-feldspar ratios than the

coarser river sediments, and all of the less than 62  $\mu$  fraction quartz-feldspar ratios will be higher than those of beach and river sands.

Plagioclase and K-feldspar have essentially the same trend with size except in the 0.25 to 1  $\mu$  fraction, where K-feldspar increases. The increase is probably caused by a determinate error in the x-ray technique that becomes evident at very low concentrations. The quartz-amphibole ratio is almost constant, with a slight increase of amphibole in the finer sizes.

Causes for the variation of quartz, feldspar, and amphibole with grain size must be related to the size of the source material, degree of weathering, and to the minerals' resistance to corrosion and abrasion. Abrasion in the silt and clay sizes is insignificant (Pettijohn, 1957); therefore, the more rapid decrease of feldspar is probably caused by corrosion at the source or in transport. The persistence of relatively unstable amphibole may be related to abundant fine-grained amphibole in the source rock.

#### Less Than 2 Micron Minerals

##### General Aspects

The less than 2  $\mu$  fraction makes up from 30 percent to over 50 percent of the basin sediments; therefore, any

parameters determined for this fraction applies to the finer-grained half of the basin sediments. Conveniently, the bulk minerals of this fraction are all clay minerals, and the quantity of non-clay minerals is negligible (figs. 7, 8, 9). Therefore, a semiquantitative x-ray clay mineral analysis will give a close approximation of the total mineralogy of this fraction, and only the x-ray-amorphous material then remains an undetermined component. Large variation in x-ray-amorphous material could influence the pattern of clay mineral distribution. If it is assumed that there are no large variations in this component, the clay mineral distribution will not be affected.

Average less-than  $2\mu$  clay mineral percents are listed in Table 7. Unlike the total sediment (Table 5), where illite predominates, montmorillonite is the most abundant constituent in this fraction of the basin sediments. As in the total sediment, kaolinite, chlorite, and vermiculite are present in decreasing abundance. In the river sediments, illite remains the most abundant, and the order of abundance is the same as in the total sediment (Table 5).

The close similarity of composition is again displayed in the less than  $2\mu$  fractions of the basin sediments, with an average coefficient of variation of 16 percent, and a range from 3 to 29 percent. River sediments are considerably more varied, and have coefficients of

Table 7. Average less than 2 micron clay mineral ratio percents

Santa Monica Basin	37	47	3.3	4.2	8	30	4.3	35
Santa Barbara Basin	36	47	3.9	3.1	10	34	4.1	20
Santa Cruz Basin	34	49	3.0	4.2	10	31	4.1	31
Catalina Basin	37	45	2.5	6.5	9	25	3.3	38
Tanner Basin	36	46	3.1	4.6	11	33	4.8	41
Continental Rise	32	47	3.7	4.2	13	42	3.3	22
Santa Ynez River*	52	24	6.5	3.1	14	19	0.0	36
Gaviota Canyon	47	37	4.9	3.0	8	45	6.8	27
Ventura River	45	42	3.1	1.7	8	24	0.0	37
Ventura River*	60	18	5.6	3.1	12	33	5.1	24
Santa Clara River*	34	51	0.4	0.3	15	28	9.6	33
San Gabriel River	40	45	3.9	2.6	15	42	11.9	31
Santa Ana River	31	46	3.8	2.9	16	33	6.8	39
San Onofre Creek	48	34	2.1	0.2	16	27	18.3	29
Santa Margarita River	46	41	0.1	0.0	12	23	2.1	48
Ave., basins	35	47	3.2	4.5	10	32	4.0	31
Ave., rivers	45	38	3.4	1.9	12	30	6.7	34

Table 7. Average less than 2 micron clay mineral ratio percents (continued)

Coefficients of Variation, %	Illite		Montmor- illonite		Vermiculite		Chlorite		Kaolinite		Mixed-layer clay		K-fixable clay		Beidellite clay	
	Basins	Rivers	Basins	Rivers	Basins	Rivers	Basins	Rivers	Basins	Rivers	Basins	Rivers	Basins	Rivers	Basins	Rivers
	6	20	3	29	16	65	25	72	29	27	17	29	15	88	24	21

\* Suspended load, 1969 storm.

variation of 20 to 65 percent, with an average of 43 percent. The differences in scatter between basin and river sediments can be seen in Figure 11.

### Clay Minerals

Ternary diagrams in Figure 11 and Table 7 illustrate the relations of the important less-than  $2\mu$  clay mineral groups. These diagrams show a similar distribution as the clay minerals of the less-than  $62\mu$  fraction, but more clearly. Kaolinite and vermiculite contents of basin and river sediments are similar; however, illite is on the whole significantly more abundant in river sediments, whereas the basin sediments are higher in montmorillonite; and chlorite is also more abundant in the basin sediments. Three mechanisms could be invoked to explain this distribution and will be examined below. These are differential settling, diagenesis, and sources other than rivers which have been studied.

If differential flocculation is used as an explanation, it must in this case be applied to the river-ocean boundary area, since the problem above is not one of a gradient over the borderland, but a difference in sediment suites. Differential flocculation in brackish waters has been experimentally demonstrated (Whitehouse, Jeffrey, and Debbrecht, 1960) and observed in nature (Van Andel and Postma, 1954). These studies show that illite will floc-

culate and settle faster at low chlorinity than montmorillonite. Illite might thus be preferentially removed at the river mouths, whereas montmorillonite would be bypassed to the borderland. It is readily evident that this situation is unstable, and eventually illite would be flushed out of the river mouths and onto the borderland by a flood. The net effect would then be the same as if no brackish-water flocculation had occurred. As an alternative to this conclusion, one might assume that the flocculated illite is transported with the fine sand-coarse silt fraction. One would then expect higher illite concentrations on the shelf and possibly in turbidite sands. The fine fractions of coarse sediments were not investigated in this study; however, the current velocities required for sand transport are probably great enough to disperse any floccules and winnow out the finer illite.

Another problem raised by differential settling is that with this process, the other clay minerals should behave similarly to illite since their settling velocities are much closer to illite than montmorillonite (Whitehouse, Jeffrey, and Debbrecht, 1960), and this is not the case.

Diagenesis must be considered as a possible cause of chlorite enrichment in basin sediments. Preferential adsorption of  $Mg^{++}$  onto clay minerals has been experimentally demonstrated (Whitehouse and McCarter, 1958; Carroll and Starkey, 1960) and observed in nature (Powers,

1957, 1959). In most cases, diagenetic changes appear to be minor, and consist of reconstitution of degraded illite, chlorite or vermiculite, and of formation of some mixed-layering. True authigenic chlorite has been observed forming from gibbsite near Hawaii (Swindale and Fan, 1967; Moberly, Kimura, and McCoy, 1968). Tidelands soils in the San Francisco Bay area which have been drained for 60 years show chlorite destruction, which seems to indicate authigenic chlorite of marine origin (Lynn and Whittig, 1966).

The apparent dilution of illite and enrichment of montmorillonite, on the other hand, is contradictory to the diagenetic behavior of these minerals in sea water. The abundance of illite in the oceans is well known, particularly in the North Atlantic and North Pacific (Biscaye, 1965; Griffin, Windom, and Goldberg, 1968). Illite has been believed to be diagenetic in origin, as an alteration from montmorillonite (Milne and Early, 1958; Johns and Grim, 1958); and the reconstitution of illite by potassium uptake from sea water, has also been considered an important process (Grim, Dietz, and Bradley, 1949; Whitehouse and McCarter, 1958; Weaver, 1967). However, potassium-argon ages of marine illites are on the order of several hundred million years (Hurley and others, 1963; Krylov and Tedrow, 1963); therefore, authigenic and reconstituted illites must comprise only a small part, if



any, of the illite in the oceans. The distribution of illite in the oceans also suggests detrital sources rather than diagenesis. Thus, even though illite may not be forming in the oceans today, it appears to be stable in sea water by observation; and it is also stable by thermodynamic considerations (Garrels and Christ, 1965). For these reasons, diagenesis cannot be invoked to explain enrichment of illite in the basin sediments.

Montmorillonite, on the other hand, has been shown to be forming in the ocean (Griffin and Goldberg, 1963; Peterson and Griffin, 1964; Moberly, Kimura, and McCoy, 1968), but is always related to areas of oceanic volcanism and low terrigenous sedimentation. In the case of the California Continental Borderland, it is doubtful if enough unaltered volcanic material reaches the basins to account for the montmorillonite enrichment by diagenesis.

Another approach to the problem of chlorite enrichment and illite dilution in basin sediments is to examine more carefully the sources studied and to consider other sources beyond the borderland perimeter. In the case of the illite-montmorillonite problem, it is worth noting that the three rivers which have the same proportions of illite and montmorillonite as the basins are the Santa Ana, Santa Clara, and San Gabriel Rivers (fig. 11). These rivers are most centrally located with respect to the section of the borderland studied (fig. 1), and have large

drainage areas and discharges (Table 8). It is therefore possible that the mineral suites of these rivers dominate in the basin sediments and thus at least partly explain this problem.

Sediment from areas beyond the perimeter of the borderland could be transported in by two currents. One of these is the California Current, which sweeps along the North American continental margin from Alaska to Mexico (Emery, 1960). Most of the California Current bypasses the borderland, but a part of the current enters in the south and sweeps over it in a large counter-clockwise eddy (Emery, 1960); another portion of the current enters Santa Barbara basin from the west (R. L. Kolpack, oral communication).

Clay mineral suites along the North Pacific coast are largely illite-chlorite-montmorillonite. Off southeast Alaska, chlorite and illite predominate (Griffin and Goldberg, 1963); further south, off Oregon, chlorite, montmorillonite, and illite are most abundant (Duncan, Kulm, and Griggs, 1970). If these clay suites are present in the borderland, they would be most readily indicated by a net increase in chlorite. Illite and montmorillonite would not be appreciably affected because they are present in large amounts on the borderland. In fact, montmorillonite might be expected to dominate over illite in the California Current because of its abundance off the coast

Table 8. Drainage areas and discharges of southern California rivers (from U. S. Geol. Survey Water-Supply Paper 1735)

	Drainage Area		Average		Years Discharge Data Available
	sq mi	sq mi	Annual Discharge Acre- Feet/Yr	Hectare- Meters/Yr	
Santa Ynez River	2320	895	13,700	3710	13
Gaviota Canyon	39*	15*	-	-	-
Ventura River	545	210	16,000	4320	33
Santa Clara River	4410*	1700*	33,100	8950	8
San Gabriel River	1440	557	8590	2320	30
Santa Ana River	6460	2490	4070	1100	20
San Onofre Creek	109	42	340	93	14
Santa Margarita River	1920	740	8500	2300	37

\* Planimetrically determined.

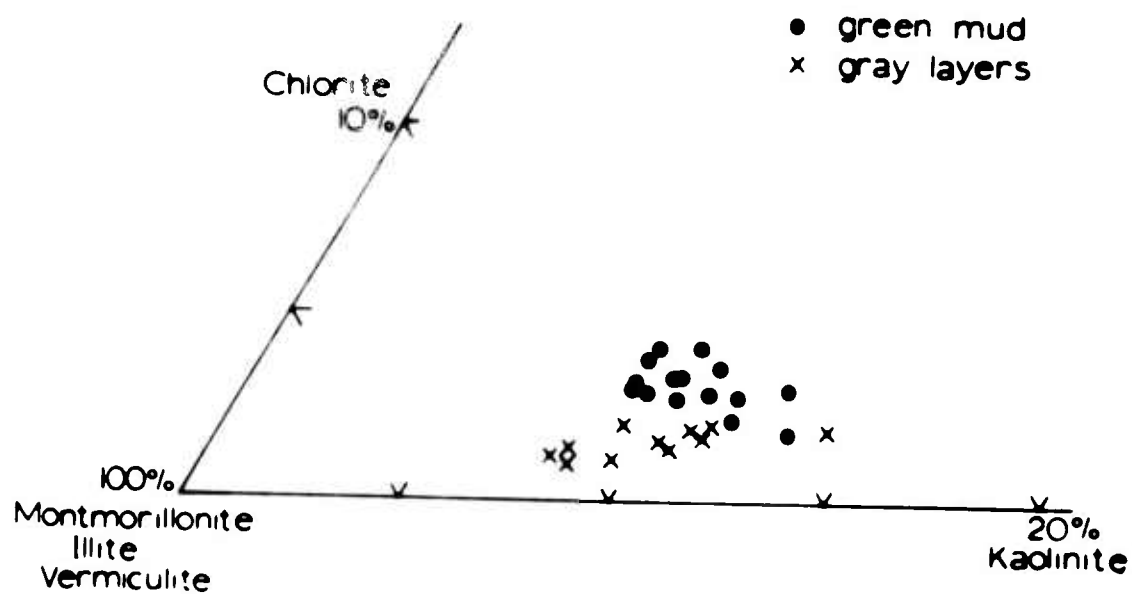
of the northwestern United States, and because it has a lower settling velocity than illite or chlorite.

Chlorite enrichment by this process can be demonstrated in Santa Barbara Basin. Here laminated green hemipelagic mud alternates with gray silt layers that are almost entirely local river sediments deposited during storms (fig. 2) (see following section). The average chlorite content of the gray layers is 1.6 percent, whereas the green mud contains 3.1 percent chlorite on the average, nearly twice as much (fig. 13); but still less than the other basins. The small quantities of chlorite in the gray layers suggests that the chlorite enrichment in the basins is not due to diagenesis. River sediments from the perimeter of Santa Barbara Basin contain an average of 1.9 percent chlorite, and it is unlikely that diagenesis would affect only the green mud and not the thin gray layers. The fact that even the green mud contains less chlorite than the other basin sediments also suggests enrichment from the California Current; sedimentation rates in the other basins studied are lower than in Santa Barbara Basin (Emery, 1960), and a greater California Current contribution would be expected.

The amount of the California Current contribution can be estimated from the chlorite content of sediments derived from the North Pacific coast. Off Oregon, the chlorite content of marine and river sediments averages

Figure 13. Less than 2 $\mu$  clay mineral composition diagram of Santa Barbara Basin sediments, showing chlorite enrichment of green, laminated mud as compared to rapidly deposited gray silt layers of local origin.

CLAY MINERAL RATIO PERCENTS  
 < 2 microns  
 SANTA BARBARA BASIN



25 percent (Duncan, Kulm, and Griggs, 1970). If the California Current carries this proportion of chlorite, the total sediment contribution from this source to Santa Barbara Basin, assuming a 1.5 percent chlorite enrichment, would amount to 7 percent. A very small portion of the chlorite may be derived from streams entering the borderland south of Santa Barbara Basin; however, sediments from these sources do not contain enough chlorite to cause significant enrichment in Santa Barbara Basin.

Another supplier of clay minerals to the borderland may be Southern water, which moves into the borderland at intermediate depths (Emery, 1954). Although information on clay minerals off Mexico and Central America is scant, montmorillonite apparently increases along the east equatorial Pacific margin (Griffin, Windom, and Goldberg, 1968). Thus, any contribution from Southern water would be mainly montmorillonite. The effects, if any, of this source cannot be delineated, and would be minor owing to less runoff from Central America.

#### Expandable Clays

##### Mixed-Layer Clays

Ratio percents of expandable mixed-layer clays in the total less-than  $2\mu$  clay mineral fraction, as determined by the method of Schultz (1964) average about 31 percent; and range from 19 percent to 45 percent for basin

and river sediments (Table 7). As with the other clay minerals, the basin sediments exhibit much less variation than the river sediments. A ternary diagram of mixed-layer clays, montmorillonite, and illite (fig. 14) shows the enrichment of montmorillonite in the basin sediments, but no trend as regards the mixed-layer clays. There is no evidence that diagenesis is affecting this component; neither a decrease that might result from reconstitution of degraded illite, nor an increase by alteration of montmorillonite as proposed by Whitehouse and McCarter (1958). It should be recalled here that the clays were analysed in a magnesium-saturated state; this treatment may destroy superficial diagenetic alterations such as Whitehouse and McCarter found in their experimental work.

#### Potassium-Fixable and Beidellitic Clays

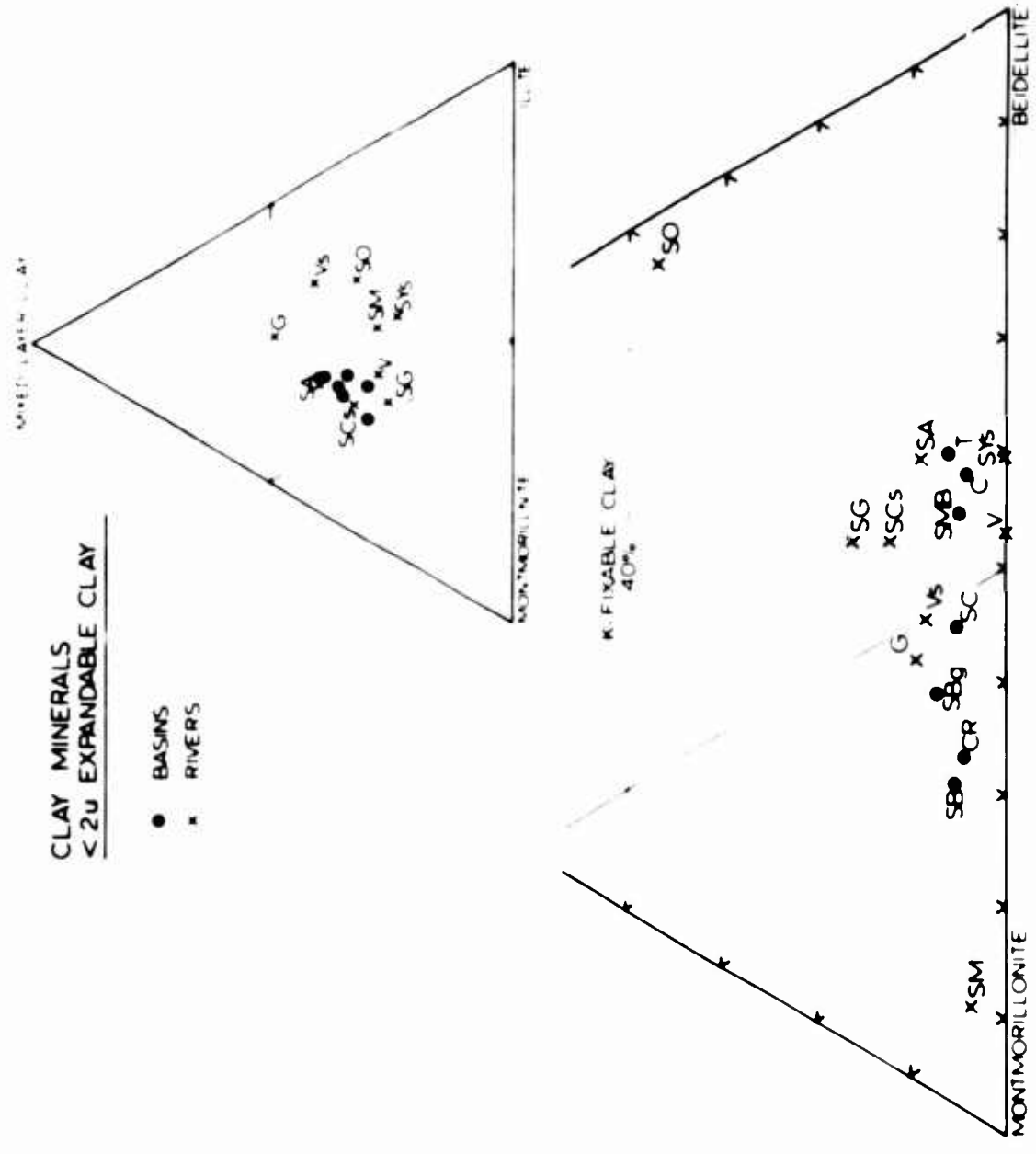
Some potassium fixation of the expandable clays can be achieved in both basin and river sediments (Table 7). On the average, about 7 percent of the total less than  $2\mu$  clay fraction of the river sediments, and 4 percent of the basin sediments can be made to contract irreversibly by this method. The exact quantity of fixation depends to a degree on the treatment, but the relative proportions give a clue to the effectiveness of this process. The degree of potassium-fixing in the basin sediments is fairly uniform; but the rivers show appreciable variation, from zero to 18



Figure 14. Less than 2 $\mu$  clay mineral composition diagrams of expandable clays for average basin and river sediments. SMB, Santa Monica Basin; SB, Santa Barbara Basin, green mud; SBg, Santa Barbara Basin, gray layers; SC, Santa Cruz Basin; C, Santa Catalina Basin; T, Tanner Basin; CR, continental rise. SYS, Santa Ynez River, suspended load; G, Gaviota Canyon; V, Ventura River; Vs, Ventura River, suspended load; SCs, Santa Clara River, suspended load; SG, San Gabriel River; SA, Santa Ana River; SO, San Onofre Creek; SM, Santa Margarita River.

CLAY MINERALS  
< 2μ EXPANDABLE CLAY

- BASINS
- × RIVERS



percent. From these figures, it appears that some potassium-fixation, presumably reconstitution of degraded illite, occurs when the sediment enters the ocean, probably rather quickly (Weaver, 1956). Quantitatively, this process appears to be minor, and would result in a net increase of illite under 10 percent. This result is in agreement with the idea that diagenetic illite is relatively unimportant in recent marine sediments (Griffin, Windom, and Goldberg, 1968).

About one-third of the total less-than  $2\mu$  clay-mineral fraction consists of "beidellitic" montmorillonite (beidelite, nontronite, saponite, and related minerals) as determined by lithium-glycerol treatment (Green-Kelly, 1953). Basin and river sediments contain equal amounts of this material with equal degrees of variability (Table 7). Although the results must be considered tentative because of the large errors in the technique, they suggest that the beidellitic montmorillonite is inherited and unaffected by diagenesis.

A ternary diagram of potassium-fixable clay, beidellitic clay, and montmorillonite (fig. 14) indicates that the degree of potassium fixing poses a limit on the proportion of beidelite. Since the determinations of potassium fixing and beidelite are not necessarily mutually exclusive, this relation suggests that a part of the potassium-fixable clay is "beidelite." Beidelite and the

trioctahedral montmorillonites carry most of their charge deficiency in the tetrahedral layer, as does illite; therefore potassium fixing would be easier to accomplish with these clays than with true montmorillonite, which carries its charge deficiency in the octahedral layer. It is likely that some of the beidellite-like material is degraded biotite, as this material would also have potassium-fixing properties.

By plotting mixed-layer clay, potassium-fixable clay, and beidellitic clay, phases which again are not mutually exclusive, essentially the same distribution is obtained as when montmorillonite is included. This suggests that the expandable mixed-layer clays are found with no preference among all expandable components.

### Geographic Distribution of Minerals

#### Rivers

##### Drainage

The mainland drainage areas on the perimeter of the borderland are by far the most important suppliers of sediments to the basins. Island sources and the California Current contribution are detectable, but quantitatively are minor. Similarly, wind-transported sediment from the Mojave and Colorado Deserts comprises a minor contribution, but is difficult to resolve because of its similarity to

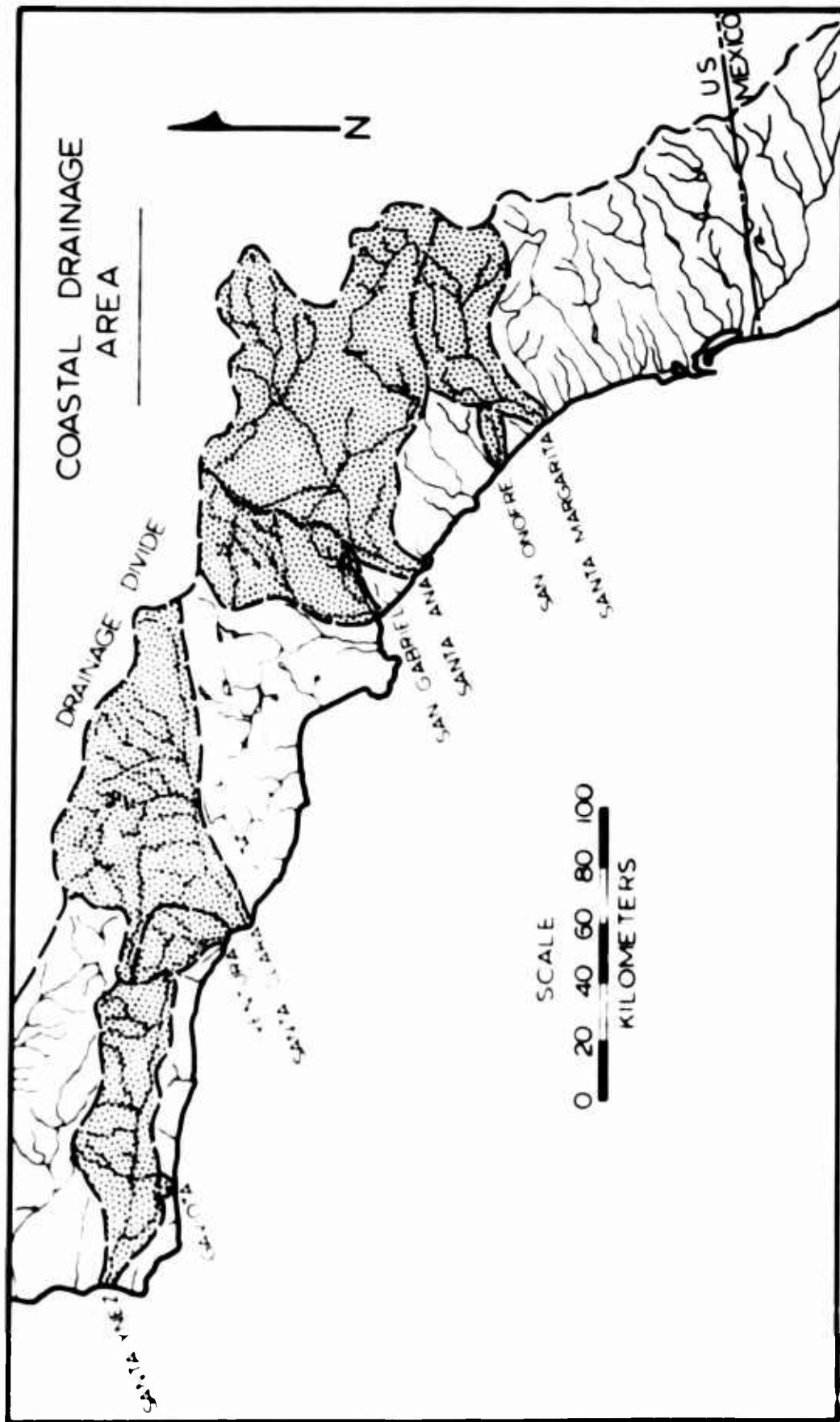
other sediment.

The total Pacific drainage area facing the borderland (fig. 15) is about 34,000 km<sup>2</sup>; with a total discharge of 185,000 hectare-meters (Gorsline, 1968). Discharges of the major drainage basins have been measured for the last 20 to 30 years, but are almost useless in comparing drainage basins because approximately one-half of the drainage area in southern California is controlled by dams, spreading basins, and irrigation diversion (Norris, 1964). Comparative estimates of sediment discharges are therefore better reflected by drainage areas rather than by present-day discharges (Table 8).

Estimates of total sediment discharge for southern California (Point Conception to the Mexican border) are 5 million tons by Emery (1960) who used depositional rates in the borderland; and 10 million tons by Handin (1951), who worked with silting rates of reservoirs. Total suspended-sediment discharge has been estimated at 3.5 million tons by Rodolfo (1964) on the basis of Los Angeles, San Gabriel, and Santa Ana River runoffs. Of this figure, 2.7 million tons were estimated to consist of silt, clay colloids, and dissolved matter.

Four rivers, the Santa Ana, Santa Clara, Los Angeles, and San Gabriel Rivers drain over one-half of the area facing the northern borderland. To the South, the Tia Juana, Santa Margarita, and San Luis Rey Rivers are the

Figure 15. Coastal drainage area, southern California. Stippling indicates drainage areas of rivers sampled.



major suppliers. To the north, the Santa Ynez River, just north of Point Conception, probably has an appreciable quantity of its suspended load carried into the borderland by the California Current.

### Lithology

The Pacific drainage of southern California is in parts of the Transverse and Penninsular Range provinces. Their complex structural relations and heterogeneous lithologies have been summarized by Bailey and Jahns (1954) and Jahns (1954).

The western Transverse Range are an east-west trending anticlinal structure that extends eastward from Point Arguello to Castaic, a distance of 100 miles. The Santa Ynez Mountains make up the narrow western part of the structure and parallels the coast for 80 miles. The Topatopa and Piru Mountains continue inland, and comprise the wider eastern portion of this structure. These three ranges contain almost exclusively Cretaceous to Quaternary clastic sediments; mainly continental and marine sandstones, mudstones, and shales of early to middle Tertiary age. In the northeastern part of these mountains, Mesozoic granitic rocks and older schists and gneisses are exposed. A few small outcrops of Franciscan serpentines are located in the western part, and Miocene basaltic and andesitic volcanics are scattered sparsely throughout the



ranges.

The Santa Monica Mountains, and their westward extension, the Channel Islands, are an anticlinal structure similar, and parallel to the Santa Ynez-Topatopa Mountains. Early and middle Tertiary sediments and basaltic volcanics make up the western part of the Santa Monica Mountains; slate and granitic rocks are exposed in the eastern part.

The eastern Transverse Ranges consist of the Libre Mountains, the Sierra Pelona, and the extensively faulted horsts of the San Gabriel and San Bernardino Mountains. These Ranges are composed of a large variety of crystalline rocks; schists, gneisses, and granitic igneous rocks. A gabbroic complex composed of anorthosite and other basic rocks is located in the western part of the San Gabriel Mountains. Metamorphosed Paleozoic sediments, including marble, occur in the San Bernardino Mountains.

The southern California portion of the Peninsular Range Province includes a group of southeast-northwest trending ranges that, taken together, present a rough, asymmetric cross-sectional profile with a gentle western slope. The San Jacinto-Santa Rosa Mountains form the high, fault-bounded eastern ridge of the province; and extending southward, the Santa Ana, Agua Tibia, and Laguna Mountains form the somewhat lower central and western part of the

province.

gabbroic to granitic rocks, primarily tonalites and granodiorites, of the Mesozoic California Batholith. A variety of metamorphic rocks, older than the batholith, are widespread but subordinate in quantity. Upper Cretaceous to Quaternary marine and continental clastic sediments are exposed in the Santa Ana Mountains on the coastal terraces in the vicinity of Oceanside and San Diego.

#### Mineralogy of River Sediments

Mineralogy of silts and clays from eight rivers draining into the continental borderland was determined in this study. Drainage areas, discharges, and locations are shown in Figure 15 and Table 8. A representative sampling of drainage areas was obtained, and all major rivers except the Los Angeles River were sampled. Sediments of the Santa Ynez River, Gaviota Creek, and Ventura River are derived mainly from the sedimentary rocks of the Santa Ynez Mountains; and the Santa Clara River carries a sedimentary suite with some metamorphic and igneous components from the Topatopa and Piru Mountains. The San Gabriel River drains the igneous-metamorphic complex of the San Gabriel Mountains. Both the Transverse and Peninsular Range provinces are drained by the Santa Ana River which derives a mixed igneous-metamorphic suite from the San Bernardino, San Jacinto, and Santa Ana Mountains. San

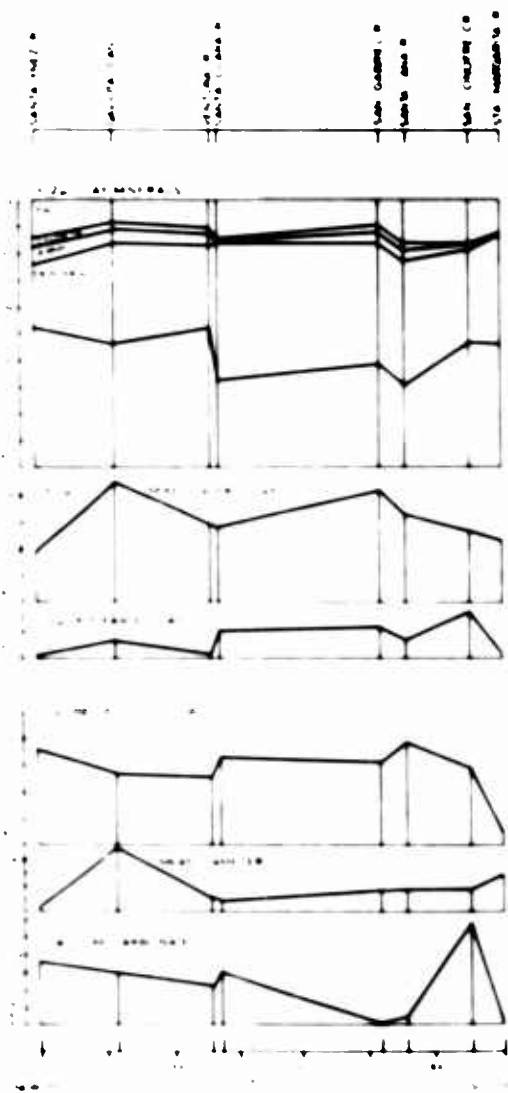
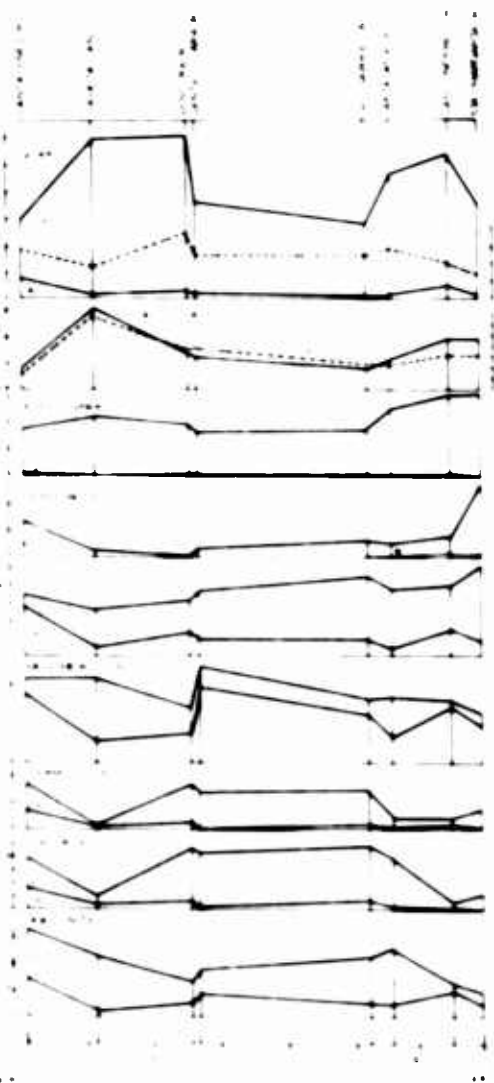
Onofre Creek drains coastal sediments and some batholithic terrain, and the Santa Margarita River carries a largely batholithic suite with a subordinate sedimentary component.

Except for a few analyses by Fan (1963) and Rodolfo (1964), no information is available on the mineral composition of fine-grained sediments from southern California rivers. The mineralogy of river sands has been examined by Gorsline (1968), and the mineralogy of southern California beach sands is well-known (Handin, 1951; Trask, 1952, 1955; Azmon, 1960; Emery, 1960).

Mineral percents, less-than  $2\mu$  clay mineral ratios, calcium carbonate, and mean diameters of river sediments are plotted in relative geographic position in Figure 16. Examination of histograms of river sediments (figs. 8, 9) show that the mineralogy of the silt fraction is strongly influenced by the size modes of the sediment, particularly by the sand fraction. For this reason, mean diameter must be considered when interpreting compositional variations in these sediments.

Quartz and feldspar show similar geographic variations. Both are low in Santa Clara and San Gabriel Rivers, and higher in the northern and southern rivers. Quartz-feldspar ratios are a little lower in the southern portion, but are generally erratic. Plagioclase-K-feldspar ratios decrease southward, but are again higher in the two

Figure 16. Mineral profiles of southern California river silts and clays.



southern rivers. The quartz and feldspar compositions reflect the stable mineralogy of the sedimentary sources in the north, the metamorphic and igneous terrain of the central area, and the batholithic terrain in the south. Similarly, the southward decrease of plagioclase-K-feldspar ratios shows the influence of igneous and metamorphic sources. Decreasing quartz-feldspar ratios and increasing plagioclase-K-feldspar ratios in the southern rivers result from the intermediate igneous rocks of the batholith. A more detailed survey of river sand-mineralogy by Gorsline (1968) shows similar trends.

Amphibole increases southward from the Ventura River; it serves as an indicator of the increasingly crystalline nature of the terrain in that direction.

Among the clay minerals, discrepancies exist between percentages and ratios, and between the less-than  $2\mu$  and the 2 to  $62\mu$  fractions. Silt-size chlorite and vermiculite is higher in the central area and is probably of metamorphic origin. The same minerals, however, show a less well-defined opposing trend in the less-than  $2\mu$  clay mineral ratios percents. Kaolinite in the silt and clay fractions exhibits a similarly inconsistent behavior. Illite and montmorillonite, on the other hand, behave uniformly in the silt and clay fractions. Coarse "montmorillonite" and fine illite are more abundant in the northern area, and fine montmorillonite and coarse illite

dominate in the central and southern areas. Total illite increases northward; total montmorillonite increases southward.

Inconsistencies between the silt and clay fractions lead to the conclusions that the clay minerals of these fractions are of different origin. The silt-size clay minerals doubtless represent igneous and metamorphic detritus, whereas the less than 2  $\mu$  clays are probably products of weathering and diagenesis. Thus the abundance of coarse illite, chlorite, and vermiculite is related to muscovite, chlorite, and biotite in the crystalline rocks of the central and southern areas. Fine-grained illite and coarse "montmorillonite" reflect diagenesis and alteration in the sediments of the northern area; but higher fine-grained montmorillonite in the central and southern areas must result from weathering of the less stable crystalline rocks.

Potassium-fixability of the less-than 2  $\mu$  clays increases to the south, probably as a result of more degradation of the igneous and metamorphic micas than for the sedimentary micas. Beidellitic montmorillonite is somewhat lower in the northern area; as discussed above, some of this material may represent degraded biotite, and much of it is probably derived from weathering of ferromagnesian silicates. Expandable mixed-layer clays show no consistent variation among these rivers.

Calcium carbonate generally decreases southward, and is apparently derived from sedimentary rocks.

### Basins

#### General Aspects

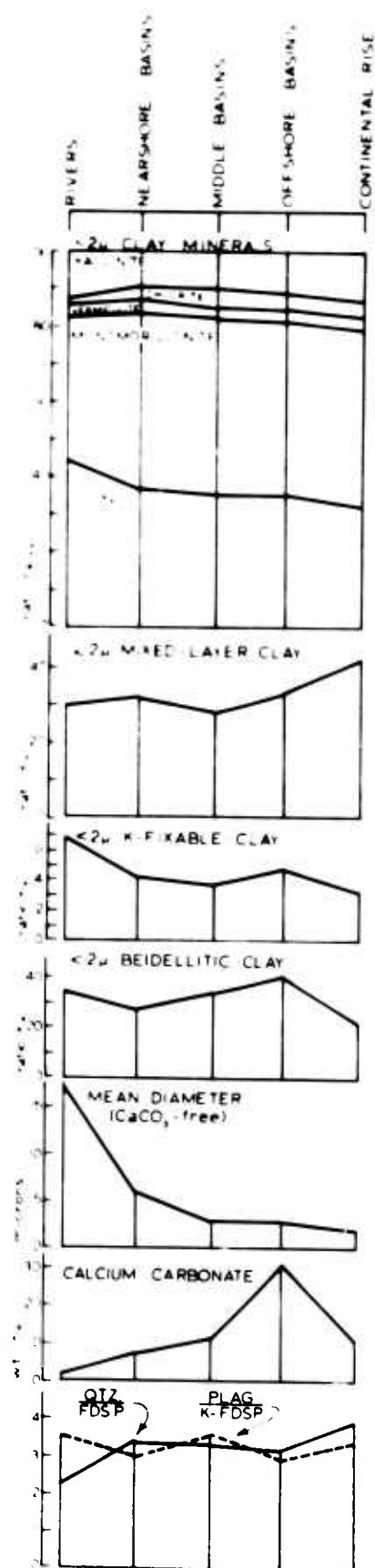
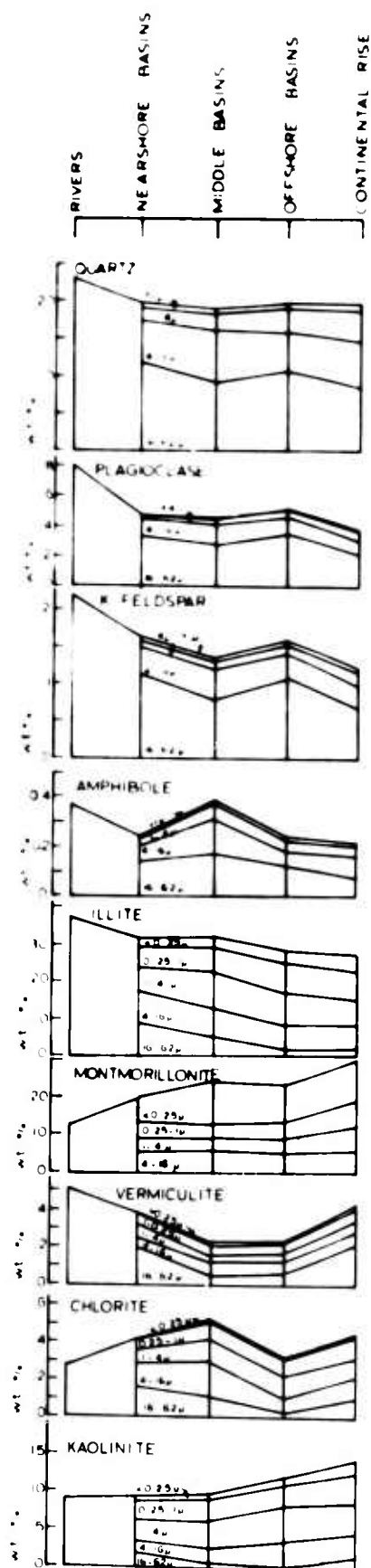
Average mineralogic and sedimentary parameters of borderland sediments are plotted as a function of distance from the mainland in Figure 17. Sedimentary parameters for depositional environments of the borderland have been presented in this manner by Emery (1960). The divisions used here, rivers, nearshore, middle, and offshore basins, and the continental rise are similar, but not identical, with the divisions used by Emery.

Mean diameter of the carbonate-free sediments decreases offshore in a way similar to the total sediment size as shown by Emery (1960). The curve is smoother because the effect of increasing coarse biogenic carbonate offshore has been eliminated. Tanner Basin sediments are still slightly coarser, due to the turbidite influx from Santa Rosa-Cortez Ridge.

Calcium carbonate reaches a maximum in the outer basins, and drops sharply on the continental rise. The offshore increase in carbonate is largely the result of a decreasing terrigenous sedimentation rate, although an increase in biologic activity offshore contributes to this trend (P. W. Barnes, oral communication). The drop in



Figure 17. Variation of mineralogy with distance from shore. Nearshore basins, Santa Barbara and Santa Monica Basins; Middle basins, Santa Catalina and Santa Cruz Basins; Offshore Basins, Tanner Basin.



carbonate on the rise is caused by solution in the deeper and colder waters, and by a reduced sedimentation rate, which allows longer exposure of carbonates to solution before burial.

#### Non-Clay Minerals

The non-clay minerals, quartz, feldspars, and amphibole all show a general decrease in quantity offshore (fig. 17). This trend is a product of the medium and coarse silts, and implies current transportation from the mainland. Quartz-feldspar ratios increase offshore; this is in part a result of decreasing grain sizes, but also related to high quartz-feldspar ratios on the Santa Rosa-Cortez Ridge. Plagioclase-K-feldspar ratios, on the other hand, show no consistent variation over the borderland.

Higher concentrations of quartz and feldspar in the silt fractions of Tanner Basin reflect the turbidite components from Santa Rosa-Cortez Ridge, and high amphibole in the middle basins is due to Santa Catalina Basin sediment, which is derived in part from the metamorphic rocks of Santa Catalina Island.

It is of interest to examine here the influence of eolian transport on the basin sediments. For this purpose, the non-clay silicates are most suitable in this area because of their presence in the silt fraction, which

also seems to be the dominant size range for eolian sediment. Quartz in particular is a good indicator because of its stability, detrital nature, and continental origin. Rex and Goldberg (1958) found quartz concentrations of about 15 percent in the East Pacific, with highest concentrations in a belt at  $30^{\circ}$  N Lat. The mean diameter of this material is about  $5\mu$ . Rex and others also found quartz in Hawaiian soils; most of this quartz is between 2 and  $10\mu$ . The illite distribution in the Pacific is similar to the quartz distribution (Griffin, Windom, and Goldberg, 1968). Both are coincident with the mid-latitude jetstream, and there is little reason to doubt their eolian origin. Windom (1969) attempted to show that all of the greater-than  $2\mu$ , and 50 percent of the less-than  $2\mu$  nonbiogenic sediment in the North Pacific is eolian. Bramlette and Arrehenius (1965) consider a sub-bottom reflecting layer off northern Mexico to be of eolian origin on the basis of a medium silt size and a quartz-feldspar composition. Its age of over 40,000 years suggests periods of high eolian transport during the Pleistocene.

Eolian quartz of the North Pacific is derived from three sources, Asia, North America, and a global component. The mid-latitude jetstream carries the Asian dust in a wide band across the central Pacific (Griffin, Windom, and Goldberg, 1968). Dust from the North American deserts

is frequently carried over the East Pacific by Santa Ana winds that are active when the North Pacific high moves over western North America. Bonatti and Arrhenius (1965) attribute the eolian silt off northern Mexico to these winds. Dust often collects on ships passing by the California coast when Santa Ana winds are blowing according to Emery (1960) who concluded from these observations that North America is the dominant source of eolian sediment in the East Pacific, and constitutes a significant portion of the sediment. Global dust, as defined by Windom (1969), is probably insignificant off North America.

Examination of the quartz (fig. 17) profile reveals that the total quantity of quartz remains at about 20 percent over the borderland because of an increase of less-than  $4\mu$  quartz. The feldspars show a similar but much weaker trend. The offshore increase of fine silt- and clay-sized quartz appears to be caused by an eolian component. If current transport were the only process responsible, a shift to finer sizes offshore would result in a relative increase of fine quartz, but would be accompanied by an quantitative decrease. A true offshore increase of fine quartz implies an enriching process, in this case the emergence of eolian sedimentation as the quantity of current-transported sediment drops off.

The eolian component on the borderland, and even on the continental rise, is minor compared to the central

Pacific because of much higher sedimentation rates of current-transported sediment. Windom (1969) has shown that dust accumulations on snowfields are seldom over  $0.1 \text{ mg/cm}^2/\text{yr}$ , even where local sources are important, whereas the terrigenous sedimentation rate on the Continental Rise is about  $3.3 \text{ mg/cm}^2/\text{yr}$  (Emery, 1960). Thus the eolian component may amount to only 3 percent on the rise; and even when assuming much higher fallout rates from Santa Ana winds, it is unlikely that the eolian component exceeds 10 percent to 15 percent on the outer borderland. Nearer to the coast eolian accumulation may be several  $\text{mg/cm}^2/\text{yr}$  (Emery, 1960), but current-transported sedimentation rates are proportionately higher.

#### Clay Minerals

As previously demonstrated, clay minerals in the basin sediments are derived from nearby mainland sources, and in small part from the California Current. From the estimates above, wind-transported clay also appears to be minor, but adequate mineralogic data on eolian sediments are not available. The clay mineral distribution on the borderland must therefore be related mainly to source areas and transport processes, especially segregation by differential flocculation and settling.

Settling rates in sea water for a number of clay minerals have been determined by Whitehouse, Jeffrey, and

Debbrecht (1960). They found that illite and kaolinite settle at about 15.8 and 11.8 m/day, respectively, and montmorillonite at 1.3 m/day. Chlorite settles somewhat faster than kaolinite, and vermiculite slightly faster than illite. Concentration does not affect the order of settling appreciably, but mixtures may result in intermediate rates.

Differential settling seems to be most readily observed in deltaic and estuarine environments; for instance, on the Niger Delta (Porrenga, 1966), and in the Gulf of Paria (Van Andel and Postma, 1954). On the Niger Delta, effects were found 80 km from the river mouth, the limit of the area sampled, and along the shelf. Whitehouse, Jeffrey, and Debbrecht (1960) have shown that above 15 ppt chlorinity, settling rates in sea water are almost constant; therefore, material that escapes flocculation at the initial fresh water-sea water mixtures continues to settle differentially in the ocean at the same rate. Work in the Gulf of Mexico (Pinsak and Murray, 1960) indicates some differential settling of montmorillonite on the abyssal plain, and increasing kaolinite offshore in northeastern parts of the Gulf of Mexico (Griffin, 1962) may also be caused by differential settling in the open ocean. On the other hand, such differential settling has not been found in the northern Adriatic Sea (Brambati, 1968), possibly, however, because the area sampled was too small.

An examination of clay mineral variation over the borderland reveals several coincident trends in the total mineralogy and in the less-than 2  $\mu$  clay mineral ratios (fig. 17). Most significant are illite and montmorillonite because they make up 70 percent of the less-than 2  $\mu$  fraction and over 50 percent of the total sediment.

Illite decreases offshore when measured as a less-than 2  $\mu$  fraction and in the total sediment over 1  $\mu$ . In the less-than 1  $\mu$  fraction, it increases slightly. Montmorillonite increases offshore when measured by both approaches, and the increase is restricted to the clay size-ranges. These trends strongly suggest that appreciable quantities of montmorillonite are deposited further offshore than illite. The slight absolute increase of illite in the finer clay sizes may be due to montmorillonite-like settling rates of this illite, or it may reflect the eolian component.

Kaolinite (fig. 17) also increases offshore when examined by percentage of ratio. Since kaolinite settles more slowly than other clay minerals except montmorillonite, it appears that this trend is also caused by differential settling. Chlorite and vermiculite fluctuate considerably in the coarser fractions, which implies variability caused by local sources; in the finer sizes, they appear to remain fairly constant over the borderland. In this case, the influx of chlorite from the California



Current is great enough to mask or reverse the differential settling effect on chlorite.

Expandable mixed-layer clays tend to increase offshore, whereas potassium-fixable clays decrease (fig. 17). Although trends might suggest diagenetic processes, they may also be caused by differential settling. The expandable mixed-layer clays are basically montmorillonitic, and the potassium-fixable clays illitic, therefore they might be expected to behave similarly to montmorillonite and illite, as they do. Beidellitic montmorillonite may also increase offshore like montmorillonite, but fluctuates too much to reveal a trend.

## CORE MINERALOGY

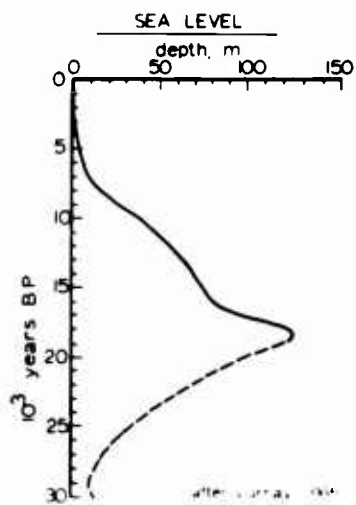
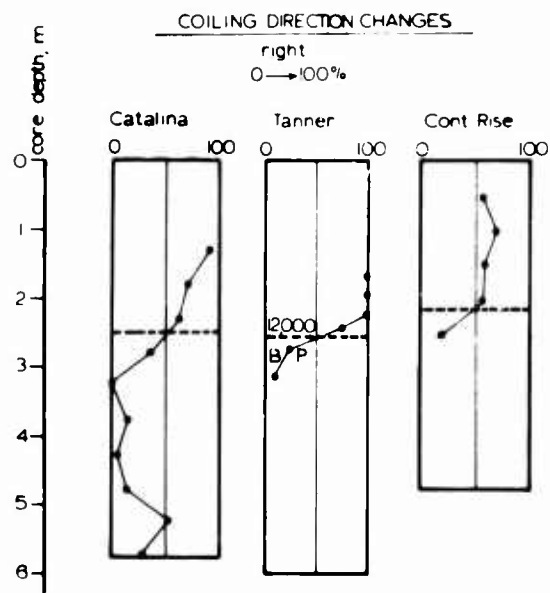
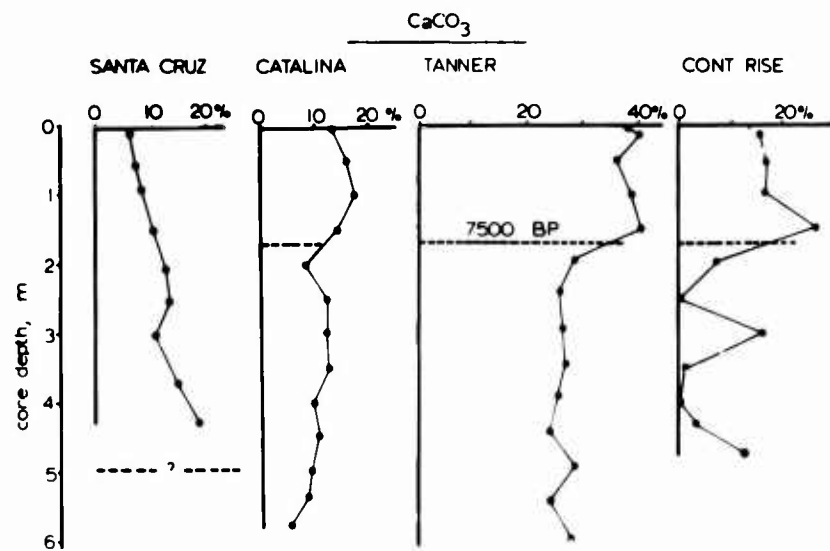
## Correlation of Cores

The cores collected in Santa Cruz, Santa Catalina, and Tanner Basins, and on the continental rise, cover sufficient time spans to allow correlation by carbonate-content stratigraphy and by Globigerina pachyderma coiling ratios. On the basis of these correlations, it is then possible to determine the mineral distribution in the middle and outer California Continental Borderland basins since the late Pleistocene.

The Pleistocene-Holocene boundary in the borderland has been based on a change in coiling direction in the planktonic foraminifer Globigerina pachyderma. In water colder than 8°C, this organism grows a left-coiling test, and above 8°C, a right-coiling test (Bandy, 1960). On the borderland, warming water at the end of the Pleistocene resulted in a change in coiling direction from left to right. The coiling change has been dated with radio-carbon techniques at 12,000 BP (Emery and Bray, 1962).

Coiling ratios were determined in the Santa Catalina Basin, Tanner Basin, and continental rise cores. The Pleistocene-Holocene boundary in these cores, based on identical quantities of left- and right-handed forms, is at a depth of 250, 260, and 220 cm, respectively (fig. 18).

Figure 18. Carbonate content and coiling directions of Globigerina pachyderma in California Continental Borderland cores with time markers established by Gorsline, Drake, and Barnes (1968) and Emery and Bray (1962). Late Quaternary sea level fluctuation after Curray, 1965.



A minor reversal occurs near the bottom of the Santa Catalina Basin core and may correspond to an earlier warm period in the Wisconsin; a similar trend was reported by Gorsline, Drake and Barnes (1968) in Tanner Basin. In the core from the rise, the change to right-handed coiling is incomplete, probably due to inclusion of Pleistocene forams through slumping and reworking of the sediment.

A second stratigraphic marker in the borderland is a sharp increase of calcium carbonate in the Holocene that was apparently caused by an increase of productivity. The inflection point at the base of the high-carbonate sediment has been radiocarbon-dated at 7500 BP in Tanner Basin (Gorsline, Drake, and Barnes, 1968), which places it at the beginning of the Hypsithermal. This marker is located at approximately 170 cm in the Santa Catalina Basin, Tanner Basin, and continental rise cores (fig. 18).

In the Santa Cruz Basin core, the carbonate increase is not present; instead, carbonate decreases upward in the core (fig. 18). This trend is characteristic of post-Hypsithermal sections of other cores. A detailed study of carbonate stratigraphy in Santa Cruz Basin by P. W. Barnes (oral communication) has shown this trend to be consistent in a large number of cores. From comparison with these cores, it appears that the core used here penetrates all but the base of the high-carbonate sediment. The age of the bottom of this core is therefore

close to 7000 years BP.

The late Pleistocene carbonate stratigraphy of the borderland has not been studied in detail, and correlation in the Pleistocene sections of the cores must be considered tentative. The Santa Catalina and Tanner Basin cores appear to span equal amounts of time. By extrapolating the 90-cm sediment thickness of the 4500 yr Pleistocene-Hypsithermal interval to the Pleistocene sections of these cores, the core bottoms have an age of 28,000 to 29,000 yr (fig. 18).

Correlation of the continental rise core is more difficult, because of its disturbed nature, and because of extensive solution of calcium carbonate in the Pleistocene section. Solution was undoubtedly caused by the lower temperature of the water during the Pleistocene. Increasing carbonate at the base of the core may be due to warming of water during a warm interval in the Wisconsin. Using the same sedimentation rates as for the other cores, an age of 25,000 yr is obtained for the core bottom.

#### Pleistocene Sea Level

Sea level fluctuation is an important, if not the predominant factor in understanding Pleistocene-Holocene sedimentation on the borderland. A review of work on Pleistocene sea levels by Curray (1969) shows some agreement on a low sea-level stand 15,000 or 18,000 BP, and high

sea level around 25,000 to 30,000 BP (fig. 18). On the basis of the above correlations, a complete high-low-high sea level cycle is therefore covered in three of the cores.

There is general agreement that the last low sea-level stand was at 100 to 130 m (Curry, 1969). A sea-level drop of this magnitude has considerable effect on the bathymetry and oceanography of the borderland. Figure 19 shows the extent of subaerial and wave-base exposure that would result from a 100 m drop in sea level. It is apparent from the paleobathymetry that offshore banks, especially Santa Rosa-Cortez Ridge, must have been significant sediment sources for the outer basins and the continental rise. It may also be inferred that circulation was restricted, increasing the importance of local sources by reducing the mainland contribution to offshore areas. Uplift and subsidence may also have played a role in the paleobathymetry, but there is little data on the degree to which this process was effective.

#### Grain-Size Parameters

Mean diameters of carbonate-, organic-, and iron oxide-free sediments (fig. 20) increased to the present in all but the Santa Catalina Basin core, where there is some indication of decreasing grain size. Variation in mean diameter is minor. It is caused in large part by the fine

Figure 19. Pleistocene low sea level, 18,000 BP; map shows areas exposed to erosion and locations of cores penetrating Pleistocene sediments.



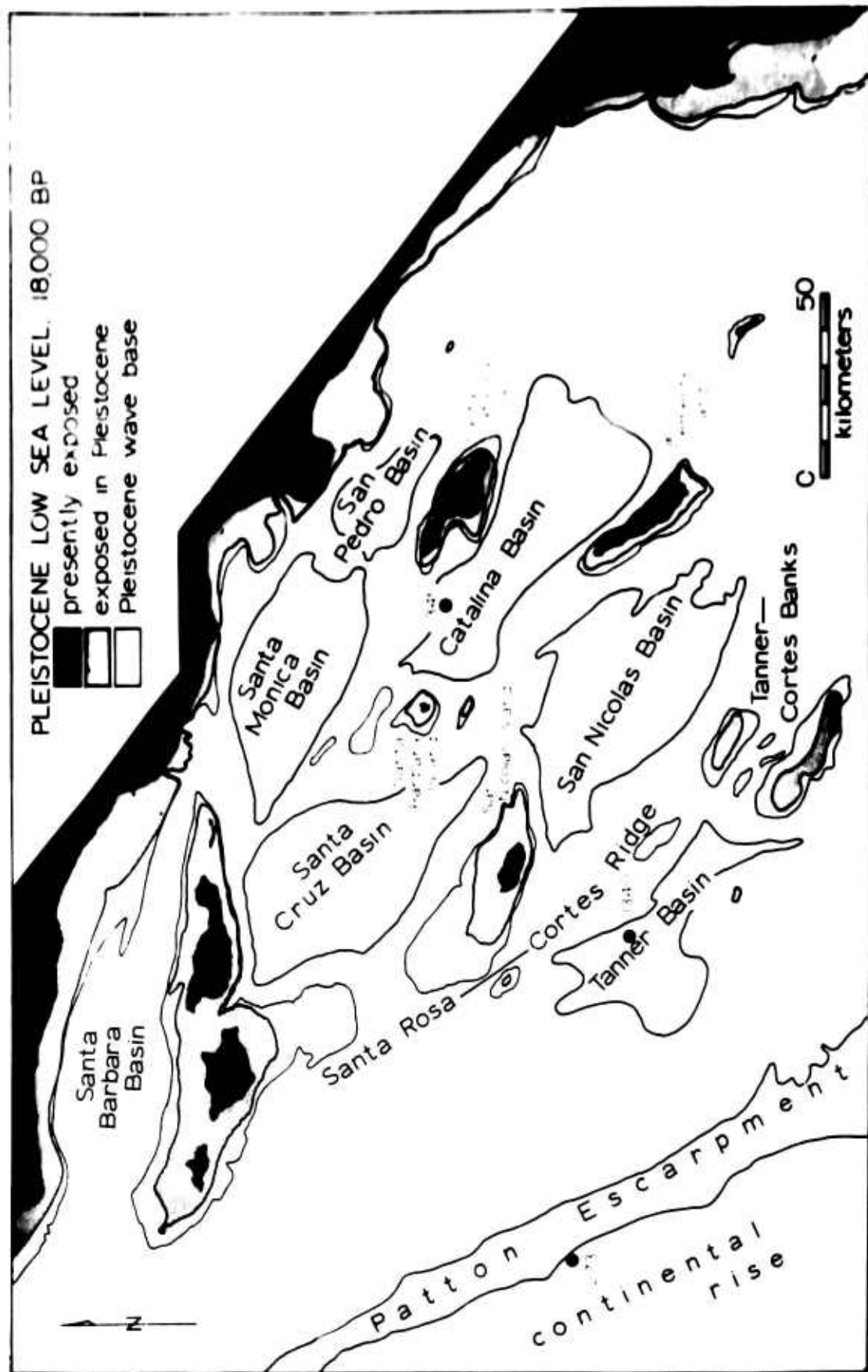
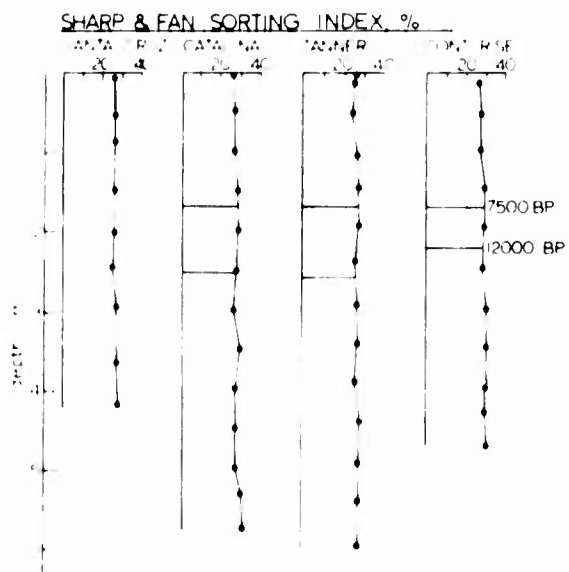
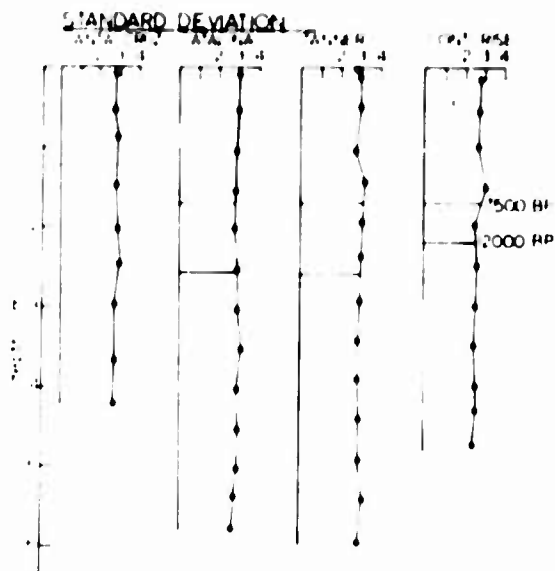
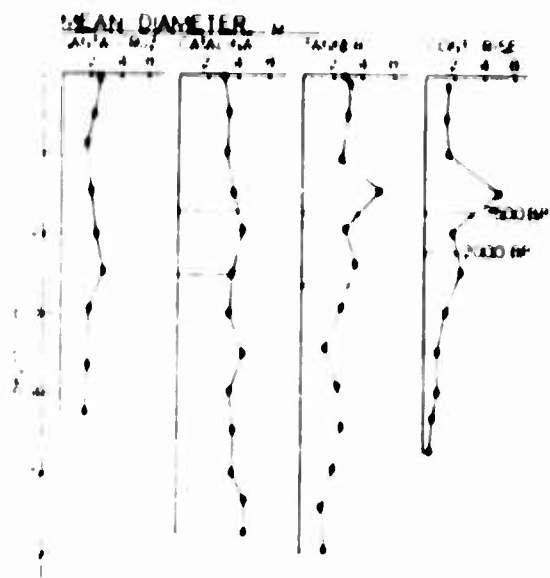


Figure 20. Mean diameter, standard deviation,  
and Sharp and Fan sorting index of  
cores from California Continental  
Borderland basins (carbonate-free).



sand-coarse silt tail of the distribution which also accounts for the two apparently coarser samples in the Tanner Basin and continental rise cores. This effect obscures small shifts in mean diameter of the body of the distribution. For this reason, mean diameter does not appear to be a particularly useful parameter in these sediments. Similarly, sorting (fig. 20) varies even less.

### Silt Mineralogy

#### Non-clay Minerals

Two characteristics of non-clay mineral distributions within the cores are apparent in Figures 21 and 22. First, most of the variation is in the coarse and medium silt fractions. Second, these minerals exhibit varying trends in different basins. Quartz and feldspar trends are similar, but the amphibole pattern does not seem to be related to these. Although there is considerable range of compositional variation in the coarse silts, these trends are not nearly as evident in variation of mean diameter. Thus they are more related to changes in sediment sources and supply than to grain size. The diversity of patterns among these cores implies that the silt fractions of these minerals are derived mainly from local sources.

In the Tanner Basin and continental rise cores, quartz and feldspar are low in the Pleistocene sections, and increase at about the time of the last sea level rise.

Figure 21. Quartz and amphibole size-fraction weight-percents; cores plotted on time scale.

SEE FIG. 10-11, 12, 13, 14, 15, 16, 17, 18, 19, 20, 21, 22, 23, 24, 25, 26, 27, 28, 29, 30, 31, 32, 33, 34, 35, 36, 37, 38, 39, 40, 41, 42, 43, 44, 45, 46, 47, 48, 49, 50, 51, 52, 53, 54, 55, 56, 57, 58, 59, 60, 61, 62, 63, 64, 65, 66, 67, 68, 69, 70, 71, 72, 73, 74, 75, 76, 77, 78, 79, 80, 81, 82, 83, 84, 85, 86, 87, 88, 89, 90, 91, 92, 93, 94, 95, 96, 97, 98, 99, 100, 101, 102, 103, 104, 105, 106, 107, 108, 109, 110, 111, 112, 113, 114, 115, 116, 117, 118, 119, 120, 121, 122, 123, 124, 125, 126, 127, 128, 129, 130, 131, 132, 133, 134, 135, 136, 137, 138, 139, 140, 141, 142, 143, 144, 145, 146, 147, 148, 149, 150, 151, 152, 153, 154, 155, 156, 157, 158, 159, 160, 161, 162, 163, 164, 165, 166, 167, 168, 169, 170, 171, 172, 173, 174, 175, 176, 177, 178, 179, 180, 181, 182, 183, 184, 185, 186, 187, 188, 189, 190, 191, 192, 193, 194, 195, 196, 197, 198, 199, 200, 201, 202, 203, 204, 205, 206, 207, 208, 209, 210, 211, 212, 213, 214, 215, 216, 217, 218, 219, 220, 221, 222, 223, 224, 225, 226, 227, 228, 229, 230, 231, 232, 233, 234, 235, 236, 237, 238, 239, 240, 241, 242, 243, 244, 245, 246, 247, 248, 249, 250, 251, 252, 253, 254, 255, 256, 257, 258, 259, 260, 261, 262, 263, 264, 265, 266, 267, 268, 269, 270, 271, 272, 273, 274, 275, 276, 277, 278, 279, 280, 281, 282, 283, 284, 285, 286, 287, 288, 289, 290, 291, 292, 293, 294, 295, 296, 297, 298, 299, 300, 301, 302, 303, 304, 305, 306, 307, 308, 309, 310, 311, 312, 313, 314, 315, 316, 317, 318, 319, 320, 321, 322, 323, 324, 325, 326, 327, 328, 329, 330, 331, 332, 333, 334, 335, 336, 337, 338, 339, 340, 341, 342, 343, 344, 345, 346, 347, 348, 349, 350, 351, 352, 353, 354, 355, 356, 357, 358, 359, 360, 361, 362, 363, 364, 365, 366, 367, 368, 369, 370, 371, 372, 373, 374, 375, 376, 377, 378, 379, 380, 381, 382, 383, 384, 385, 386, 387, 388, 389, 390, 391, 392, 393, 394, 395, 396, 397, 398, 399, 400, 401, 402, 403, 404, 405, 406, 407, 408, 409, 410, 411, 412, 413, 414, 415, 416, 417, 418, 419, 420, 421, 422, 423, 424, 425, 426, 427, 428, 429, 430, 431, 432, 433, 434, 435, 436, 437, 438, 439, 440, 441, 442, 443, 444, 445, 446, 447, 448, 449, 450, 451, 452, 453, 454, 455, 456, 457, 458, 459, 460, 461, 462, 463, 464, 465, 466, 467, 468, 469, 470, 471, 472, 473, 474, 475, 476, 477, 478, 479, 480, 481, 482, 483, 484, 485, 486, 487, 488, 489, 490, 491, 492, 493, 494, 495, 496, 497, 498, 499, 500, 501, 502, 503, 504, 505, 506, 507, 508, 509, 510, 511, 512, 513, 514, 515, 516, 517, 518, 519, 520, 521, 522, 523, 524, 525, 526, 527, 528, 529, 530, 531, 532, 533, 534, 535, 536, 537, 538, 539, 540, 541, 542, 543, 544, 545, 546, 547, 548, 549, 550, 551, 552, 553, 554, 555, 556, 557, 558, 559, 560, 561, 562, 563, 564, 565, 566, 567, 568, 569, 570, 571, 572, 573, 574, 575, 576, 577, 578, 579, 580, 581, 582, 583, 584, 585, 586, 587, 588, 589, 590, 591, 592, 593, 594, 595, 596, 597, 598, 599, 600, 601, 602, 603, 604, 605, 606, 607, 608, 609, 610, 611, 612, 613, 614, 615, 616, 617, 618, 619, 620, 621, 622, 623, 624, 625, 626, 627, 628, 629, 630, 631, 632, 633, 634, 635, 636, 637, 638, 639, 640, 641, 642, 643, 644, 645, 646, 647, 648, 649, 650, 651, 652, 653, 654, 655, 656, 657, 658, 659, 660, 661, 662, 663, 664, 665, 666, 667, 668, 669, 670, 671, 672, 673, 674, 675, 676, 677, 678, 679, 680, 681, 682, 683, 684, 685, 686, 687, 688, 689, 690, 691, 692, 693, 694, 695, 696, 697, 698, 699, 700, 701, 702, 703, 704, 705, 706, 707, 708, 709, 710, 711, 712, 713, 714, 715, 716, 717, 718, 719, 720, 721, 722, 723, 724, 725, 726, 727, 728, 729, 730, 731, 732, 733, 734, 735, 736, 737, 738, 739, 740, 741, 742, 743, 744, 745, 746, 747, 748, 749, 750, 751, 752, 753, 754, 755, 756, 757, 758, 759, 760, 761, 762, 763, 764, 765, 766, 767, 768, 769, 770, 771, 772, 773, 774, 775, 776, 777, 778, 779, 780, 781, 782, 783, 784, 785, 786, 787, 788, 789, 790, 791, 792, 793, 794, 795, 796, 797, 798, 799, 800, 801, 802, 803, 804, 805, 806, 807, 808, 809, 810, 811, 812, 813, 814, 815, 816, 817, 818, 819, 820, 821, 822, 823, 824, 825, 826, 827, 828, 829, 830, 831, 832, 833, 834, 835, 836, 837, 838, 839, 840, 841, 842, 843, 844, 845, 846, 847, 848, 849, 850, 851, 852, 853, 854, 855, 856, 857, 858, 859, 860, 861, 862, 863, 864, 865, 866, 867, 868, 869, 870, 871, 872, 873, 874, 875, 876, 877, 878, 879, 880, 881, 882, 883, 884, 885, 886, 887, 888, 889, 890, 891, 892, 893, 894, 895, 896, 897, 898, 899, 900, 901, 902, 903, 904, 905, 906, 907, 908, 909, 910, 911, 912, 913, 914, 915, 916, 917, 918, 919, 920, 921, 922, 923, 924, 925, 926, 927, 928, 929, 930, 931, 932, 933, 934, 935, 936, 937, 938, 939, 940, 941, 942, 943, 944, 945, 946, 947, 948, 949, 950, 951, 952, 953, 954, 955, 956, 957, 958, 959, 960, 961, 962, 963, 964, 965, 966, 967, 968, 969, 970, 971, 972, 973, 974, 975, 976, 977, 978, 979, 980, 981, 982, 983, 984, 985, 986, 987, 988, 989, 990, 991, 992, 993, 994, 995, 996, 997, 998, 999, 1000

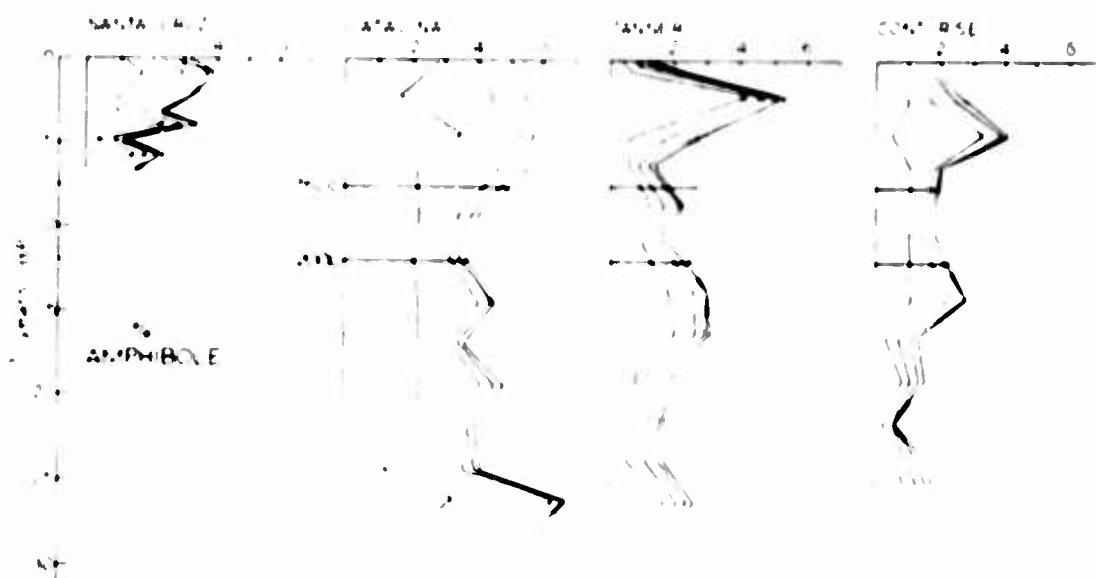
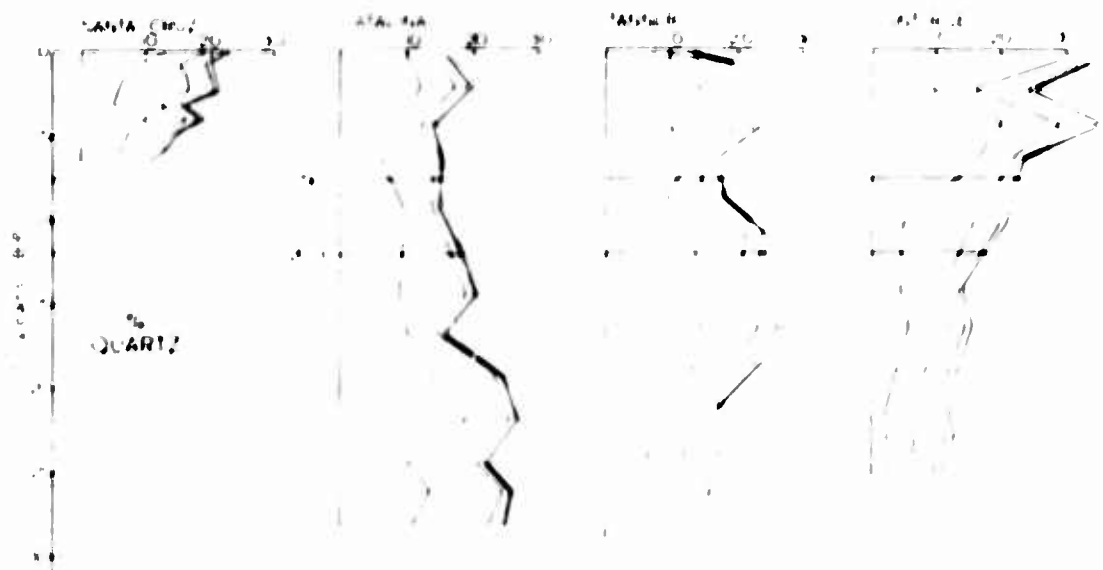
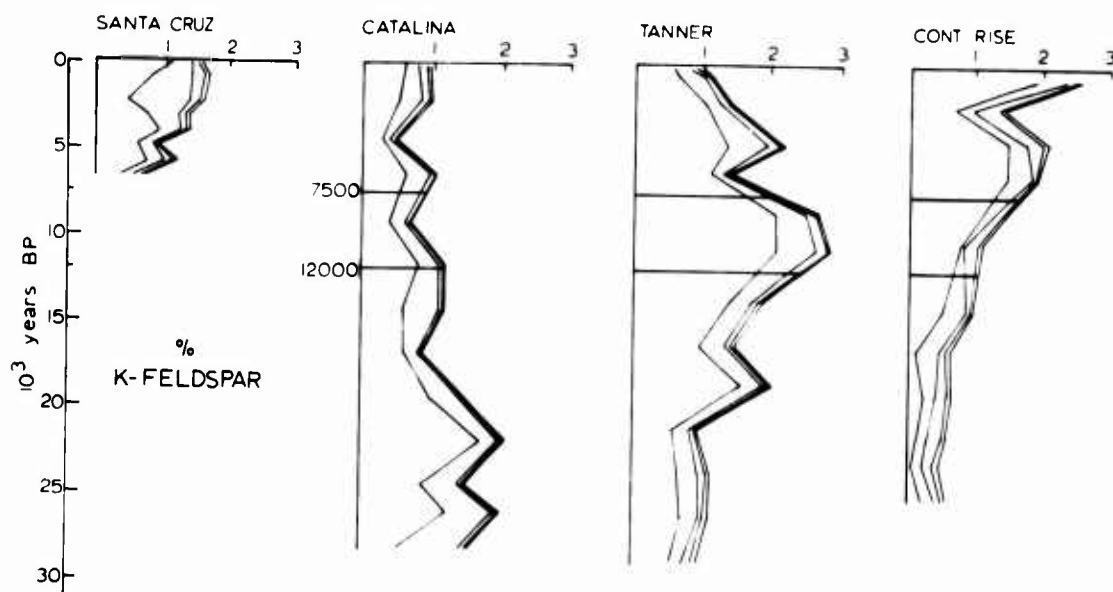
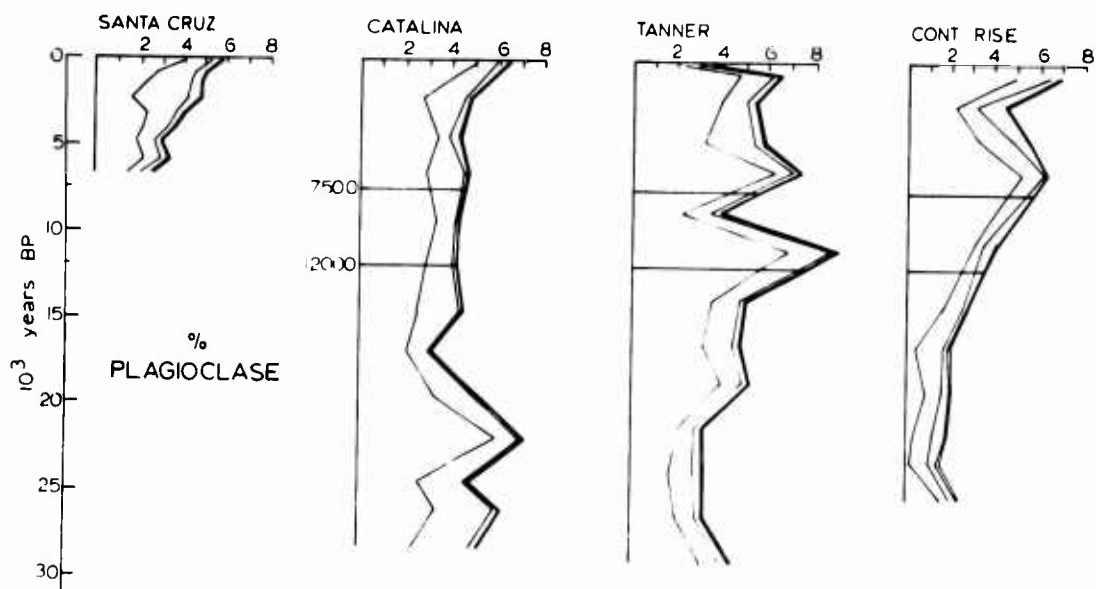


Figure 22. Plagioclase and potassium feldspar  
size-fraction weight-percents;  
cores plotted on time scale.

size fractions $\mu$			
62-16	16-4	4-1	<1



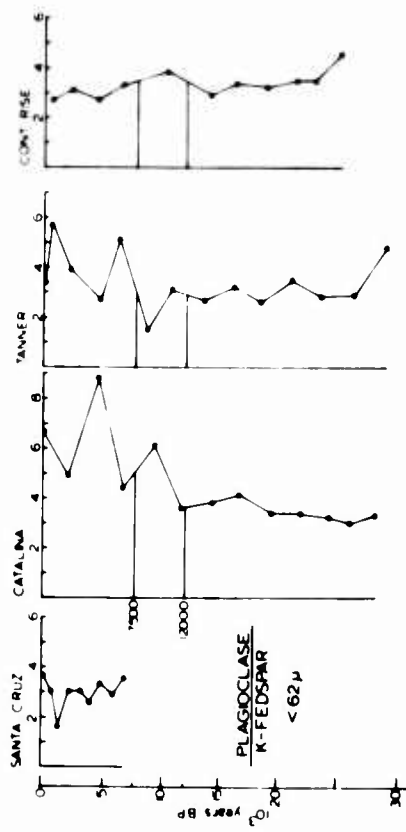
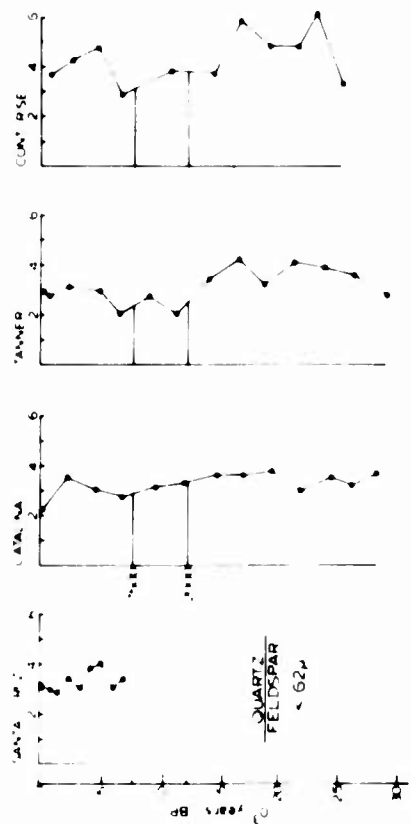
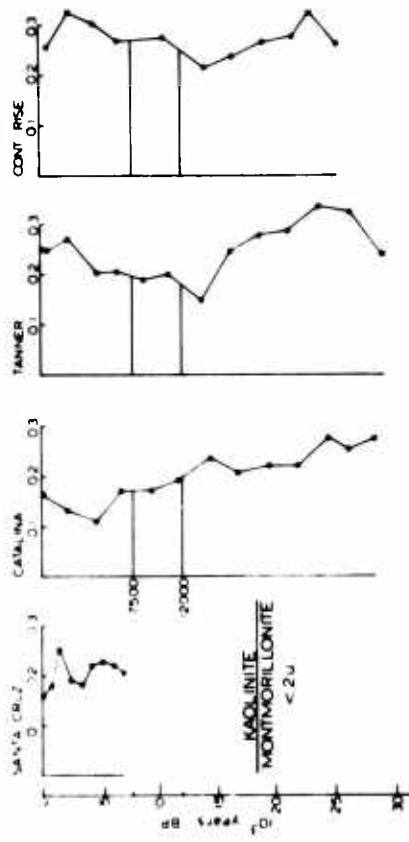
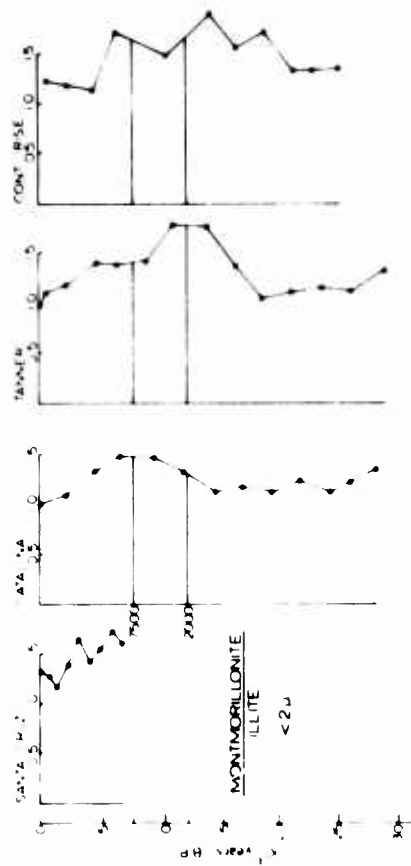


In the Holocene sections, these minerals generally remain high; and in Santa Cruz Basin they have increased to the present. Amphibole shows a similar but less well-defined trend in these three cores.

Quartz-feldspar ratios in the Tanner Basin and rise cores (fig. 23) correlate well with sea level, and were high during the last low sea-level stand. The source of the low-feldspar sediment is doubtless the Santa Rosa-Cortes Ridge, which is underlain by Miocene sediments, where quartz-feldspar ratios of sands are about 6 (Emery, 1960). Sand on the Tanner-Cortes Banks to the southeast, on the other hand, has a very low quartz-feldspar ratio of 0.17, probably as a result of outcrops of Miocene basalts (Holzman, 1952). Plagioclase-K-feldspar ratios seem to be somewhat lower during low sea level. This may also be related to the ridge mineralogy, but plagioclase-K-feldspar ratios on the ridge are not known.

That the Santa Rosa -Cortes Ridge is an important sediment source for Tanner Basin, and was even more important during the Pleistocene, is evidenced by the frequency of turbidite sands. Sand layers are more abundant in the Pleistocene sediment, and increase in the direction of the ridge (Gorsline, Drake, and Barnes, 1968). The core used in this study also contains a higher proportion of sand layers in the Pleistocene section (fig. 2).

Figure 23. Quartz-feldspar, plagioclase-K-feldspar, montmorillonite-illite, and kaolinite-montmorillonite ratios; cores plotted on time scale.



#### Mineral constituents of northern Santa Catalina

Basin sediments are derived mainly from pre-Tertiary metamorphic rocks of Catalina Island via Catalina Submarine Canyon; and from Miocene volcanics of Santa Barbara Island and shelf to the north. At low sea level, the volcanic suite would be expected to become more important because of increased exposure. Exposure of the metamorphic rocks, however, has not varied much because of the steep scarps along Santa Catalina Island (fig. 1).

The effect of changing sources is displayed among the non-clay minerals by amphibole (fig. 21). Being of predominantly metamorphic origin, amphibole is most abundant at times of high sea level when it is not diluted by the volcanic suite. Quartz and feldspar do not show this trend as clearly since their origin is not unique, and the increase of these minerals near the bottom of the core may not be directly related to either source. The high plagioclase-K-feldspar ratios in the upper portion of the core (fig. 23) are clearly related to Santa Catalina Island, which contributes a plagioclase-rich suite. The absence of high plagioclase-K-feldspar ratios in the lower section of the core, and the increase in quartz and feldspar, may indicate that a third, possibly sedimentary source may have been important at that time.

### Clay Minerals

The clay mineral distribution in the cores must be considered in two ways. Clay minerals of the medium and coarse silt fractions are primarily of local origin like the non-clay minerals; but for clay minerals in the fine fractions, long-distance transport as a significant factor must be considered.

Coarse clay minerals (figs. 24 and 25) on the whole have trends that are opposite to those of the non-clay minerals. Particularly the two most abundant constituents, illite and montmorillonite, are present in inverse abundance to the non-clays. There is a slight general decrease of most clay minerals since the Pleistocene in the Tanner Basin and continental rise cores; and in the Holocene of the Santa Cruz Basin core, all clay minerals decrease toward the top.

Trends in the Santa Catalina Basin core are more complex. The chlorite distribution follows the sea level curve like amphibole, and increases with high sea level. Like amphibole, the chlorite reflects the metamorphic suite from Santa Catalina Island.

Vermiculite, which is found primarily in the coarse fractions, is prominent in the Holocene section of the Santa Catalina Basin core, and in the upper Pleistocene of the continental rise core. Since this mineral probably consists in large part of altered biotite, it can be

Figure 24. Montmroillonite and illite size-  
fraction weight-percents; cores  
plotted on time scale.

size fractions $\mu$				
62.5	16.4	4.1	1.0	<0.25

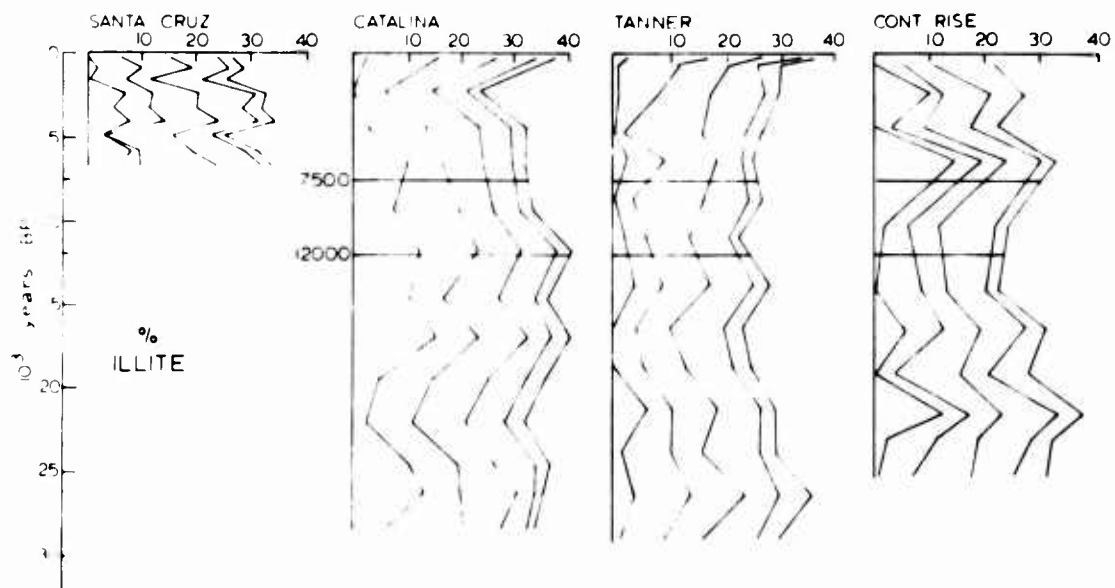
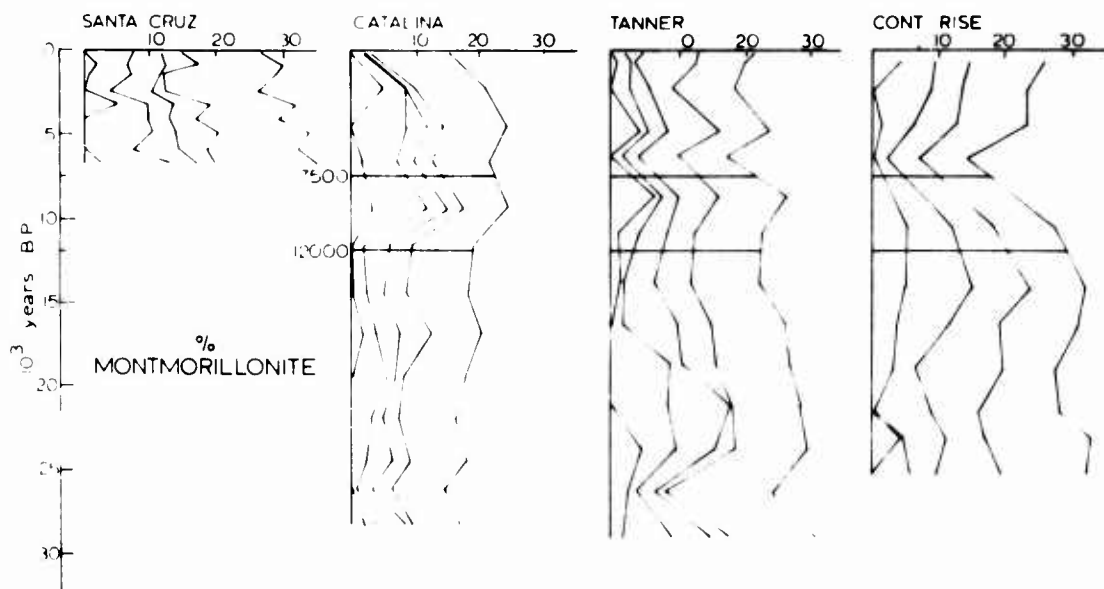
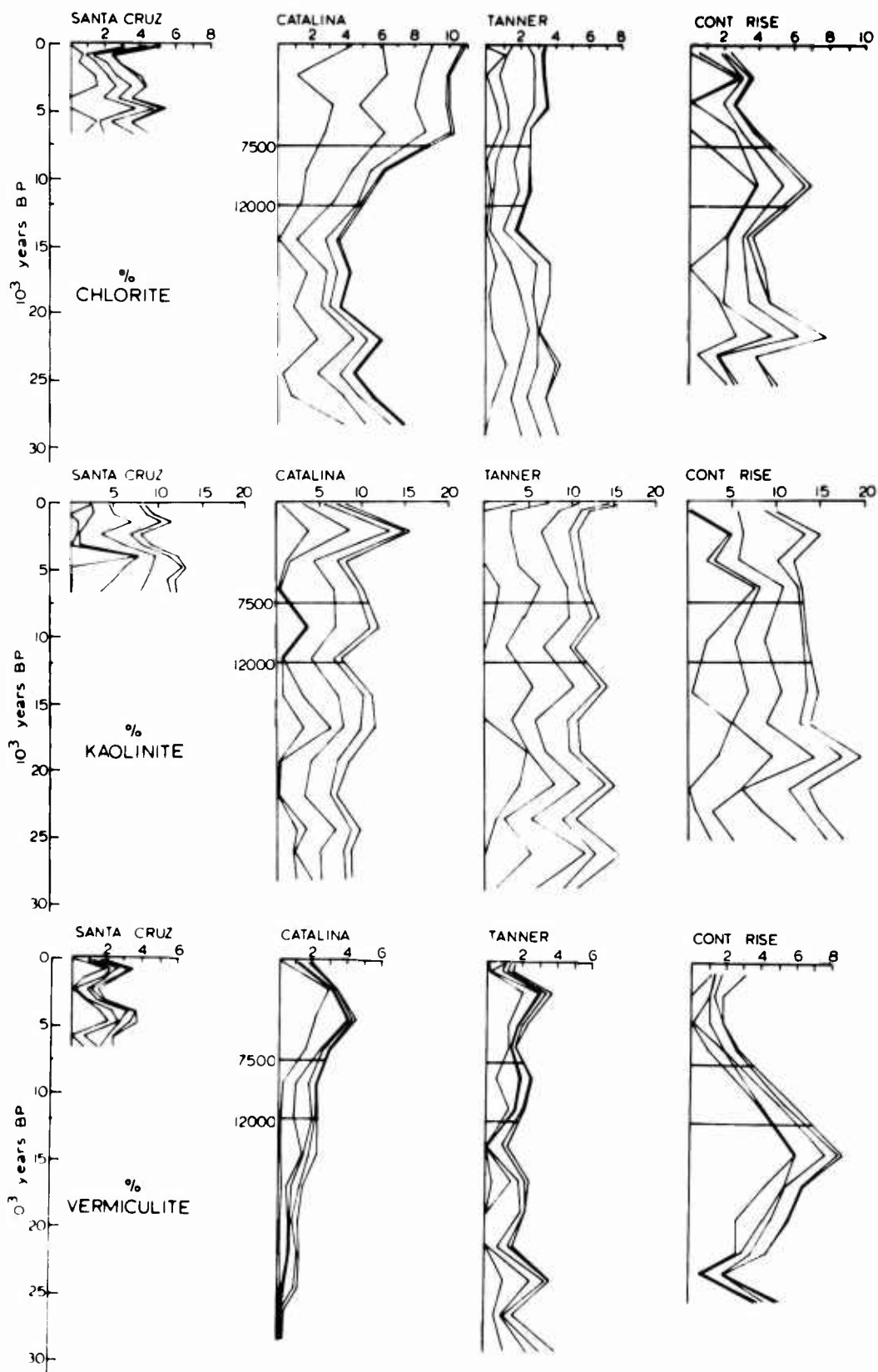


Figure 25. Chlorite, kaolinite, and vermiculite size-fraction weight-percents; cores plotted on time scale.



size fractions, $\mu$					
62-16	16-4	4-1	1-0.25	0.25	<0.25



expected in the metamorphic Santa Catalina Island suite, but its abundance in the rise core is at present unexplained.

It is apparent that, with the exception of chlorite and amphibole in Santa Catalina Basin, the coarse clays and the non-clay minerals show no direct variation with sea level fluctuations. The clay mineralogy of the offshore banks is at present unknown, and therefore no comparison of compositions or ratios can be made as was done with quartz-feldspar ratios on Santa Rosa-Cortes Ridge. Pleistocene-Holocene variation in silt mineralogy, although significant and undoubtedly related to changes in local sources as controlled by sea-level fluctuation, has a complexity that requires more data for an adequate interpretation.

#### Less Than 2 Micron Clay Minerals

Less than 2  $\mu$  clay minerals, which comprise the bulk of this size fraction, are derived from both local and distant sources. The well-mixed nature of fine fractions from borderland basin sediments has been previously discussed. Because of mixing and smoothing-out of local effects in the clay-size fractions, it is possible to examine this fraction for regional effects on the clay mineral distribution since the late Pleistocene.

Less than 2  $\mu$  clay mineral ratio percents (figs.

26, 27, and 28) show some similarity to the coarser clay minerals, but also considerable differences. Illite increases slightly to the tops of the cores and montmorillonite remains constant or decreases slightly. Kaolinite has decreased to the present; whereas chlorite has generally increased, and vermiculite trends are variable.

Trends of illite and montmorillonite ratio percents, which include about two-thirds of the clay minerals, are almost mirror images and appear unaffected by the minor clay minerals. The three long cores contain a bulge in illite and montmorillonite trends that is located in the central sections. The montmorillonite bulge is better expressed by a plot of montmorillonite-illite ratios (fig. 23). The montmorillonite increase appears first in the rise core at about the time of minimum sea level, a little later in Tanner Basin, and near the end of the Pleistocene in Santa Catalina Basin. Montmorillonite decreases in the Holocene sections of all four cores. The similarity of these trends suggests that this is a regional pattern, and the sequence is such that a gradual landward progression of higher montmorillonite-illite ratios results. Montmorillonite-illite ratios are generally higher in the outer borderland as had been previously shown, and the montmorillonite bulge is also greater in the outer borderland.

Clay-mineral segregation by differential settling

Figure 26. Less than 2  $\mu$  montmorillonite and  
illite ratio percents; cores  
plotted on time scale.

# <2 $\mu$ CLAY MINERALS

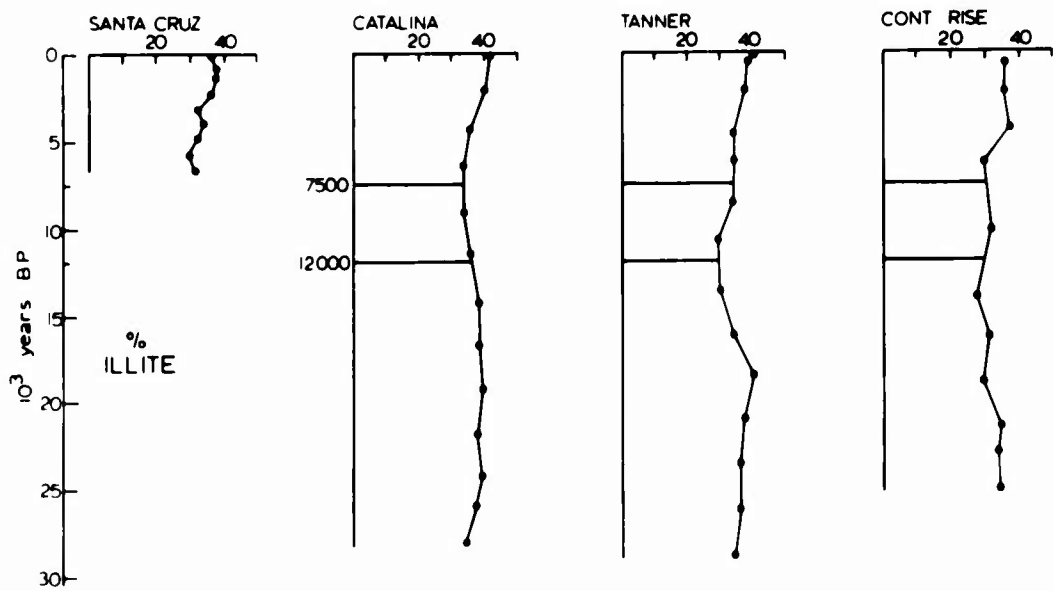
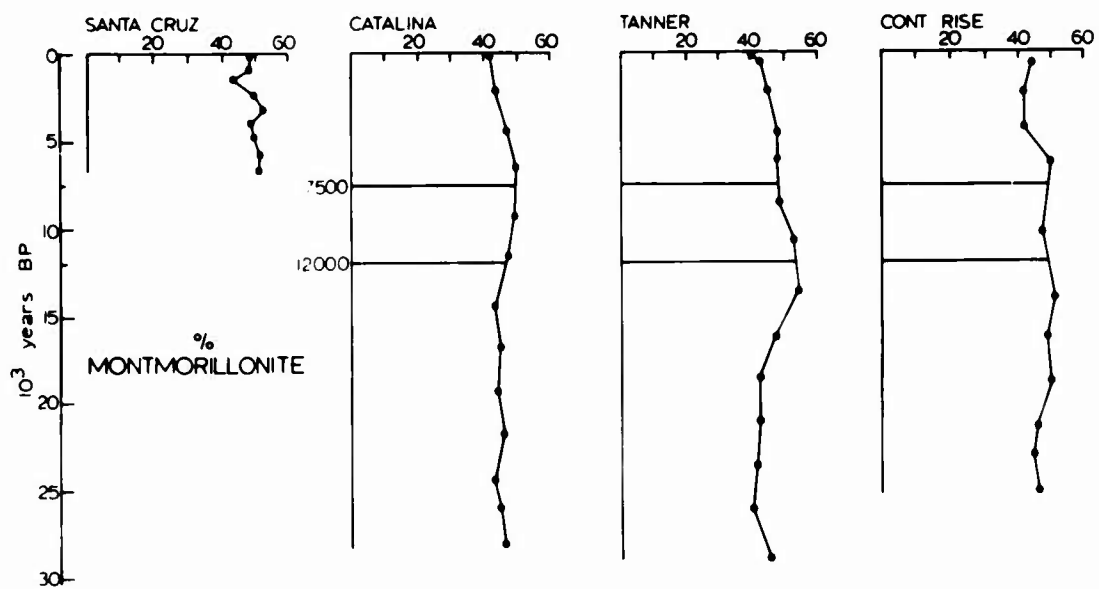


Figure 27. Less than 2 $\mu$  kaolinite and  
chlorite ratio percents; cores  
plotted on time scale.

# <2 $\mu$ CLAY MINERALS

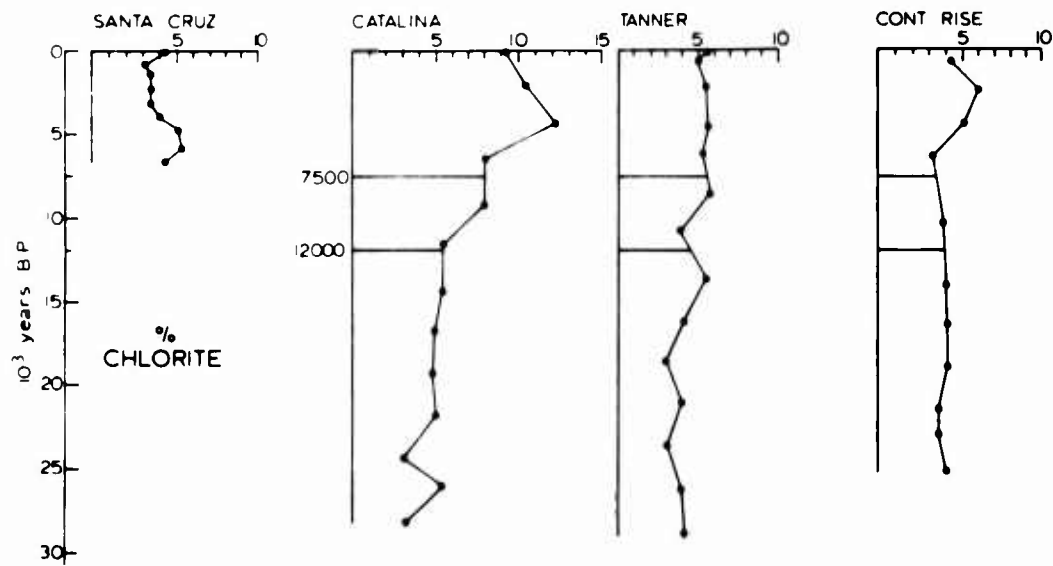
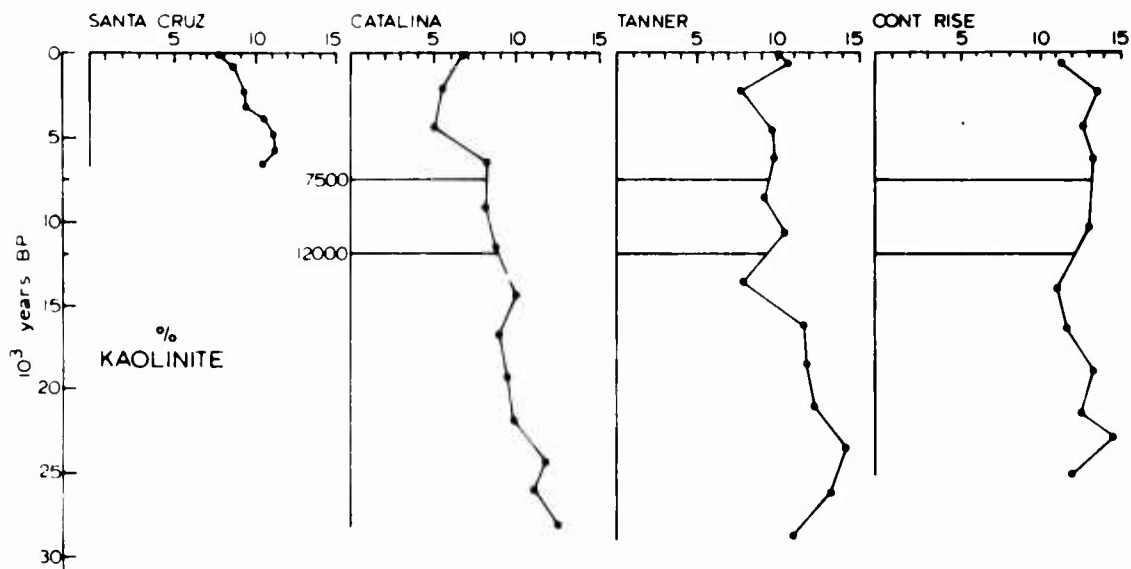
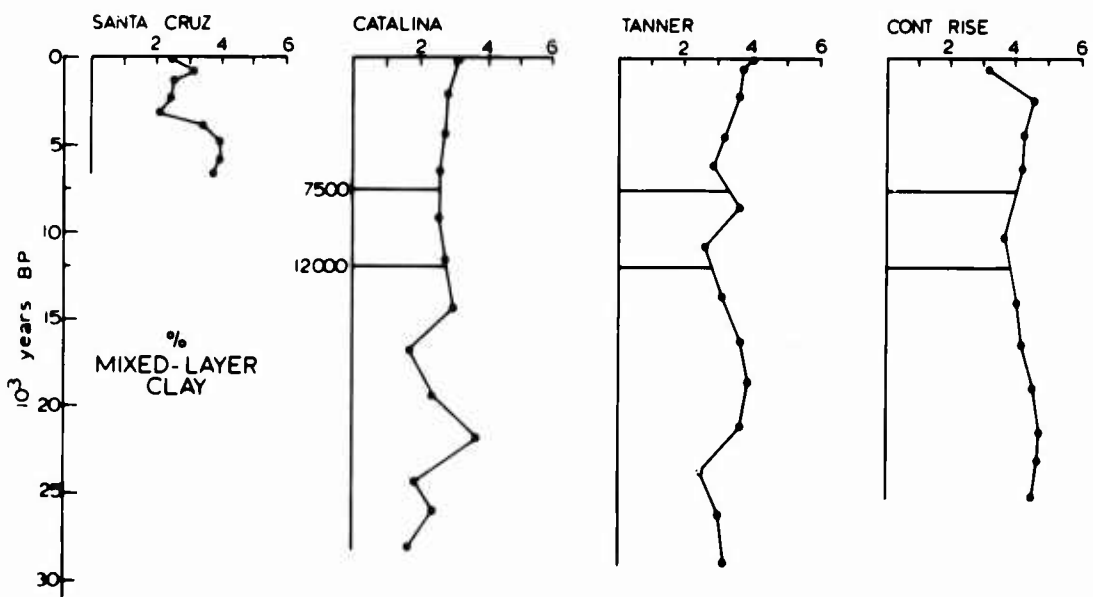
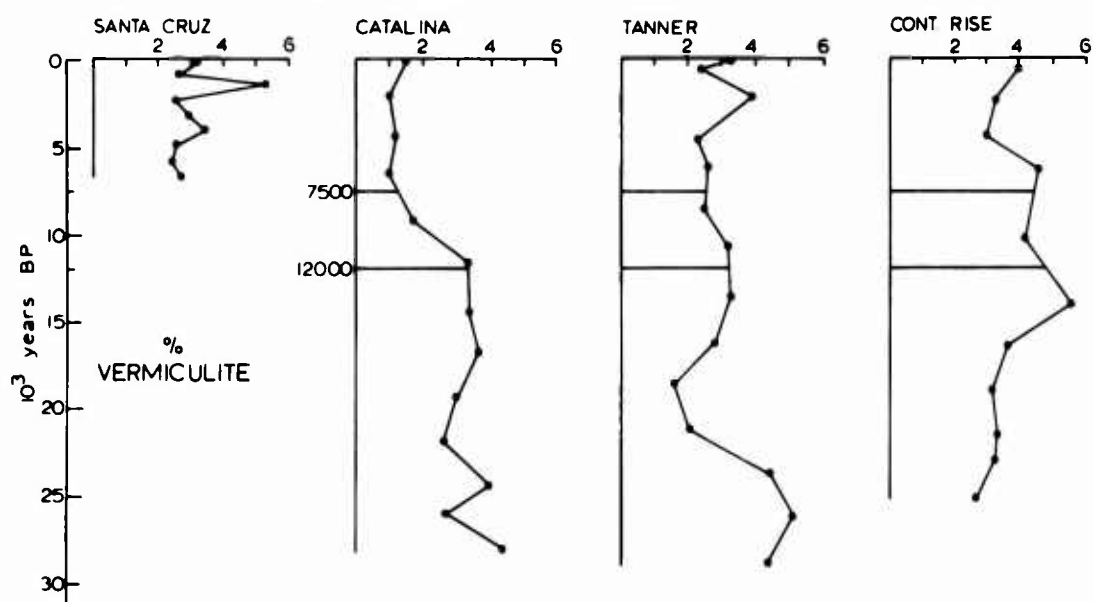


Figure 28. Less than 2/μ vermiculite ratio  
percents and mixed-layer clay;  
cores plotted on time scale.



# <2 $\mu$ CLAY MINERALS



which accounts for higher montmorillonite on the outer borderland also appears to have caused the montmorillonite bulge in the cores. A minimum sea level, when island and offshore-bank sediment-sources were important, the average transport distance for basin sediment was reduced, resulting in a greater abundance of faster-settling illite. As sea level began to rise at the close of the Pleistocene, the importance of the offshore sources decreased, and mainland sediment sources contributed a relatively greater proportion. This process is analogous to increasing the average transport distance of an average source. If differential settling is active, an increase in the montmorillonite-illite would be preferentially deposited in the nearshore areas. The increase of montmorillonite would be expected first on the outer borderland because here the cumulative effect of all sources is felt most, whereas in the inner borderland, a larger rise of sea level will be required to initiate the apparent removal of sources.

The overall decrease of montmorillonite-illite ratios as of the Hypsithermal is not explained by the differential settling process and remains a puzzling problem. A possible explanation (D. S. Gorsline, oral communication) is that the decreasing montmorillonite-illite ratios reflect an equilibration of southern Cali-

fornia streams to the present sea level, and that Pleistocene stream deposits with lower montmorillonite contents are presently being eroded.

The decrease of less than 2 u kaolinite in the Holocene sections of the cores is probably related to a drier climate in southern California since the end of the Pleistocene inasmuch as it can be resolved from the effect of local variations. Kaolinite is thought to form most readily under fairly humid conditions; Sherman (1952) has shown that kaolinite content in Hawaiian soils increases with rainfall, and that montmorillonite decreases proportionately under these conditions. A plot of kaolinite-montmorillonite ratios (fig. 23) shows that these decrease toward the end of the Pleistocene; during the Holocene, they remain constant or increase slightly. The general coincidence of these trends in the cores suggests that climatic change is responsible for much of the kaolinite distribution.

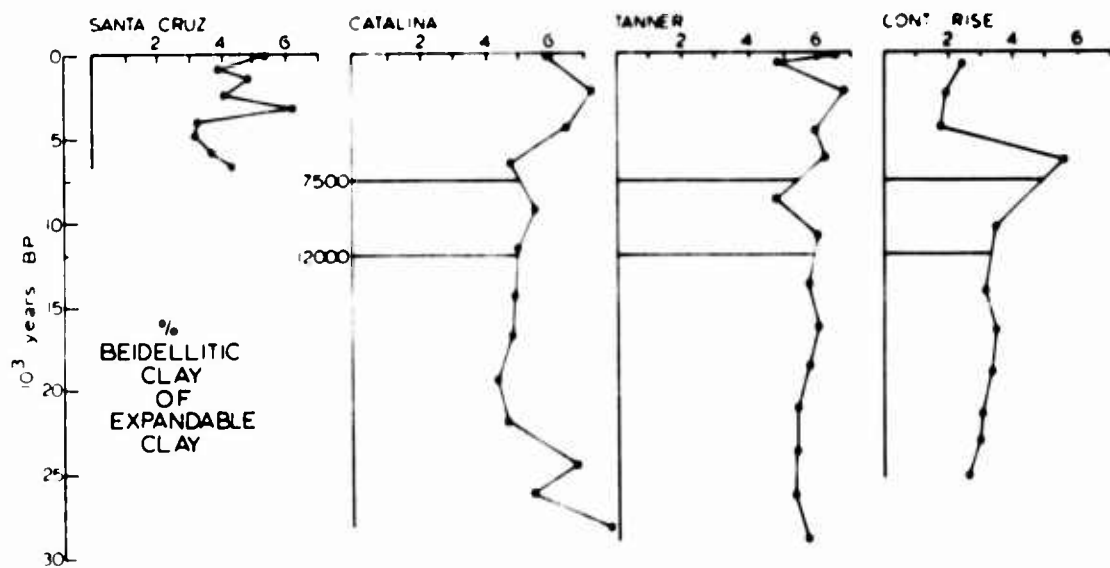
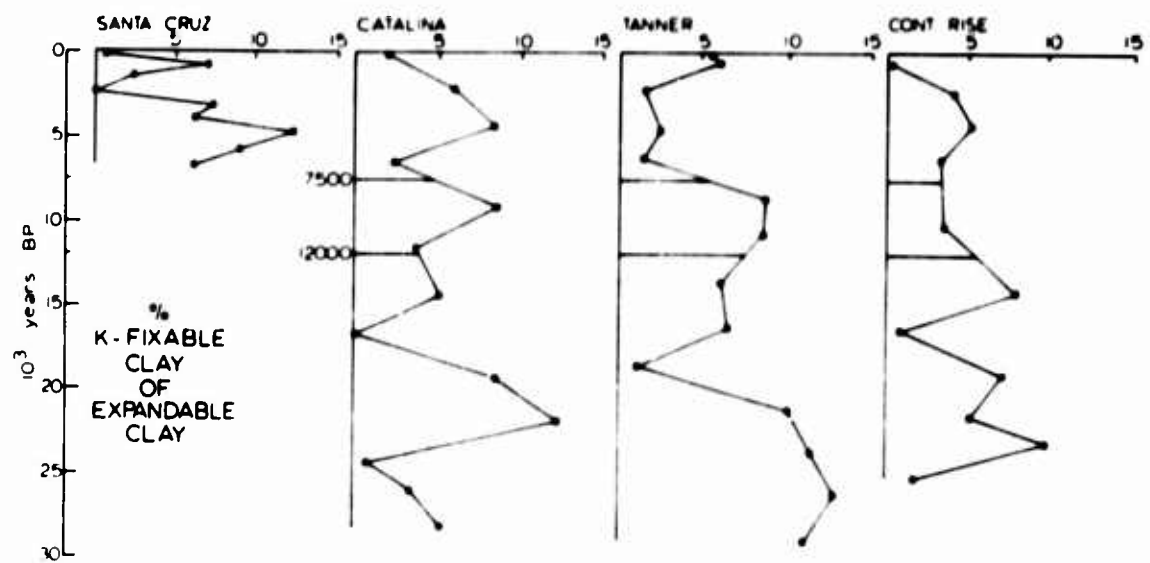
Higher chlorite in the Holocene sections of the cores is partly related to local sources, as in Santa Catalina Basin. Higher chlorite concentrations in the outer borderland may reflect a relatively higher California Current contribution as bank-top and island sources became submerged at the end of the Pleistocene.

### Expandable Clays

Parameters for less than 2 $\mu$  expandable clays, mixed layering, beidellitic montmorillonite, and potassium fixing are shown in Figures 28 and 29. The low precision of these values makes it difficult to evaluate these trends. There appears to be no consistent pattern to the mixed-layer clays. Potassium fixing increases toward the bottoms of the Tanner Basin and continental rise cores; this trend is probably related to the bank-top sources rather than to diagenesis, as it is not observed in the Santa Catalina Basin core. Beidellitic montmorillonite content does not vary much except in Santa Catalina Basin, where a high beidellite concentration occurs at the top and bottom of the core. This trend is similar to that of chlorite and amphibole, and like them, records the sea-level fluctuations. The beidellite probably represents in large part iron-rich montmorillonite derived from weathering of ferromagnesian minerals in the metamorphic suite from Catalina Island.

Figure 29. Potassium-fixable clay and  
beidellitic clay in the less-  
than 2 $\mu$  expandable clay fraction;  
cores plotted on time scale.

# <2 $\mu$ CLAY MINERALS



## SANTA BARBARA BASIN MINERALOGY

## General Aspects

The sediments of Santa Barbara Basin (fig. 1) are exceptional in the California Continental Borderland in that they are undisturbed by postdepositional processes. Coupled with one of the highest sedimentation rates on the borderland, this feature results in an extremely detailed depositional history for the basin, and allows one to elucidate depositional processes to a degree not possible elsewhere in the borderland.

The cause for the undisturbed state of the sediments is a very low oxygen content of bottom water that is inhospitable to larger, bottom-disturbing benthic organisms. Emery (1960) has shown that waters below sill depth in California Continental Borderland basins have the characteristics of water entering the basin at the depth of the sill. The sill of Santa Barbara Basin is at its western end at a depth of 475 m and lies within the oxygen minimum of North Pacific water. As a result, the subsill water of the basin has an oxygen content of about 0.3 ml/L. This value decreases to less than 0.1 ml/L, due to depletion by organisms, in the deepest part of the basin, between 600 and 625 m (Hülsemann and Emery, 1961).

Circulation in Santa Barbara Basin, although an

important factor in acquiring a detailed knowledge of the sediment distribution, is not well known. Part of the water comes from the California Current, and enters the basin at the western end. This water makes a counter-clockwise eddy in the western two-thirds of the basin and departs through the western end as a coastal counter-current (R. L. Kolpack, oral communication). In addition, the Davidson Current, part of a larger eddy over the borderland, brings in warm Southern Water through the eastern passage of the basin. This water is entrained in the California Current eddy (Kolpack, oral communication).

The sediments of the basin have been classified by Hülsemann and Emery (1961) into laminated mud, homogenous mud, and turbidites. The laminated mud consists of couplets of light and dark layers approximately 2 mm thick. The dark layers are composed of terrigenous material deposited in fall and winter; the light laminae are rich in diatoms and radiolarians, and were deposited in spring and summer. Detailed study of the laminae by R. E. Casey (oral communication) and Soutar (1969) established their seasonal nature. Casey demonstrated that the diatom concentrations are related to plankton blooms; and that the dark laminae are rich in sub-polar radiolarians which are carried into the basin by the California Current, where they suffer mass mortality as the cold water mixes with warmer Southern Water.



The homogenous mud appears to be disturbed laminated sediment. Hulsemann and Emery (1961) found that homogenous sediment increases toward the perimeter of the basin, and is more common in shallow depths. Post-depositional disturbance of laminated mud by benthic organisms, slumping, and turbidites is responsible for the uniform appearance of the so-called homogenous mud.

Intercalated with the olive-green laminated and homogenous sediment are numerous gray silt layers which are from a few millimeters to several centimeters thick (fig. 2). They are easily distinguished on the basis of their color, low organic matter, and low carbonate content. Hulsemann and Emery (1961) considered these layers to be turbidites. As evidence, they cited graded bedding in some of the thicker layers, an occasional oxidized zone at the base, supposedly coarser grain size, and an increase in the number of layers to the northern margin of the basin. These characteristics, coupled with the low carbonate and organic content, led them to postulate the northern mainland shelf as the source of the turbidites.

A comparative mineralogic study of gray silt layers and laminated green mud was made on the core collected for this work with the purpose of examining the source and depositional mechanism of the gray layers. The location of the core, in the deepest, central part of the basin (fig. 1) is well-suited for this purpose; and the recovered

length of about 7 m provides a substantial depositional record. Examination of the core revealed 34 gray silt layers 0.5 cm or thicker (fig. 2); 25 of these, or 70 percent, are 2 cm or less in thickness; 5 are over 2 cm and under 10 cm thick, and 4 are 10 to 12 cm thick. The thicker layers occur below 300 cm; Hülsemann and Emery found a similar sequence in their cores. There is some indication of graded bedding in the thicker layers. No distinction has been made between laminated and homogeneous sediment, because they are essentially the same material. Eleven gray layers and 15 samples of green mud in 50-cm intervals were analyzed.

The span of time covered in the core can be estimated on the basis of a radiocarbon-dated core recovered in the same area of the basin (Emery, 1960). At a depth of 425 cm, this core had an age of 2700 yr; by extrapolation, the bottom of the core used in this work would have an age of approximately 4200 yr.

Sediment sources, discussed in the previous section, for Santa Barbara Basin are mainly the Santa Clara and Ventura Rivers, located at the eastern end of the basin. Additional sediment from the Santa Ynez River is probably transported into the basin in significant quantities. A minor contribution is made by coastal drainage of the Santa Ynez Mountains along the northern margin of the basin. Suspended-sediment representative of these sources

was collected from the Santa Ynez, Ventura, and Santa Clara Rivers during the 1969 flood; in addition, bedload sediment was collected from Gaviota Canyon and the Ventura River (fig. 1).

### Comparative Core Mineralogy

#### Grain Size and Carbonate

Comparison of average organic matter- and carbonate-free grain-size parameters (Table 9) revealed that both types of sediment have mean diameters in the fine-silt range, but that the gray layers are a little finer and better sorted than the green mud. Variation of grain-size parameters in the core is minor; there is a slight coarsening down the core (fig. 30). These differences in the two types of sediment are made more apparent by their size-frequency distributions (fig. 31). The gray silt has a considerably more peaked distribution, even though the silt-clay ratios for the two sediments are about the same and vary little with depth (fig. 30). Average values for kurtosis are -0.60 and -0.42 for the green and gray sediments, respectively, and confirm the observed modal differences. The frequency distributions also show another significant difference between the two sediments: the green mud contains appreciably more sand and coarse silt than the gray silt.

Table 9. Composition of green mud and gray layers,  
Santa Barbara Basin

<u>Sediment Parameters and Carbonate Content</u>						
	No. Sples.	Mean Diam., Microns	Std. Dev.	Sort- ing Coef. %	Skew- ness	CaCO <sub>3</sub> , %
Green	15	2.8	2.74	28	0.40	9.76
Gray	11	2.2	2.48	31	0.55	2.49

<u>Average Less Than 62 Micron Weight Percents</u>									
	Quartz	Plagioclase	K-feldspar	Amphibole	Illite	Montmoril- lonite	Vermi- culite	Chlorite	Kaolinite
Green	20.9	4.3	1.4	0.08	27.5	25.6	4.2	3.5	12.9
Gray	22.0	4.5	1.5	0.0	33.5	22.6	1.9	2.3	11.2

<u>Average Less Than 2 Micron Clay Mineral Ratio Percents</u>								
	Illite	Montmor- illonite	Vermiculite	Chlorite	Kaolinite	Mixed-layer clay	K-fixable clay	Beidellitic clay
Green	35.9	46.6	4.0	3.1	10.4	34.5	4.1	20.4
Gray	37.6	47.5	3.1	1.6	10.2	31.4	5.7	25.5

Figure 30. Grain-size parameters and  
carbonate content, Santa Barbara  
Basin, core 11270.

SANTA BARBARA BASIN, 11270

—●— GREEN MUD      - - - ○ - - - GRAY LAYERS

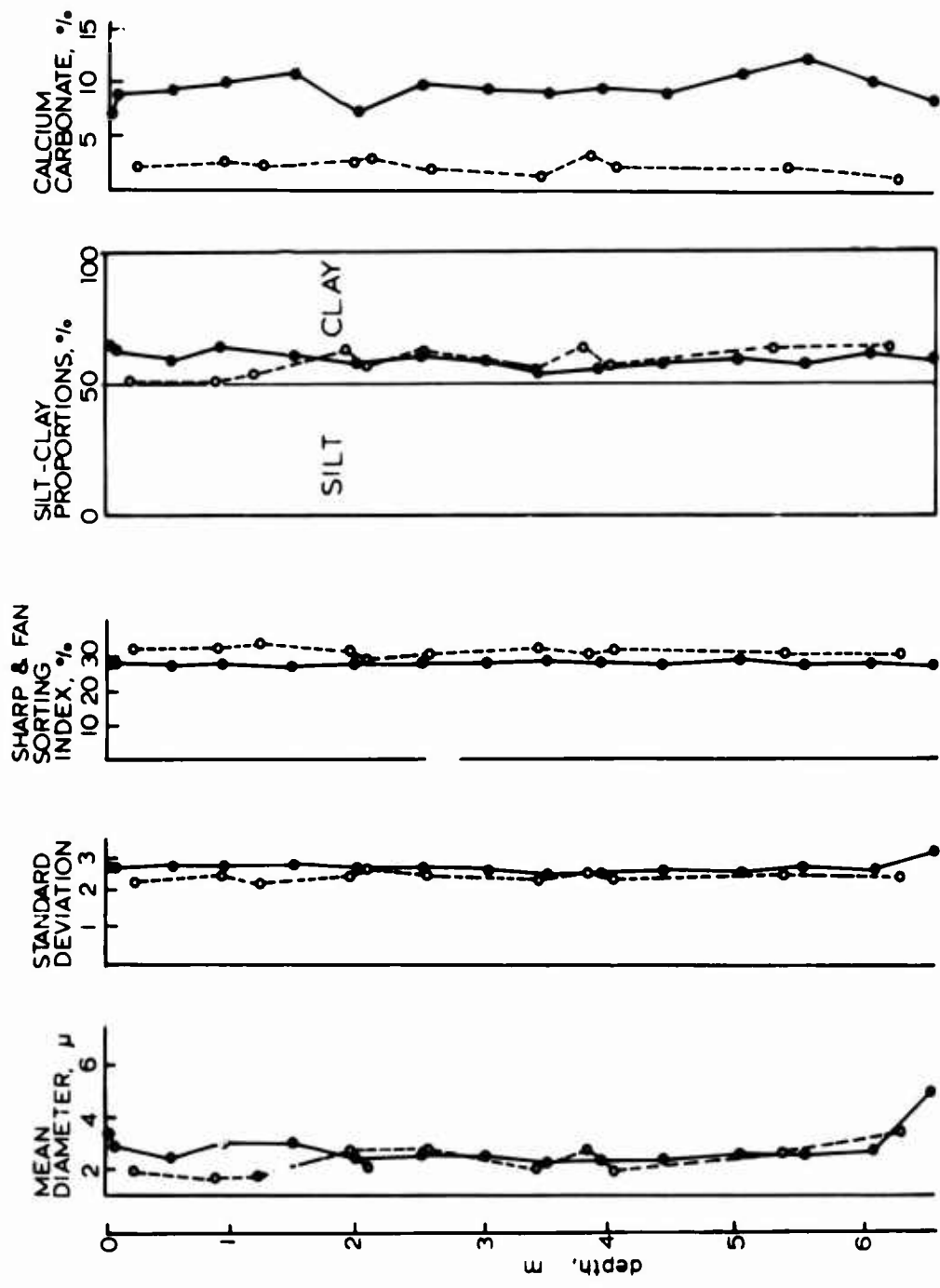
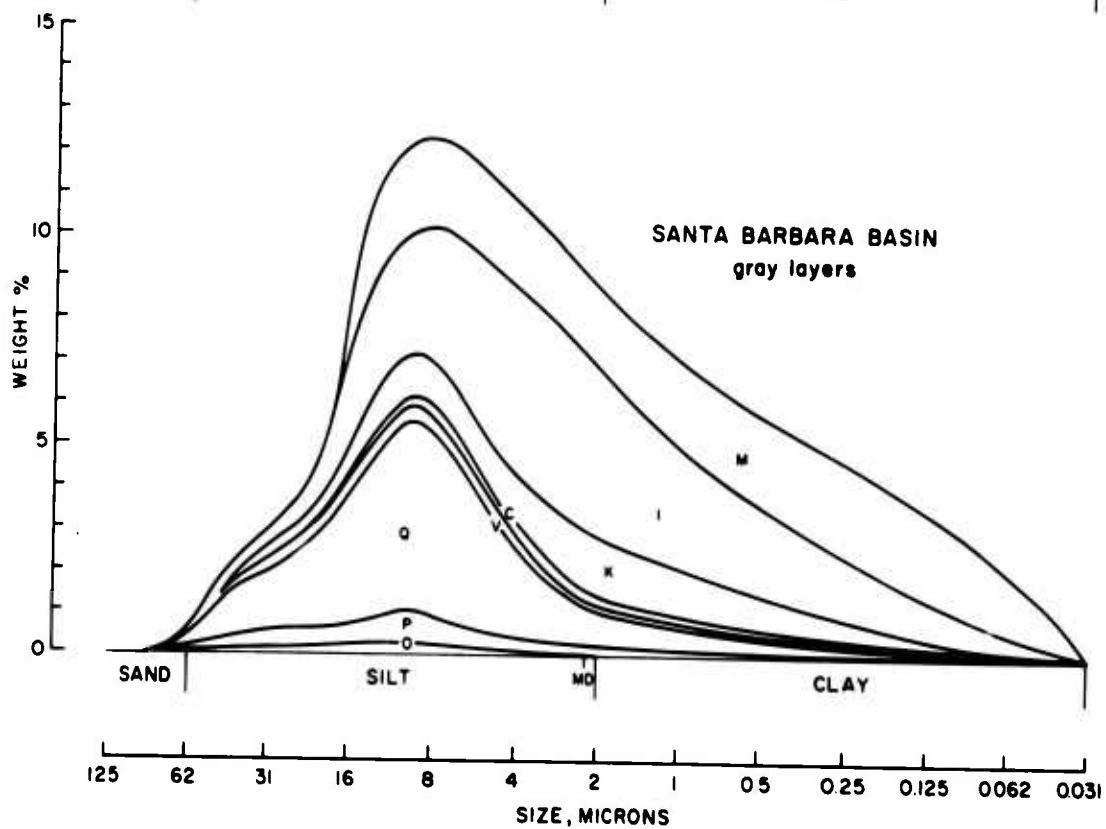
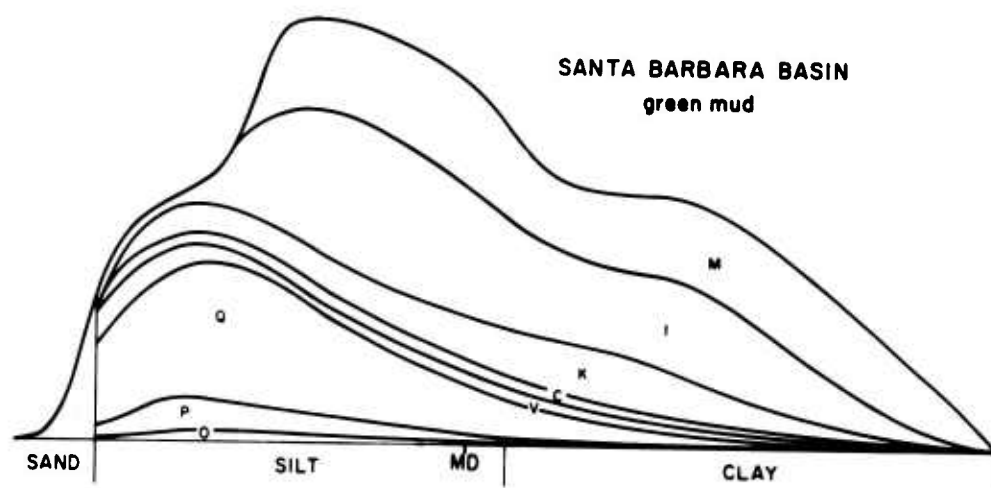


Figure 31. Average mineral size-distributions for Santa Barbara Basin green mud and gray layers. M, montmorillonite; I, illite; K, kaolinite; C, chlorite; V, vermiculite; Q, quartz; P, plagioclase; O, K-feldspar; MD, mean diameter.





These findings conflict with those of Hülsemann and Emery (1961), who stated that the gray layers are coarser than the green mud. A proposed depositional process for the gray layers then must explain the better sorting, finer grain size, and the near-absence of sand.

Calcium carbonate content (Table 9, fig. 30) in the gray layers is only 25 percent of that in the green mud; this value corresponds to the carbonate content on the shelf (Hülsemann and Emery, 1961); it also approximates the carbonate content of the rivers (Table 3).

### Minerals

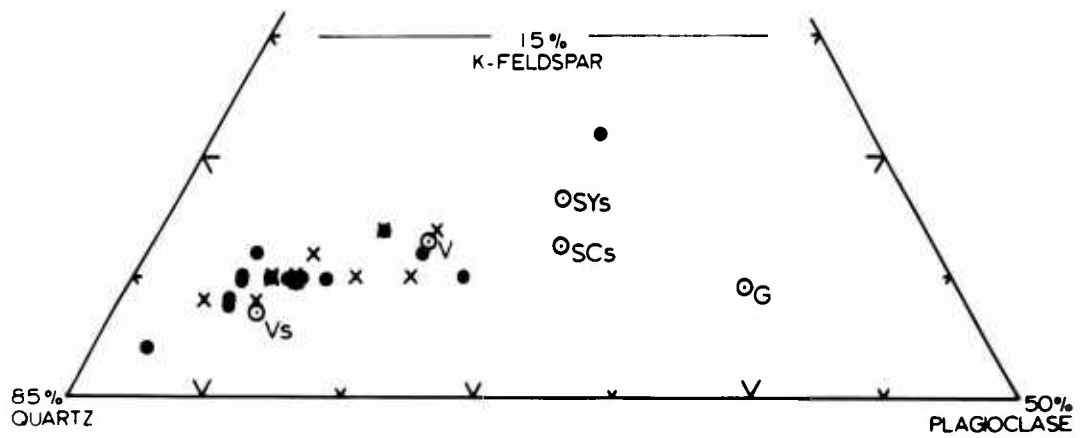
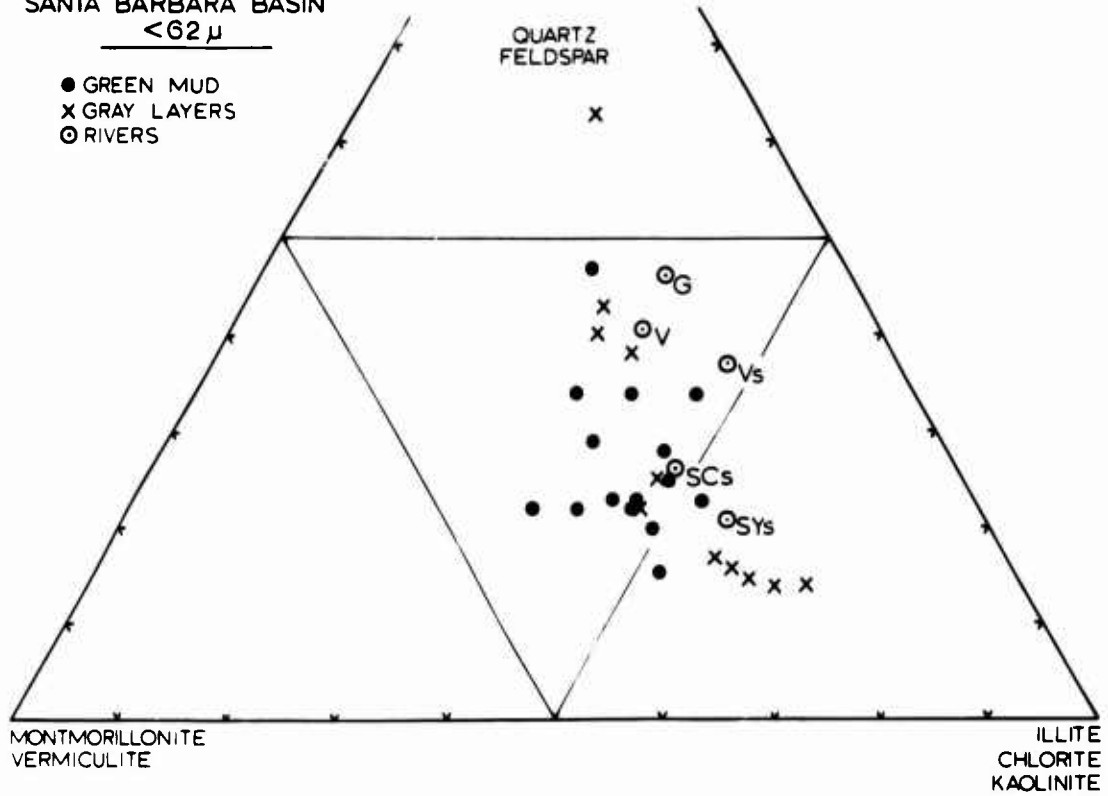
Average mineral compositions of the green mud and the gray layers are given in Table 9 where it can be seen that the gray layers are a little higher in quartz and illite, and lower in chlorite and vermiculite. When plotted on a total-composition ternary diagram (fig. 32) the green mud appears enriched in montmorillonite as compared to the river sediments, whereas the gray silt occupies a narrow intermediate band. A number of gray layers are higher in illite and kaolinite than either river sediments or green mud. This may be caused by either a change in composition of source material, or by segregation of illite and kaolinite during transport.

Quartz-feldspar ratios for green mud and gray layers are about 3.8; for rivers, the ratios are somewhat

Figure 32. Bulk mineral and quartz-feldspar composition diagrams of less than 62  $\mu$  Santa Barbara Basin and river sediments. SYS, Santa Ynez River, suspended load; G, Gaviota Canyon; V, Ventura River; Vs, Ventura River, suspended load; SCs, Santa Clara River, suspended load.

SANTA BARBARA BASIN  
 $< 62 \mu$

- GREEN MUD
- x GRAY LAYERS
- RIVERS



higher. As has been previously shown, quartz-feldspar ratios are size-dependent and increase in the silt and clay sizes. This explains the large spread in quartz content in Figure 32. Plagioclase-K-feldspar ratios are about 3.0 for the basin sediment and a little higher for river sediments, but do not vary appreciably (fig. 32).

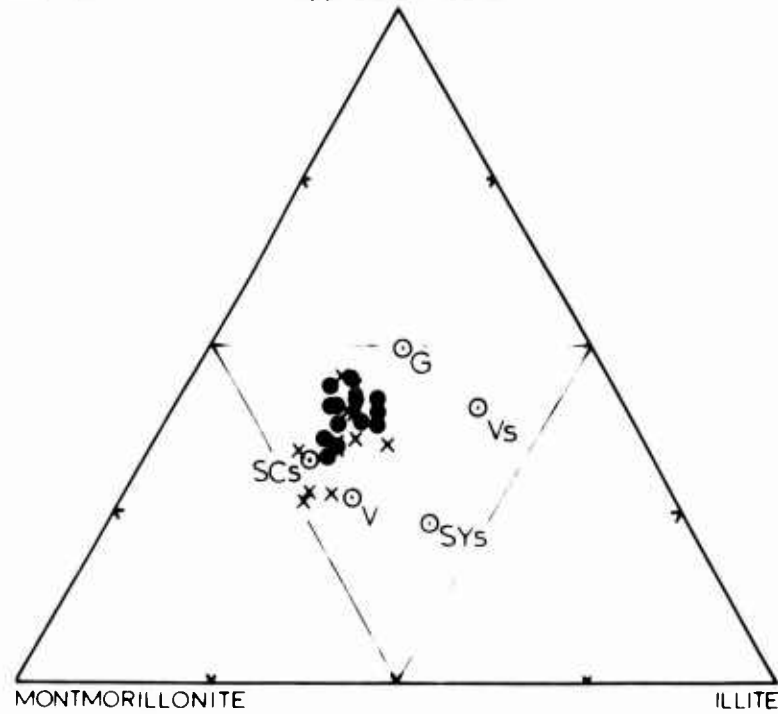
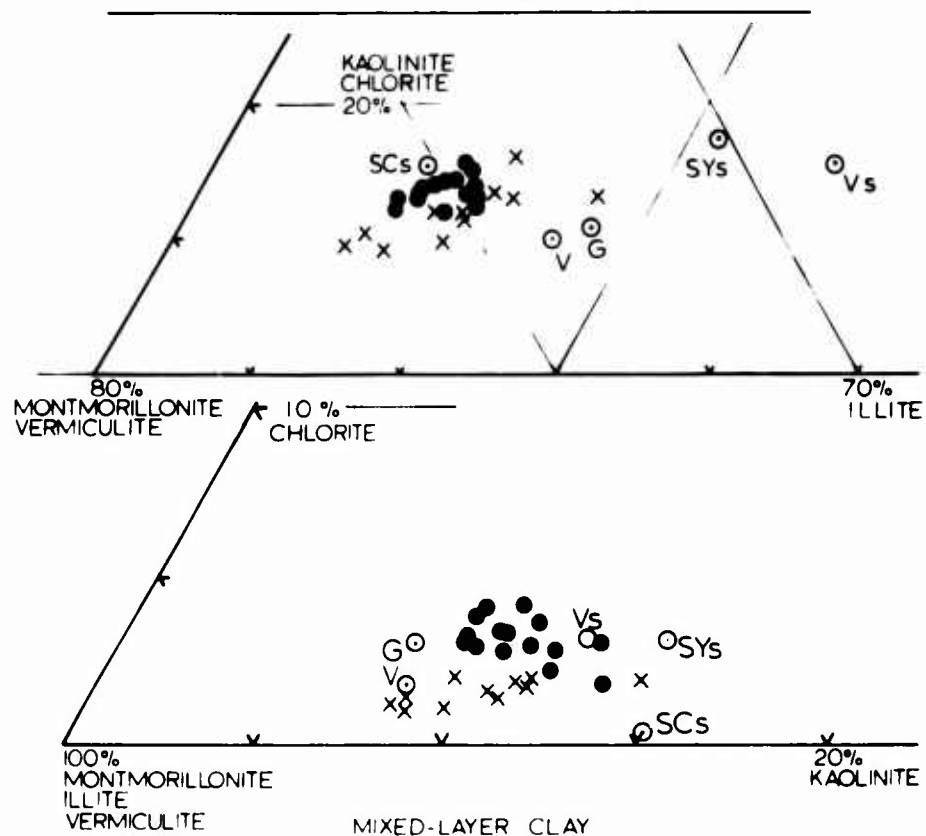
Amphibole (Table 9) was detected in about one-half of the samples of green mud, but not at all in the gray layers. It occurs in small but detectable amounts in all rivers except the Ventura River. The presence of amphibole in the rivers, and its absence in the gray layers, is a result of the lower detection limit of the method used to analyze the river sediments. For these, silt and clay fractions were separated, giving good resolution of silt-size minerals like amphibole. The basin sediments were analyzed in cumulative pipette fractions, and the presence of the clay size-fraction here raises the detection limit by diluting the silt fraction.

Less-than  $2\mu$  clay mineral ratio percents (fig. 33) show decreasing scatter from river sediments to gray layers to green mud. Ternary diagrams for the less than  $2\mu$  fraction also show an apparent enrichment of montmorillonite in the basin sediments and of chlorite in the green mud. The percent of expandable mixed-layer clay does not vary greatly in these sediments, although the green mud contains a little more of this material than the gray

Figure 33. Less than 2  $\mu$  clay mineral composition diagrams, Santa Barbara Basin and rivers. SYS, Santa Ynez River, suspended load; G, Gaviota Canyon; V, Ventura River; Vs, Ventura River, suspended load; SCs, Santa Clara River, suspended load.

# SANTA BARBARA BASIN <2 $\mu$

- GREEN MUD
- x GRAY LAYERS
- RIVERS



layers.

Considerable mineralogic variation down the core occurs in the gray layers, whereas the composition of the green mud remains more constant (figs. 34, 35). Chlorite, kaolinite, and illite decrease; and vermiculite, quartz, and feldspars increase in abundance down the core within the gray layers. In the green mud, only chlorite decreases, and vermiculite and amphibole increase downward. This variation takes place mainly in the silt fraction, and the changes in the less than  $2\mu$  clay minerals are considerably less (fig. 35). Potassium-fixable clay decreases downward, and expandable mixed-layer clay decreases downward in the gray layers. These two trends appear to be inherited rather than diagenetic, as they are not always reproducible in cores from other borderland basins.

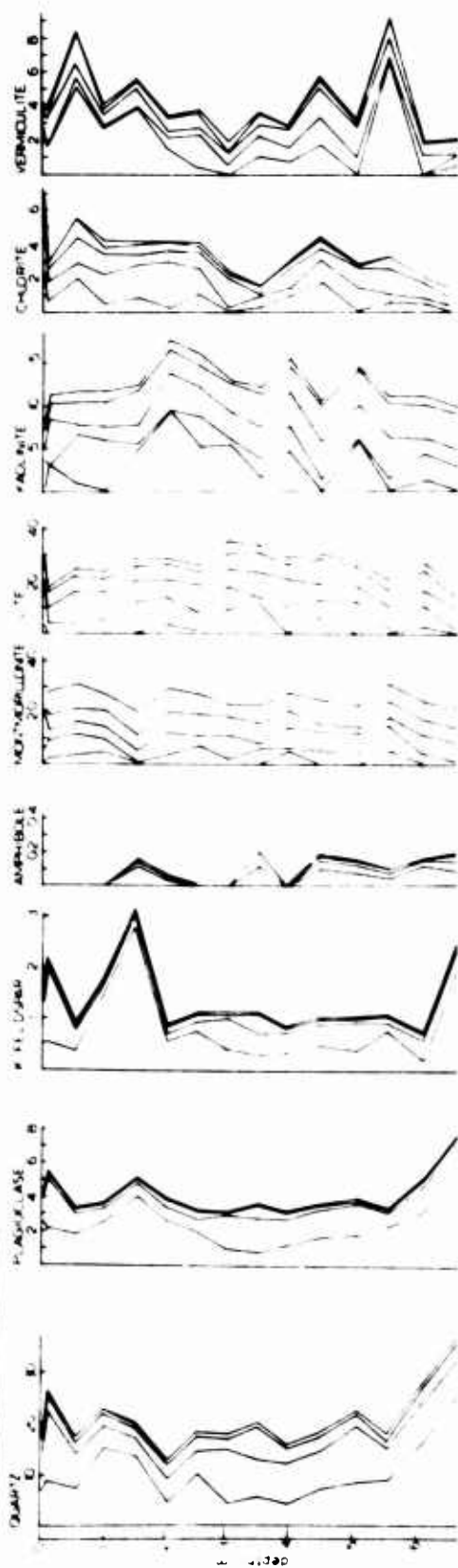
A significant fact is that these variations, especially those in the silt fractions, represent true compositional differences, and are not simply related to a shift in sediment size. Thus, the small shift in mean diameter down the core (fig. 30) is not sufficient to account for the variation in mineral composition. This anomaly must then be caused by changing sources, or by variations within the source areas.

Figure 34. Less than 62  $\mu$  size-fraction  
mineralogy, Santa Barbara Basin,  
core 11270.



SANTA BARBARA BASIN, 11270

GREEN MUD



GRAY LAYERS

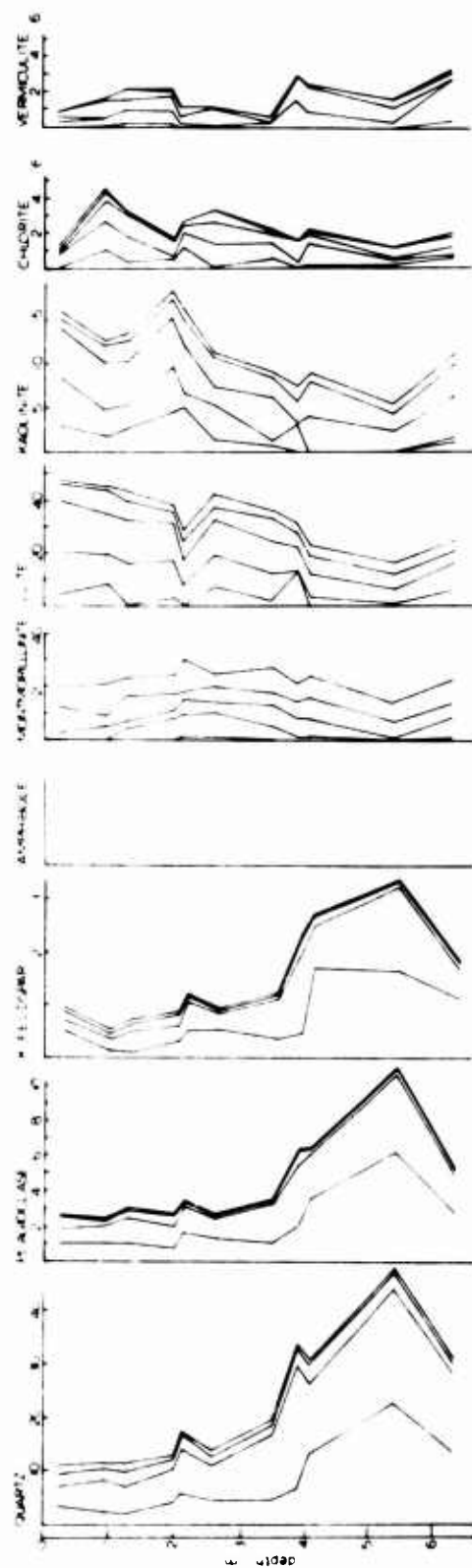
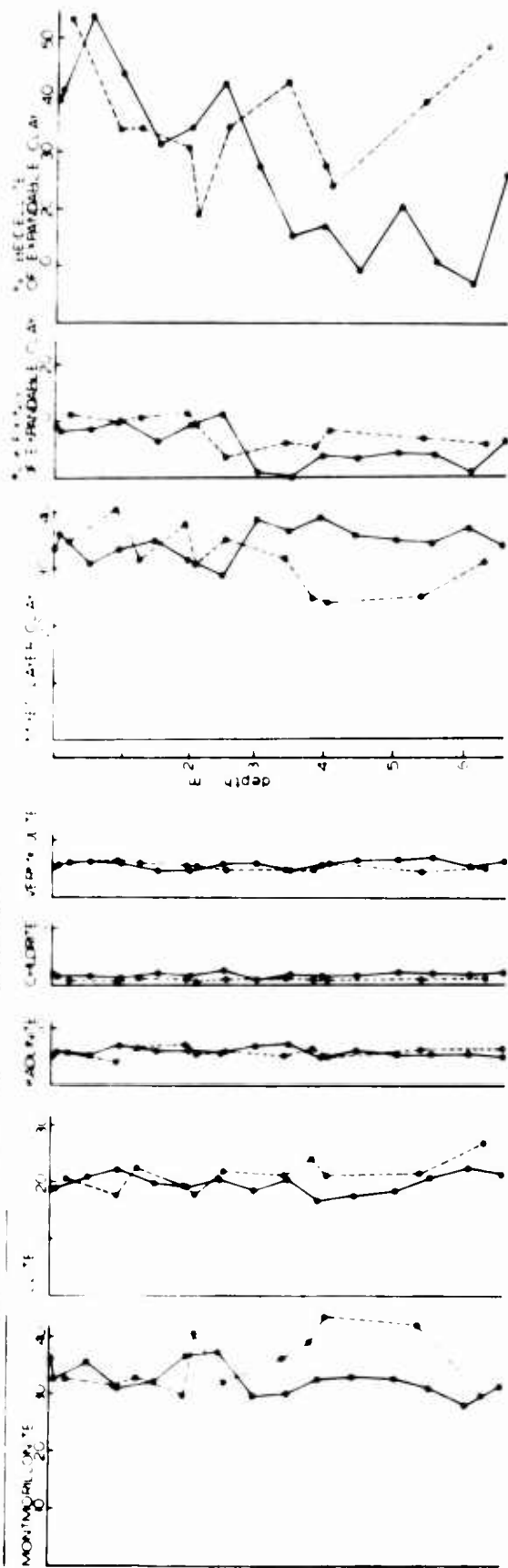


Figure 35. Less than 2  $\mu$  clay mineral ratio  
percents, Santa Barbara Basin,  
core 11270.

SANTA BARBARA BASIN 11270  
- 24 CLAY MINERALS. %



## Source of Sediment

Among the compositional diagrams (figs. 32 and 33), it is important to note the relation of the Santa Clara River. On the total-composition diagram, it fits most closely to the basin sediments, as it does in the montmorillonite-mixed-layer clay-illite diagram. It is the only river that does not show an illite deficiency compared to the basin sediments. The Santa Clara River has the lowest chlorite content among the rivers; making the chlorite content of the gray layers intermediate between it and the green mud. Since the sedimentological properties of the gray layers point to a local origin on the basin margin and to a rapid depositional process, it is probable that the Santa Clara River is the major contributor to the gray layers and to the green mud as well.

In order to make a more comprehensive comparison of the basin sediments with the rivers, a technique was employed which enables comparison by ranking of the river mineral suites with a basin mineral suite. For this purpose, the mineral suite of the less than 62 $\mu$  fraction is most appropriate for a comparison with the gray layers or the green mud. Ranking was used to give equal weights to each mineral in the suite, since the composition of different minerals ranged from zero to over 50 percent.

The method used allows a rapid multiple comparison

of a large number of data sets,  $N$  (mineral suites in this case), composed of a large number of variables,  $v$  (mineral percents), with a null set (the basin sediments). A ranking number,  $R$ , where  $R = 0, 1, 2, \dots, N-1$ , is assigned to each variable.  $R$  is determined by ranking the absolute values of the differences of each variable in the data sets and its corresponding value in the null set. A ranking coefficient,  $C_N$ , can then be determined for each data set by

$$C_n = 1 - \frac{\sum_{j=1}^v R_j}{V(N-1)}$$

when  $R$  is summed over all variables of  $N$ .  $C_N$  is not an independent coefficient for each data set, because

$$\sum_{j=1}^N C_{Nj} = \frac{\sum_{j=1}^N R_j}{N-1}$$

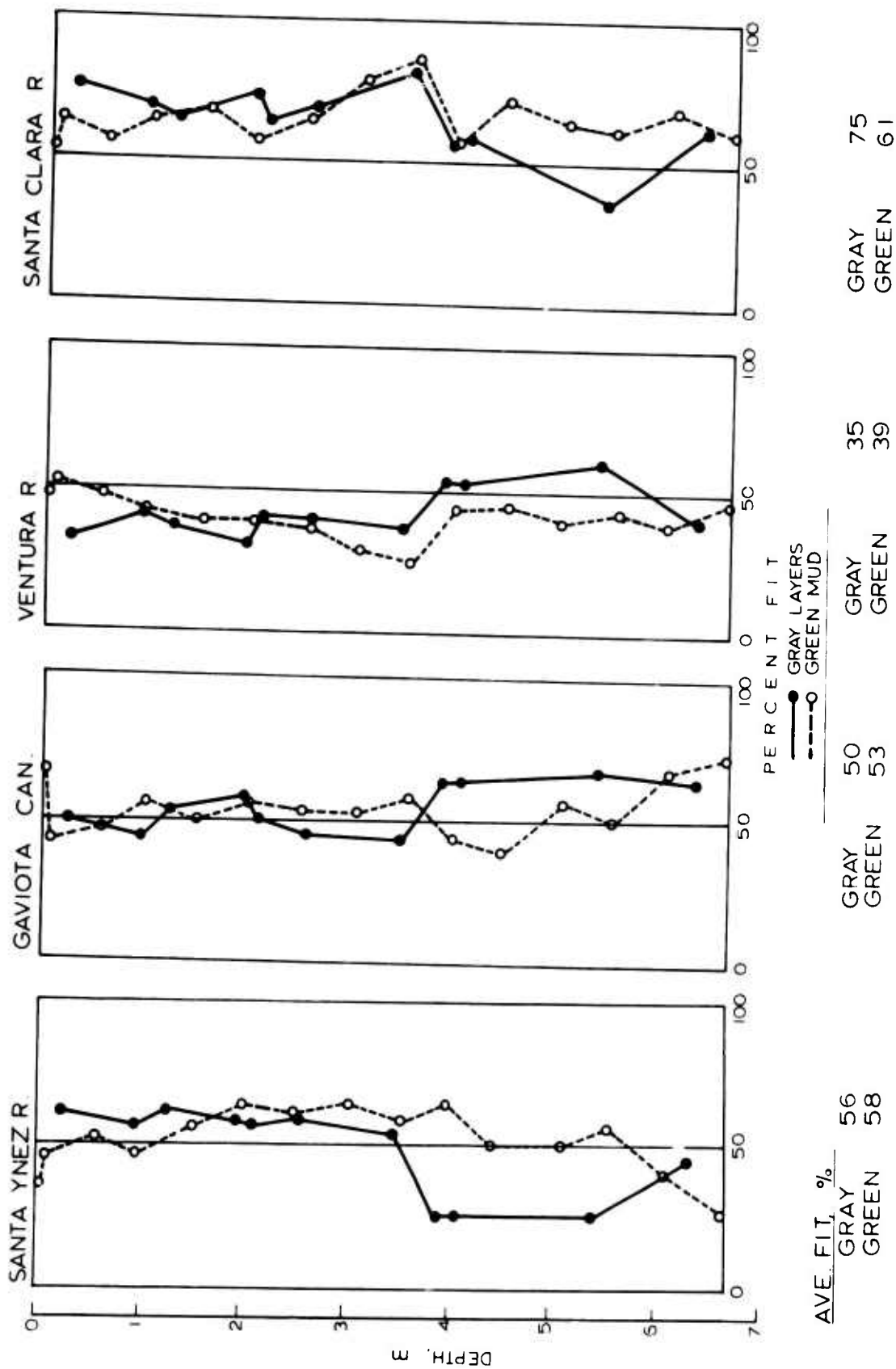
where  $R$  for one variable is summed over  $N$ . Instead, it gives the degree of fit of a particular data set to the null set relative to the other data sets.  $C_N = 1$  is a best fit, and  $C_N = 0$  is a worst fit.  $C_N = 0.5$  means an average fit; a value of 0.5 for all data sets would indicate equal degrees of fit to the null set, but does not imply that the fit is good or bad. No absolute measure of correlation is made by  $C_N$ . Similarly, a very

high value of  $C_H$  does not imply a high similarity with the null set, but simply a greater similarity than for the other data sets.

This method was applied to the nine-mineral suites of the less-than 2  $\mu$  fractions of the five river sediments, both as averages and as individual analyses. The results are similar for gray layers and green mud, but the gray layers reveal a greater range and diversity (fig. 36). This suggests a greater effect of variation in local sources on the gray layers. The Santa Clara River suite fits the basin sediments best; the Santa Ynez River and Gaviota Canyon have intermediate fits. The Ventura River shows the least agreement in both suspended- and bottom-sediment suites.

A rather abrupt change in mineral suites of the basin sediments, particularly the gray layers, and already indicated by mineral percents (figs. 34, 35), is suggested by the ranking coefficients. In the upper half, the Santa Clara-Santa Ynez River suites dominate, whereas in the lower half, a Gaviota-Ventura River suite is dominant. The shift corresponds to the appearance of the thicker gray layers in the core (fig. 2). The cause of the shift is conjectural, but could be related to a sediment supply on the northern mainland shelf, which decreased at some time before the upper 3 m of sediment were deposited in the basin.

Figure 36. Fit of less than 62  $\mu$  river mineral-suites to gray layers and green mud of Santa Barbara Basin by ranking (see text).





From all of the above considerations, it is proposed that the Santa Clara River was the dominant source of Santa Barbara Basin sediment, and particularly to the gray layers in the upper half of the core. It should be emphasized that it does not follow from the above analysis that a good fit in itself defines the dominant source. The Santa Ynez River, for instance, has a better than average fit, but lies outside of the perimeter of the basin and probably supplies a subordinate quantity of sediment. The Santa Clara River, on the other hand, is by far the largest single drainage area on the basin perimeter (fig. 15), and makes the other sources almost insignificant.

Additional evidence that the Santa Clara River is the main source of the basin sediment, and especially of the gray layers, is the fine-silt size range of the gray layers. Stevenson, Uchupi, and Gorsline (1959) first reported that the mainland shelf east of Santa Barbara is the only location in southern California where silt is abundant on the shelf. Wimberly (1964) divided this area into the Santa Clara River prodelta deposit and the Las Pitas mud deposit to the west. Mean diameters of the Las Pitas mud deposit range from 8 to 16  $\mu$ , usually 7 to 8  $\mu$ ; and the sand content is less than 1 percent (Wimberly, 1964). This shelf deposit, derived from the Santa Clara River, indicates the magnitude of this source and may it-

self be a supplier.

#### Depositional Process

The turbidite origin of the gray layers proposed by Hülsemann and Emery (1961) does not appear to be suitable for several reasons. First, the northern shelf is not an important sediment source because of its small drainage area. Second, mineral suites of the gray layers do not match those of the Santa Ynez Range drainage, but rather the Santa Clara River. Third, the fine-silt size of the gray layers makes a turbidite origin questionable. Turbidites are common in some borderland basins (Gorsline and Emery, 1959; Gorsline, Drake, and Barnes, 1967) and are often present in similar late Tertiary strata (Bramlette, 1946), but are always sand-sized. The gray silt layers of Santa Barbara Basin appear to be unique in this respect.

An explanation of the gray layers that is more consistent with their characteristics is that they are flood-year deposits. Rather than being derived from re-suspended shelf sediments, they are deposited more or less directly from the heavy suspended load that southern California rivers carry during severe seasonal storms. Such floods, popularly called "100-year storms," coincide well with the frequency of the gray layers. With an estimated age of 4200 yr for the core in this work, the

gray layers counted occur at an average interval of 120 yr.

A storm of this kind occurred in winter 1969 when two successive two-week storms in January and in February-March caused record rainfalls in southern California. Unpublished United States Geological Survey records from the gauging station on the Santa Clara River indicate that 54 million tons of suspended sediment were carried into the ocean during these two storms.

An approximation of thickness of the deposit resulting from the above quantity of suspended sediment can readily be made. The bulk density of the sediment can be estimated confidently at about 1.5 using water content, sediment size, and core penetration data for California basin sediments using data given by Emery (1960). The areal extent of such a deposit is more difficult to estimate. An area of  $2700 \text{ km}^2$ , a 70 km by 15 km rectangle extending westward from the Santa Clara River, was used. This area covers all of the basin floor, sides, and a good portion of the shelf; and is probably high. These figures result in a layer 1.3 cm thick, well within the range of most of the gray layers.

This figure is affected by a number of factors. It can be increased by reducing the area of the deposit, which is probably considerably less than  $2700 \text{ km}^2$ . Subordinate contributions from the Ventura and Santa Ynez

Rivers, and from the coastal drainage would also add to the deposit. On the other hand, two factors act to decrease the deposit. One is that much of the suspended matter, especially the sand and coarse silt, either is deposited on the shelf near the river mouth or is lost to the south in the longshore drift. In addition, a large quantity of the suspended sediment that bypasses the shelf may be carried to the south and deposited in Santa Monica Basin. However, even if one-half of the suspended sediment is removed by these processes, an easily recognizable deposit would form on the basin floor.

Two transporting mechanisms may be responsible for the gray layers; their relative importance and the processes at work are not yet clearly understood. Revelle and Shepard (1939) long ago recognized the importance of suspended sediment from storms in sedimentation on the California Continental Borderland, and concluded that suspended sediment dispersion of this kind occurs over the inner basins. Using a settling velocity of 15 m/day for flocculated sediment (corresponding to a hydraulic diameter of  $15\mu$ ), they showed that currents are sufficient to transport sediment over an entire basin during a settling period of one to two months.

That direct settling of suspended matter from the water column has occurred to some degree after the 1969 flood may be evidenced by turbidity measurements by D. E.

Drake (oral communication). These data show a large plume of suspended sediment from the Santa Clara River moving over the shelf and into the water column of the central basin, becoming detached from the bottom at the shelf break.

Bottom samples collected in Santa Barbara Basin by Drake and R. L. Kolpack (oral communication) at intervals for one year after the flood indicate, however, that the reddish Santa Clara River silt did not start to collect on the basin floor until three or four months after the flood. The pattern of appearance of this "red layer," first in the eastern part of the basin and then gradually further westward, suggests that this material may be creeping slowly over the basin floor as a near-bottom turbid layer. One year after the flood, the sediment covered most of the deeper parts of the basin with a watery layer 1 to 2 cm thick, and the reddish color of the sediment is changing to a grayish buff as the iron oxides are reduced in the near-anaerobic bottom water (Drake, oral communication).

At present, there is insufficient evidence to make any firm conclusions about the efficacy of the near-bottom turbid layer in distributing the "red layer" over the basin floor. The sediment-water interface in Santa Barbara Basin is characteristically indistinct and soupy, and the slow appearance of the flood deposit in the bottom samples may simply be due to a loss of the still watery

material in months immediately after the flood. Whatever the depositional mechanism, however, it is highly probable that the majority of the gray layers in Santa Barbara Basin are of a similar flood-deposit origin. An exception may be the thicker layers in the lower half of the core, and these may be of a more conventional turbidite origin.

## SUMMARY AND CONCLUSIONS

Hemipelagic basin sediments of the California Continental Borderland consist of approximately equal proportions of silt and clay on a carbonate-free basis. Illite, quartz, and montmorillonite are predominant in the silt sizes; montmorillonite and illite are most abundant in the clay sizes. Kaolinite, chlorite, vermiculite, and talc(?) in addition to plagioclase, potassium feldspar, and amphibole in the silt sizes, are present in subordinate amounts. Montmorillonite consists in part of beidellite or trioctahedral varieties, and about one-third of this mineral contains random mixed-layering of illite. A small portion of the expandable clay is potassium-fixable. No evidence of diagenesis was found in this component or among the other clays.

Coastal drainage is the major sediment source for the basins. The fine-grained sediments of these sources are similar in mineral composition, but three suites can be distinguished. These are a northern quartz-feldspar-illite suite from sedimentary rocks of the western Transverse Ranges, an igneous-metamorphic chlorite-vermiculite-illite suite from the central Transverse Ranges, and a southern quartz-feldspar suite from the California Batholith.

The mineral composition of basin sediments is more

uniform than that of river sediments because of mixing by currents. Quartz-feldspar ratios are 3.0, higher than for rivers, in the total sediment, and plagioclase-orthoclase ratios are 3.5. Variation of quartz-feldspar ratios is in part related to sources, but is strongly dependent on grain size because quartz is more persistent in the fine silt sizes than feldspar. Basin sediments contain more montmorillonite and chlorite, and less illite than the river sediments. Excess chlorite is carried into the borderland from the northwest Pacific coast by the California Current. Evidence for this process is found in Santa Barbara Basin, where rapidly deposited flood-layers of local origin contain only one-half as much chlorite as the continuously-deposited sediment. A current influx of 5 percent to 10 percent is sufficient to cause the enrichment. A portion of the montmorillonite may also be derived from this source, although enrichment of this mineral may only be apparent because three major rivers have similar montmorillonite and illite contents as the basins.

A decrease in particle size, differential settling, and eolian transport determine mineralogic variations from nearshore to offshore areas. Quartz, feldspar and amphibole generally decrease offshore. Fine silt- and clay-size quartz, however, increases offshore and is probably of eolian origin. The quantity of wind-borne



sediment increases offshore because of a decrease in the total terrigenous sedimentation rate. Eolian sediment is derived mainly from Santa Ana winds, but its overall contribution to the basin sediments is probably under 10 percent. Segregation by differential flocculation causes faster-settling illite to be deposited in greater quantities in nearshore areas, and slower-settling montmorillonite in the outer borderland.

Core mineralogy of late Pleistocene-Holocene sediments in Catalina Basin, Tanner Basin, and the continental rise show that sea-level fluctuations, and to some extent climatic change, has determined the mineral distribution. Silt-size minerals are largely of local origin, and exposure of offshore banks and islands during low sea level 18,000 BP is reflected by these minerals. High quartz-feldspar ratios during the Pleistocene in Tanner Basin and on the continental rise indicate erosion of quartz-rich sediment on the Santa Rosa-Cortez Ridge. In Santa Catalina Basin, which is characterized by a distinctive plagioclase-amphibole-chlorite suite derived from metamorphic rocks of Santa Catalina Island, an influx of volcanic sediment from Santa Barbara Bank occurred during the Pleistocene. The dilution of the Santa Catalina Island suite, the quantity of which remained constant during the Pleistocene, is closely related to sea-level fluctuations.

Clay minerals in late Pleistocene-Holocene sediments reflect the effects of long-distance transport and climatic change to the extent that these processes can be resolved from local source variations. Differential settling is responsible for variation of illite and montmorillonite. Beginning on the outer borderland, montmorillonite-illite ratios increased with inception of sea-level rise. This trend was caused by the gradual submergence of the offshore banks and islands, which resulted in a relative increase in the proportion of mainland sediment. The net effect of sea-level rise thus was to increase the average transport distance of sediment to the offshore areas. Because the average transport distance was increased, faster settling illite reached the outer borderland in lesser amounts, and the proportion of montmorillonite increased. A decrease of montmorillonite-illite ratios since the Hypsithermal may be related to gradual adjustment of stream profiles after the sea-level rise.

Numerous well-sorted gray silt layers in Santa Barbara Basin originated as flood deposits. They occur at an average interval of 120 yr, and are caused by unusually heavy storms. Low carbonate and organic matter content of the layers indicates rapid deposition. Comparison of river mineral-suites with gray-layer mineral-suites shows that the Santa Clara River is the major

source of these deposits. The origin by floods of the gray layers is confirmed by a similar deposit that was laid down after the 1969 flood.

## REFERENCES

## REFERENCES

## REFERENCES

- Azmon, E., 1960, Heavy minerals in sediments of southern California: Ph.D. dissert., Univ. of Southern California, Los Angeles, California, 148 p.
- Bailey, T. L. and Jahns, R. H., 1954, Geology of the Transverse Range Province, in Jahns, R. H., Editor, Geology of southern California: California Div. of Mines Bull. 170, p. 65-106.
- Bandy, O. L., 1960, Geological significance of coiling ratios in the foraminifer Globigerina pachyderma (Ehernburg): Jour. Paleontology, v. 34, p. 671-681.
- Biscaye, P. E., 1965, Mineralogy and sedimentation of Recent deep-sea clay in the Atlantic Ocean and adjacent seas and oceans: Geol. Soc. America Bull., v. 76, p. 803-832.
- Bonatti, E. and Arrhenius, G., 1965, Eolian sedimentation in the Pacific Ocean off northern Mexico: Marine Geology, v. 3, p. 337-348.
- Brambati, A., 1968, Mixing and settling of fine terrigenous material (less than 16 microns) in the northern Adriatic Sea between Venice and Trieste: Studi Trentini di Scienze Naturali, v. 45, p. 103-117.
- Bramlette, M. N., 1946, The Monterey Formation of California and the origin of siliceous rocks: U. S. Geol. Survey Prof. Paper 212, 57 p.
- Brindley, G. W., 1961, Kaolin, serpentine, and kindred minerals, in Brown, G., Editor, The x-ray identification and crystal structures of clay minerals: London, Mineralogical Society, p. 51-131.
- Carroll, D. and Starkey, H. C., 1960, Effect of sea water on clay minerals, in Swineford, A., Editor, Proc. 7th National Conf. on Clay Minerals: New York, Pergamon, p. 80-101.
- Clarke, F. W., 1924, Data of geochemistry: U. S. Geol. Survey Bull. 770, 841 p.

- Copeland, L. E., 1963, Quantitative analysis by x-ray diffraction, in Clark, G. L., Editor, Encyclopedia of x-rays, New York, Rheinhold, p. 875-877.
- Curray, J. R., 1969, History of continental shelves, in The new concepts of continental margin sedimentation: American Geological Institute, Short Course Lecture Notes, p. JC-VI-1 - JC-IV-18.
- Dietz, R. S., 1941, Clay minerals in recent marine sediments: Ph.D. dissert., Univ. of Illinois, Urbana, Illinois, 68 p.
- Duncan, J. R., Kulm, L. D., and Griggs, G. B., 1970, Clay mineral composition of late Pleistocene and Holocene sediments of Cascadia Basin, Northeastern Pacific Ocean: Jour. Geology, v. 78, p. 213-221.
- Emery, K. O., 1954, Source of water in basins off southern California: Jour. Marine Research, v. 13, p. 1-21.
- \_\_\_\_\_, 1960, The sea off southern California: New York, John Wiley & Sons, 366 p.
- Emery, K. O. and Bray, E. E., 1962, Radiocarbon dating of California basin sediments: Am. Assoc. Petroleum Geologists Bull., v. 46, 1839-1856.
- Gaal, R. A. P., 1966, Marine Geology of the Santa Catalina Basin area: Ph.D. dissert., Univ. of Southern California, Los Angeles, California, 268 p.
- Garrels, R. M. and Christ, C. L., 1965, Solutions, minerals, and equilibria: New York, Harper and Row, 450 p.
- Gibbs, R. J., 1965, Error due to segregation in quantitative clay mineral x-ray diffraction mounting techniques: Am. Mineralogist, v. 50, p. 714-751.
- \_\_\_\_\_, 1967a, Quantitative x-ray diffraction using clay mineral standards extracted from the samples to be analysed: Clay Minerals, v. 7, p. 79-90.
- \_\_\_\_\_, 1967b, The factors that control the salinity and the composition and the concentration of the suspended solids; Geochemistry of the Amazon River System: Part I: Geol. Soc. America Bull., v. 78, p. 1203-1232.

- Gorsline, D. S., 1968, Marine geology of the California Continental Borderland: Report No. USC GEOL 68-1, Annual Report for the first contract year, University of Southern California, Los Angeles, California, 92 p.
- Gorsline, S., Drake, D. E., and Barnes, P. W., 1968, Holocene sedimentation in Tanner Basin, California Continental Borderland: Geol. Soc. America Bull., v. 79, p. 659-674.
- Gorsline, D. S. and Emery, K. O., 1958, Turbidity current deposits in San Pedro and Santa Monica Basins off southern California: Geol. Soc. America Bull., v. 70, p. 279-290.
- Greene-Kelly, R., 1953, Identification of Montmorillonoids: Jour. Soil Science, v. 4, p. 233-237.
- Griffin, G. M., 1962, Regional clay mineral facies--products of weathering intensity and current distribution in the northeastern Gulf of Mexico: Geol. Soc. America Bull., v. 73, p. 737-768.
- Griffin, J. J. and Goldberg, E. D., 1963, Clay-mineral distribution in the Pacific Ocean: in Hill, M. N., Editor, The sea: New York, Interscience, v. 3, p. 728-741.
- Griffin, J. J., Windom, H., and Goldberg, E. D., 1968, The distribution of clay minerals in the world ocean: Deep-Sea Research: v. 15, p. 433-459.
- Grim, R. E., 1968, Clay mineralogy, 2nd ed., New York, McGraw-Hill Book Company, 596 p.
- Grim, R. E., Bradley, W. F., and White, W. A., 1957, Petrology of the Paleozoic shales of Illinois: Illinois Geol. Survey Rept. Inv. 203, 35 p.
- Grim, R. E., Dietz, R. S., and Bradley, W. F., 1949, Clay mineral composition of some sediments from the Pacific Ocean off the California coast and the Gulf of California: Geol. Soc. America Bull., v. 60, p. 1785-1808.
- Handin, J. W., 1951, The source, transportation, and deposition of beach sediment in southern California: Dept. of Army, Corps of Engineers, Beach Erosion Board, Tech. Memo. 22, 113 p.

- Holzman, J. E., 1952, Submarine geology of Cortez and Tanner Banks: Jour. Sed. Petrology: v. 22, p. 83-118.
- Hjulstrom, F., 1939, Transportation of detritus by moving water, in Trask, P. D., Editor, Recent marine sediments: Soc. Econ. Paleontologists and Mineralogists Spec. Pub. 4, p. 5-31.
- Hulsemann, J. and Emery, K. O., 1961, Stratification in recent sediments of Santa Barbara Basin as controlled by organisms and water character: Jour. Geology, v. 69, p. 279-290.
- Hurley, P. M. B., Heezen, B. C., Pinson, W. H., Jr. and Fairbairn, H. W., 1963, K-Ar values in pelagic sediments of the North Atlantic: Geochim. Cosmochim. Acta, v. 27, p. 393-399.
- Jackson, M. L., 1956, Soil chemical analysis--advanced course: Madison, M. L. Jackson, 991 p.
- Jahns, R. H., 1954, Geology of the Peninsular Range Province, southern California and Baja California, in Jahns, R. H., Editor, Geology of southern California: California Div. Mines Bull. 170, p. 29-52.
- Johns, W. D. and Grim, R. E., 1958, Mineral composition of recent sediments from the Mississippi River Delta: Jour. Sed. Petrology, v. 28, p. 186-199.
- Johns, W. D., Grim, R. E. and Bradley, W. F., 1954, Quantitative estimations of clay minerals by diffraction methods: Jour. Sed. Petrology, v. 24, p. 242-251.
- Klug, H. P. and Alexander, L. E., 1954, X-ray diffraction procedures: New York, John Wiley and Sons, 716 p.
- Kolpack, R. L. and Bell, A. S., 1968, Gasometric determination of carbon in sediments by hydroxide absorption: Jour. Sed. Petrology, v. 38, p. 617-620.
- Krumbein, W. C., 1934, Size frequency distributions of sediments: Jour. Sed. Petrology, v. 4, p. 65-77.
- Krumbein, W. C. and Pettijohn, F. J., 1938, Manual of sedimentary petrography: New York, Appleton-Century-Crofts, 550 p.



- Krylov, A. Ya. and Tedrow, J. C. F., 1963, Argon dating in marine geology and paleogeography, in Vinogradov, A. P., Editor, Chemistry of the earth's crust: Washington, Joint Publications Research Service, p. 413-424.
- Leith, C. K. and Mead, W. J., 1915, Metamorphic geology: New York, Henry Holt, 337 p.
- Lynn, W. C. and Whittig, L. D., 1966, Alteration and formation of clay minerals during cat clay development, in Clays and clay minerals, Proc. 14th National Conf. on Clay Minerals: New York, Pergamon, p. 241-248.
- MacEwan, D. M. C., 1961, Montmorillonite minerals, in Brown, G., Editor, The x-ray identification and crystal structures of clay minerals: London, Mineralogical Society, p. 143-207.
- Mielenz, R. C. and King, M. E., 1955, Physical-chemical properties and engineering performance of clays, in Pask, J. A. and Turner, M. D., Editors, Clays and clay technology, Proc. 1st National Conf. on Clays and Clay Technology: California Div. Mines Bull. 169, p. 196-254.
- Milne, I. H. and Early, J. W., 1958, Effect of source and environment on clay minerals, Am. Assoc. Petroleum Geologists Bull., v. 42, p. 328-338.
- Moberly, R., Jr., Kimura, H. S., and McCoy, F. W., Jr., 1968, Authigenic marine phyllosilicates near Hawaii: Geol. Soc. America Bull., v. 79, p. 1449-1460.
- Norris, R. M., 1964, Dams and beach sand supply in southern California, in R. L. Miller, Editor, Papers in marine geology, Shepard commemorative volume: New York, The Macmillan Company, p. 154-174.
- Orr, W. L., and Emery, K. O., 1956, Composition of organic matter in marine sediments: Preliminary data on hydrocarbon distribution in basins off southern California: Geol. Soc. America Bull., v. 67, p. 1247-1258.
- Peterson, M. W. A. and Griffin, J. J., 1965, Volcanism and clay minerals in the southeastern Pacific: Jour. Marine Research, v. 22, p. 13-21.

- Pettijohn, F. J., 1954, Classification of sandstones: Jour. Geology, v. 62, p. 360-365.
- \_\_\_\_\_, 1957, Sedimentary rocks: New York, Harper and Row, 718 p.
- Pinsak, A. P. and Murray, H. H., 1960, Regional clay mineral patterns in the Gulf of Mexico, in Swineford, A., Editor, Clays and clay minerals, Proc. 7th National Conf. on Clay Minerals: New York; Pergamon, p. 162-167.
- Porrenga, D. H., 1966, Clay minerals in recent sediments of the Niger Delta, in Bailey, S. W., Editor, Clays and clay minerals, Proc. 14th National Conf. on Clay Minerals: New York, Pergamon, p. 221-234.
- Powers, M. C., 1957, Adjustment of land derived clays to the marine environment: Jour. Sed. Petrology, v. 27, p. 267-287.
- \_\_\_\_\_, 1959, Adjustment of clays to chemical change and the concept of equivalence level, in Swineford, A., Editor, Clays and clay minerals, Proc. 6th National Conf. on Clays and Clay Minerals: New York, Pergamon, p. 309-338.
- Reed, R. D., 1928, The occurrence of feldspar in California sandstones: Am. Assoc. Petroleum Geologists Bull., v. 12, p. 1023-1024.
- Revelle, R. and Shepard, F. P., 1939, Sediments of the California coast, in Trask, P. D., Editor, Recent marine sediments: Soc. Econ. Paleontologists and Mineralogists Spec. Pub. 4, p. 245-282.
- Rex, R. W. and Goldberg, E. D., 1958, Quartz content of pelagic sediments of the Pacific Ocean: Tellus, v. 10, p. 153-159.
- Rex, R. W., Syers, J. K., Jackson, M. L., and Clayton, R. W., 1969, Eolian origin of quartz in soils of Hawaiian Islands and in Pacific pelagic sediments: Science, v. 163, p. 277-279.
- Rodolfo, K. S., 1964, Suspended sediment in southern California waters: M. S. thesis, Univ. of Southern California, Los Angeles, California, 91 p.

- Schultz, L. G., 1964, Quantitative interpretation of mineralogical composition from x-ray and chemical data for the Pierre Shale: U. S. Geol. Survey Prof. Paper 391-C, 32 p.
- Sharp, W. E. and Fan, P. F., 1963, A sorting index: Jour. Geology, v. 71, p. 76-84.
- Shaw, D. B. and Weaver, C. E., 1965, The mineralogical composition of shales: Jour. Sed. Petrology, v. 35, p. 213-222.
- Shepard, F. P., 1954, Nomenclature based on sand-silt-clay ratios: Jour. Sed. Petrology, v. 24, p. 151-158.
- Shepard, F. P., Dill, R. F., and von Rad, U., 1969, Physiography and sedimentary processes of La Jolla submarine fan and fan-valley, California, Am. Assoc. Petroleum Geologists Bull., v. 53, 390-420.
- Sherman, G. D., 1952, The genesis and morphology of the alumina-rich laterite clays, in Problems of clay and laterite genesis: Amer. Inst. Min. Metal. Eng., p. 154-161.
- Soutar, A., 1969, Sedimentation in Santa Barbara Basin, California (abs.): Am. Assoc. Petroleum Geologists Bull., v. 53, p. 468.
- Stevenson, R. E., Uchupi, E., and Gorsline, D. S., 1959, Some characteristics of sediments on the mainland shelf of southern California: Oceanographic survey of the continental shelf area of southern California: California State Water Pollution Control Board Pub., p. 59-110.
- Swindale, L. D. and Fan, P. F., 1967, Transformation of gibbsite to chlorite in ocean bottom sediments: Science, v. 157, p. 799-800.
- Trask, P. D., 1952, Source of beach sand at Santa Barbara, California as indicated by mineral grain studies: U. S. Army, Corps of Engineers, Beach Erosion Board, Tech. Memo. 28, 24 p.
- \_\_\_\_\_, 1955, Movement of sand around California promontories: U. S. Army, Corps of Engineers, Beach Erosion Board, Tech. Memo. 74, 60 p.

- U. S. Geological Survey, 1964, Compilation of surface waters of the United States, October 1950 to September 1960, Part 11, Pacific slope basins in California: U. S. Geol. Survey Water-Supply Paper 1735, 715 p.
- Van Andel, Tj. H. and Postma, H., 1954, Recent sediments of the Gulf of Paria, in Reports of the Orinoco shelf expedition: Amsterdam, North Holland, v. 1, 245 p.
- Walker, G. F., 1961, Vermiculite minerals, in Brown, G., Editor, The x-ray identification and crystal structures of clay minerals: London, Mineralogical Society, p. 297-324.
- Weaver, C. E., 1956, The distribution and identification of mixed-layer clays in sedimentary rocks: *Am. Mineralogist*, v. 41, p. 202-221.
- \_\_\_\_\_, 1958, The effects and geological significance of potassium "fixation" by expandable clay minerals derived from muscovite, biotite, chlorite, and volcanic material: *Am. Mineralogist*, v. 43, p. 839-861.
- \_\_\_\_\_, 1967, Potassium, illite, and the ocean: *Geochim. Cosmochim. Acta*, v. 31, p. 2181-2196.
- Whitehouse, U. G., Jeffrey, L. M., and Debbrecht, J. D., 1960, Differential settling tendencies of clay minerals in saline waters, in Swineford, A., Editor, Clays and clay minerals, Proc. 7th National Conf. on Clay Minerals: New York, Pergamon, p. 1-79.
- Whitehouse, U. G. and McCarter, R. S., 1958, Diagenetic modification of clay mineral types in artificial sea water, in Swineford, A., Editor, Clays and clay minerals, 5th National Conf. on Clays and Clay Minerals: National Acad. Sciences, National Research Council Pub. 566, p. 81-119.
- Williams, H., Turner, F. J., and Gilbert, C. M., 1954, Petrography: San Francisco, Freeman, 406 p.
- Wimberly, S., 1964, Sediments of the southern California mainland shelf: Ph.D. dissert., Univ. of Southern California, Los Angeles, California, 202 p.

Windom, H. L., 1969, Atmospheric dust records in permanent snowfields: Implications to marine sedimentation: Geol. Soc. America Bull., v. 80, p. 761-782.

Winters, E. and Simonson, R. W., 1951, The subsoil: Advan. Agron., v. 3, p. 2-92.